TWO-DIMENSIONAL ENZYME-BASED BIOSENSORS FOR SPATIALLY RESOLVED IMAGING AND MONITORING OF NEUROCHEMICALS

By

MONDE T. QHOBOSHEANE

A DISSERTATION PRESENTED TO THE GRADUATE SCHOOL
OF THE UNIVERSITY OF FLORIDA IN PARTIAL FULFILLMENT
OF THE REQUIREMENTS FOR THE DEGREE OF
DOCTOR OF PHILOSOPHY

UNIVERSITY OF FLORIDA

2003

Dedicated to my mother Nomonde Mashiqana for her agape love

ACKNOWLEDGMENTS

I would like to thank Dr. Weihong Tan for his guidance, support and encouragement during my study at the University of Florida. A special thanks to Dr. Xiaojing Liu, Dr. Xiaohong Fang, Dr. Peng Zhang and Dr. Swadeshmukul Santra for their scientific involvement. Also thanks to the members of the Tan research group for providing invaluable support, encouragement, and creating a positive working environment.

I am forever in debt to my mother for her unconditional love, support, guidance and never-ending sacrifices. My graduate efforts would not have been accomplished without my father Jeffery S. Hudson's spirit constantly with me. Also my collegiate trek would not have been completed without the love and support of my aunt and uncle Nobubele and Thami Mhlambiso.

I am grateful to Dr. Jim Deyrup and the Department of Chemistry graduate student office. I would like to express my gratitude to Lidia Matveeva for her priceless advice, companionship, and motherly guidance. I also appreciate the various secretaries who have made my graduate career manageable and enjoyable.

I thank the National Institutes of Health (NIH) department of Neurological disorders and stroke and the Vice Provost's office for their financial support through the duration of my graduate career.

TABLE OF CONTENTS

page

ACKNOWLEDGMENTS iii

ABSTRACT viii

1. INTRODUCTION 1

1.1 Neurochemicals 5
1.1.1 Neurotransmitters 5
1.1.2 Importance of L-lactate 11
1.1.3 Importance of Glutamate 13
1.2 Enzymes 17
1.2.1 Specificity of Enzymes 18
1.2.2 Naming and Classification 19
1.2.3 Enzyme Kinetics 23
1.3 Current Detection Methods 27
1.3.1 Microelectrodes 28
1.3.2 Fiber Optic Probes 30
1.3.3 Microdialysis 31
1.4 Nanotechnology 32

2. FABRICATION AND CHARACTERIZATION OF 1ST GENERATION TWO-DIMENSIONAL BIOSENSOR FOR BIO-ANALYTICAL APPLICATIONS 33

2.1 Experimental 33
2.1.1 Instrumentation 33
2.1.2 Reagents and Materials 35
2.1.3 2D Sensor Surface Modification 35
2.1.4 Enzyme Immobilization; LDH and GDH 36
2.1.5 Sensor Response Analysis 39
2.2 Sensor Characterization 42
2.2.1 Effect of Immobilization Time on the 2D Enzyme Biosensor 42
2.2.2 NAD^+ Effect on the 2D Enzyme Sensor Performance 43
2.2.3 Influence of pH on the Enzyme Sensor 45
2.2.4 Enzyme Probe for Sensitive Neurochemical Detection. 45
2.2.5 2D Enzyme Biosensor Stability 52

2.2.6 2D Enzyme Biosensor Selectivity 53
2.2.7 2D Sensor Response Time 53
2.3 2D Spatially Resolved Imaging 58
2.4 Conclusions 60

3. SYNTHESIS OF PURE SILICA NANOPARTICLES FOR BIOANALYSIS AND FABRICATION OF 2ND GENERATION TWO-DIMENSIONAL BIOSENSOR 61

3.1 Introduction 61
3.2 Experimental Section 64
3.2.1 Materials 64
3.2.2 Apparatus 65
3.2.3 Nanoparticle Synthesis 65
3.2.4 Nanoparticle Characterization 66
3.2.5 Silica Nanoparticle Surface Modification 67
3.2.6 Enzyme Immobilization 67
3.2.7 Biochemical Modification of Dye-Doped Silica Nanoparticles 69
3.2.8 Spectroscopic Measurement 69
3.3 Results and Discussion 71
3.3.1 Uniform Silica Based Nanoparticles 71
3.3.2 Particle Surface Modification 71
3.3.3 Enzyme Immobilized Nanoparticles for Glutamate and Lactate Analysis 75
3.3.4 Enzyme Immobilized Silica Nanoparticles for 2nd Generation 2D Sensor 78
3.3.5 Lifetime and Sensor Response for Glutamate and Lactate 81
3.3.6 Comparison Between Enzyme Immobilized Microspheres and Nanoparticle. 81
3.3.7 Dye-Doped Nanoparticle for Modification and Application as a Membrane Probe 83
3.4 Conclusion 87

4. ASSEMBLY OF NANOPARTICLES FOR BIOENHANCED NANOMATERIAL 88

4.1 Introduction 88
4.2 Experimental Section 90
4.2.1 Materials 90
4.2.2 Preparation of Pure Silica Nanoparticles 90
4.2.3 Silica Nanoparticle Characterization 91
4.2.4 2D Assemblies of Silica Nanoparticles 91
4.2.5 Controlled Assembly of Nanoparticles 93
4.2.6 Surface Modification of Nanoparticle Assembly 93
4.3 Results and Discussion 94
4.3.1 Nanoparticle Assembly Characterization 94
4.3.2 Nanoparticle Array Density Studies 94
4.3.3 Localized Assembly of Nanoparticles 98
4.3.4 Enzyme Immobilized Nanoparticle Array for Glutamate Analysis 99
4.4 Conclusion 99

5. A TWO-DIMENSIONAL IMAGING BIOSENSOR FOR THE MONITORING OF LACTATE RELEASE FROM BRAIN SLICES 102

5.1 Introduction 102
5.2 Experimental and Methods 104
5.2.1 Apparatus 104
5.2.2 Reagents 105
5.2.3 2nd Generation 2D Sensor Fabrication 105
5.2.4 Sensor Response Analysis 106
5.2.5 Monitoring Lactate Release from Brain Slice 107
5.3 Results and Discussion 107
5.3.1 Covalent Immobilization of LDH on Nanoparticle Modified FSP 107
5.3.2 Influence of pH and NAD^+ Effects on Lactate Sensor Performance 108
5.3.3 2nd Generation 2D Biosensor for Lactate Detection 108
5.3.4 Selectivity and Stability of the 2nd Generation 2D Biosensor. 109
5.3.5 Response Time of the 2D Biosensor 110
5.3.6 2D Imaging of Lactate from Tissue Slice 110
5.3.7 Real-Time Imaging of the Brain Slice 115
5.4 Conclusion 120

6. NICOTINE STIMULATION OF BRAIN SLICES FOR THE MONITORING OF GLUTAMATE 121

6.1 Introduction 121
6.2 Experimental and Methods 123
6.2.1 Apparatus 123
6.2.2 BioSensor Fabrication 124
6.2.3 Sensor Characterization 124
6.2.4 Preparation of Biological Samples 125
6.2.5 NAD^+ Effect on Glutamate Sensor Performance 126
6.2.6 Influence of pH on the Glutamate Sensor 126
6.2.7 GDH Probe for Sensitive Glutamate Detection 126
6.2.8 Glutamate Sensor Stability and Selectivity 130
6.3 Biological Application of the Imaging Biosensor 130
6.3.1 Nicotine Stimulation of Brain Tissue Slices for Glutamate Release 133
6.3.2 Imaging of Glutamate Release from Brain Slice 138
6.4 Conclusion 140

7. SUMMARY AND FUTURE DIRECTIONS 141

7.1 Summary 141
7.2 Future Work 144
7.2.1 Future Work for Nanoparticles 144
7.2.2 Future Work for 2D Assembly of Nanoparticles 145
7.2.3 Future Work for 2D Enzyme Biosensor for Neurochemical Detection. 145
LIST OF REFERENCES 146

BIOGRAPHICAL SKETCH 151

Abstract of Dissertation Presented to the Graduate School
of the University of Florida in Partial Fulfillment of the
Requirements for the Degree of Doctor of Philosophy

TWO-DIMENSIONAL ENZYME-BASED BIOSENSORS FOR SPATIALLY RESOLVED IMAGING AND MONITORING OF NEUROCHEMICALS
By

Monde T. Qhobosheane

May 2003

Chair: Weihong Tan
Major Department: Chemistry

This work focuses on the development of a novel two-dimensional (2D) enzyme-based biosensor for the detection of neurochemicals. There is a growing need for the elucidation of neurochemicals such as glutamate and lactate. Enzyme-based biosensors have shown to be an excellent detection technique for these neurochemicals. Current biosensors, which detect neurochemicals by single point measurements, have made much progress towards real time monitoring. However, a single point is not adequate for the complete understanding of many interesting cellular and subcellular events. The development of a spatially resolved 2D biochemical sensor will enable a better understanding of many biological processes by simultaneously imaging a large target area, not just a single point.

Our (2D) biosensor is based on a flat silica plate (FSP) with immobilized enzyme. The immobilization of the enzymes was done through a combination of covalent chemistries established for biosensor development. The enzymes (LDH and GDH for the

detection of lactate and glutamate respectively) go through a catalytic reaction with its co-substrate nicotinamide adenine dinucleotide (NAD^+) and either lactate or glutamate to yield the fluorescent product NADH. With an intensified charged coupled device (ICCD) detection system, highly sensitive glutamate and lactate monitoring was achieved.

To improve the biosensors detection capabilites, silica nanoparticles were polymerized onto the FSP. Higher silica content for enzyme immobilization increased the sensitivity down to the nanomolar range. Also individual nanoparticles were modified with enzyme and utilized for glutamate and lactate detection. Respectively, these nanoparticles have been covalently assembled onto 2D substrates for bio-analysis.

We have used the 2D biosensors for real-time monitoring of lactate released from mouse brain slices. We have studied the impact of KCl on lactate release. The variations of lactate released from the tissue slice have been spatially resolved and monitored.

Moreover, we have used the 2D biosensors for the detection of glutamate release. Nicotine, a well known addictive drug, has been used for the stimulation for glutamate release. We have found that low levels of nicotine can stimulate glutamate release, which gives more information about nicotine addiction.

The detection, monitoring and imaging of neurochemical release has shown that the 2D enzyme-based biosensor is a feasible approach to study cellular communications and possibly other biological processes that require simultaneous temporal and spatial resolutions. The two-dimensional biosensor also has the capability of monitoring many cells.

CHAPTER 1
INTRODUCTION

Stroke is the most common cause of adult disability in the United States having approximately 700,000 new cases arising each year. Moreover, stroke is the third leading cause of mortality and morbidity (Castillo et. al., 1997; Zivin and Choi 1991). This cardiovascular disease affects the blood vessels supplying blood to the brain. A stroke occurs when a blood vessel bringing oxygen and nutrients to the brain bursts or is clogged by a blood clot or some other particle. Because of this rupture, part of the brain does not get the flow of blood it needs. Neurons in the hippocampus, striatum, and cerebral cortex can be particularly vulnerable to this short period of ischemia (loss of blood flow and oxygen delivery). To account for this selective vulnerability to ischemia, the glutamate-calcium hypothesis is widely accepted (Collins et al.. 1989; Diemer et al.. 1993; Smith and Meldrum 1995; Zivin and Choi 1991). This hypothesis proposes that extracellular glutamate, a major excitatory neurotransmitter increases during ischemia, which in turn triggers an increase in intracellular calcium ion concentration [Ca^{2+}] and eventually neuronal cell death. Differential neuronal responses determine the degree and type of damage after ischemia.

There are four main types of stroke: two are characterized by the presence of blood clots, the remaining two are due to hemorrhage formation. Blood clot formation or the presence of particles in the artery is known as cerebral thrombosis and cerebral embolism respectively.

These types of strokes are by far the most common, accounting for about 70-80% of all strokes. The formation of blood clots in an artery or the presence of particles can decrease the amount of blood being delivered to the brain cells and cause a malfunction.

Cerebral and subarachnoid hemorrhages are caused by ruptured blood vessels on the surface of the brain. The escaped blood flows in the spaces between the brain and the skull. When this occurs, the loss of a constant blood supply can cause some brain cells to no longer function and eventually die. Another problem is that the accumulated blood from the burst artery may put pressure on surrounding brain tissue and interfere with how the brain functions. Severe or mild symptoms can result, depending on the amount of pressure. Consequently the hemorrhage form of stroke has a much higher fatality rate than strokes caused by clots.

Conventional approaches to the treatment of ischemic stroke focus on maintaining cardiac output, blood pressure, and cerebral blood flow (Collins et al. 1989). New therapies based on neuro-excitoxicity and reactive oxygen radicals have become a focal point due to the enhanced understanding of the cellular basis for ischemic injury. In ischemic stroke, the clinical challenge is to limit the spread of damage from one cell to another and to protect the brain as much as possible.

The detection of extracellular glutamate will be of great value in understanding the cellular and subcellular determinants of ischemic cell injury, which will ultimately lead to better treatment options for ischemic stroke. Thus, micron to submicron biosensor detection techniques is needed that have high sensitivity with nanometer spatial resolution, fast temporal resolution and excellent biochemical selectivity. The monitoring of glutamate responses to ischemic insult using these detection techniques will provide

insights into the subcellular mechanisms of glutamate excitoxicity during an ischemic event. Therefore, the real-time monitoring of neuronal responses to glutamate becomes extremely important in our understanding of the pathophysiology of stroke.

Current methodologies, which monitor cellular events, are done through the use of microelectrodes, optical microscopy or optical fiber biosensors (Hu and Wilson 1997; Lada et al. 1997; Tan et al. 1992; Xin and Wightman 1998). Of these methods, optical microscopy has several unique advantages that have led to its successful and widespread application in biology and medicine (Tan 1998). Current biosensing techniques using single point measurements such as microelectrodes and ultra-small optical fiber sensors have also made great advances in cellular monitoring. However, single point measurements are not adequate for a complete understanding of many important cellular and subcellular events and are too difficult for cellular communication studies.

The development of spatially resolved two-dimensional biochemical sensors will enable a better understanding of many biological processes by imaging a large target area, not just one single location. Currently, a conventional optical microscopy technique has been developed with two-dimensional capabilities to allow a more in-depth study of the cellular processes occurring with ischemia stroke (Bang and Tan 1999). Historically, the two-dimensional study of cell metabolism, function and pathology has been based on static images that are essentially projections of cell contents onto the image plane of optical and electron microscopes. Recent techniques, however, have focused on noninvasive real time monitoring of living cells (Chen and Ewing 1997).

Many of the current two-dimensional techniques use an array of optical fiber sensors, essentially a number of single point optical fiber probes bundled together

(Michael et al. 1998), while others form arrays by placing sensing material in microwells (Lavine et al. 1998). These biosensors (Chen and Ewing 1997; Lavine et al. 1998; Martin and Mitchell 1998; Michael et al. 1998) are mainly used for multi-analyte detection and have not been applied to obtain spatially resolved information on subcellular events. Thus, a two-dimensional biochemical sensor intended for chemical mapping of subcellular structures for real-time monitoring of cellular dynamics will have much significance in the study of living cells. For example, they could be used for the mapping of extracellular neurotransmitter concentrations and for the two-dimensional monitoring of neurotransmitter release.

To enhance the analytical capabilities of the two-dimensional sensor, nanotechnology has been included in the development of the enzyme biosensor. Nanotechnology is now poised to revolutionize the electronic, chemical and biotechnology industries (Kobayashi and Martin 1999; Martin and Mitchell 1998). One of the most important aspects of this field is the preparation and development of nanomaterials such as nanoparticles (Bruchez et al. 1998; Chan and Nie 1998; Couvreur et al. 1995; Haupt et al. 1985; Tadros 1993). There are several important areas of current interest in the field of nanoparticles, of which the following are critically important for biochemical analysis: preparation of nanoparticles with small and uniform size and nanoparticle biochemical modification for unique functionality. Recent advances in nanoparticle surface modification (Bruchez et al. 1998; Couvreur et al. 1995) have allowed nanoparticles to be biochemically modified with a variety of highly selective and biologically important molecules, resulting in different biofunctional surface properties. Nanoparticles with biocompatible surfaces are useful for a variety of applications in

biochemical analysis, such as biosensing and biomarking. The development of biochemically modified nanoparticles for enhanced measurements of signaling molecules, such as NADH will further improve the monitoring of cellular events.

In this work, highly sensitive optical biosensors with two-dimensional detection capabilities for real-time monitoring of neurochemicals and neurotransmitters have been developed. Biosensor and nanoparticle technology techniques have been combined to achieve neurochemical monitoring with high temporal and spatial resolution. Two generations of the two-dimensional sensors have been fabricated for the detection of neurochemicals and through the use of nanoparticles there has been an enhancement of sensing capabilities. With the use of these optical biosensors a more encompassing view of extra-cellular and cellular activity can be obtained to gain a better understanding of ischemic injury and cell death. The technological innovations developed from this research can be applied to greatly improve our ability to understand cellular and subcellular neurochemical mechanisms.

1.1 Neurochemicals

1.1.1 Neurotransmitters

The basic units of life that keep our physical and mental functions cycling through activation, inhibition, and modification are the cells of our central and peripheral nervous systems, the glia and neurons. Neurons make up the circuits of the nervous system, relaying information from the external and internal environment, and sending commands for reaction to the environment. The nerve cell or neuron also conveys information both electrically and chemically. Within the neuron itself, information is passed along through the movement of an electrical charge. The neuron has three main components (Nichols et

al. 1992) as shown in Figure 1-1: (1) dendrites - thin fibers that extend from the cell in branched tendrils to receive information from other neurons:, (2) Cell body, which carries out most of the neuron's basic cellular functioning and (3) Axons - long, thin fiber that carries nerve impulses to other neurons. Nerve signals often travel over long distances in the body, and dozens of neurons can be involved in such a circuit, necessitating a sophisticated communication system to rapidly convey signals between cells. Also because individually neurons can be up to 3 feet long, a rapid-rely mechanism within the neurons themselves is required to transmit each signal from the site where it is received to the site where it is passed on to neighboring cell. Two mechanisms have evolved to transmit nerve signals. First, within cells, electrical signals are conveyed along the cell membrane. Second, for communication between cells, the electrical signals generally are converted into chemicals signals conveyed by small messenger molecules called neurotransmitters (Nicholls 1994).

1.1.1.1 Signal Transmission within Nerve Cells

The mechanism underlying signal transmission within neurons is based on voltage differences (i.e. potentials) that exist between the inside and the outside of the cell (Figure 1-2). This membrane potential is created by the uneven distribution of electrically charged particles or ions; the most important of these ions are sodium (Na^+), potassium (K^+), chloride (Cl^-), and calcium (Ca^{2+}). Ions enter and exit the cell through specific protein channels in the cell's membrane. The channels "open" or "close" in response to neurotransmitters or to changes in the cells membrane potential. The resulting redistribution of electric charge may alter the voltage difference across the membrane. A decrease in the voltage difference is called depolarization. If depolarization exceeds a

certain threshold, an impulse (i.e. action potential) will travel along the neuron. Various mechanisms ensure that the action potential propagates in only one direction, toward the axon tip. The generation of an action potential is sometimes referred to as "firing" (Gonzales and Jaworski 1997).

1.1.1.2 Signal Transmission between Cells

Communication among neurons typically occurs across microscopic gaps called synaptic clefts. Each neuron may communicate with hundreds of thousands of other neurons. A neuron sending a signal (i.e. a presynaptic neuron) releases a chemical called a neurotransmitter, which binds to a receptor on the surface of the receiving (i.e., postsynaptic) neuron. Neurotransmitters are released from presynaptic terminals, which may branch to communicate with several postsynaptic neurons. Dendrites are specialized to receive neuronal signals, although receptors may be located elsewhere on the cell. Approximately 100 different neurotransmitters exist. Each neuron produces and releases only one or a few types of neurotransmitters, but can carry receptors on its surface for several types of neurotransmitters.

To cross the synaptic cleft, the cell's electrical message must be converted into a chemical one. This conversion takes place when an action potential arrives at the axon tip, resulting in depolarization. The depolarization causes Ca^{2+} to enter the cell. The increase in intracellular Ca^{2+} concentration triggers the release of neurotransmitter molecules into the synaptic cleft as shown in Figure 1-3. Many neurochemicals and

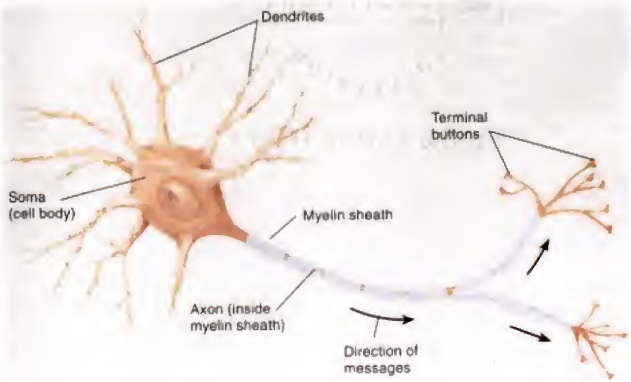

Figure 1-1. A neuron and its processes (copied from http://salmon.psy.plym.as.uk/year1/neurtotr.htm.)

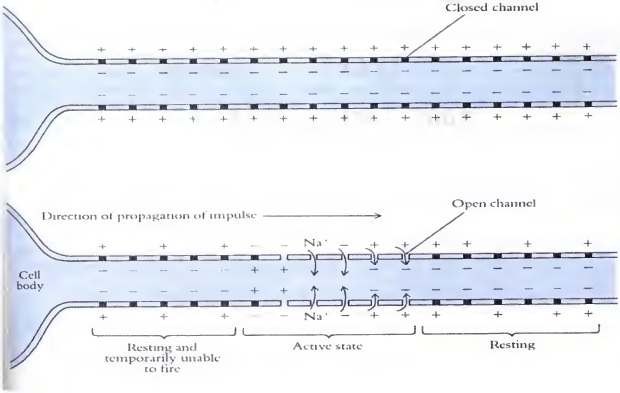

Figure 1-2. Signal transmission within neurons when an action potential happens. This diagram shows the opening and closing of sodium and potassium ion channels. (Copied from http://wwwpsych.stanford.edu/~lera/psych115s/notes/lecture3/figures1.html#spike)

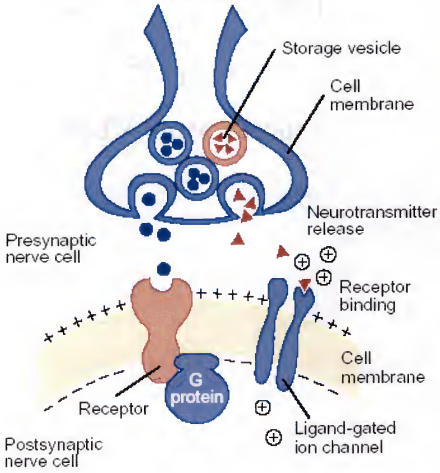

Figure 1-3. Signal transmission across the synaptic cleft. The binding of neurotransmitters (shown as triangles) to receptors that act as ligand-gated ion channels causes these channels to open, leading in some cases to a depolarization of the part of the membrane closest to the channel. Depolarization results in the opening of other ion channels, which in turn may generate an action potential. Neurotransmitters (shown as circles) that bind to second messenger-linked receptors initiate a complex cascade of chemical events that can produce changes in cell function. (Copied from http://wwwpsych.stanford.edu/~lera/psych115s/notes/lecture3/figures1.html#spike)

neurotransmitters have been identified for some time, such as dopamine and epinephrine, but some are still being discovered. The neurochemicals and neurotransmitters of interest in this work are l-lactate (lactic acid) and glutamate (glutamic acid). Both lactate and glutamate are important important bio molecules found in the brain and are involved physiological and clinical pathologies, such as ischemia and hypoxia (Mascini 1984).

1.1.2 Importance of L-lactate

The determination of L-lactate is essential in the diagnosis of respiratory insufficiencies and in sports medicine (Trettnak and Wolfbeis 1989; Toffaletti 1989). In sports medicine athletes increasingly use advance technology to fine tune their fitness and an understanding of lactate biochemistry can help them to prepare their body for peak activity. Monitoring blood lactate is an important tool for athletes in training, and portable analyzers give rapid results from a finger-prick of blood, which enables practical analysis of blood lactate changes during training.

Muscles use carbohydrates to provide energy for muscle movement, and in muscle cells the fuel can be use in two ways: aerobic (with oxygen) or anaerobic (without oxygen). Lactate is formed when carbohydrate is used anaerobically for energy, and when sufficient oxygen is available it is usually reconverted back to carbohydrate or used as a fuel itself. The aerobic pathway is limited in the amount of energy that it can supply and the duration over which it supplies energy. It does not provide energy quickly enough to satisfy the demands of high-intensity exercise or prolonged muscle activity. Muscles draw more heavily on the anaerobic pathway to support intensive or prolonged

exercise, resulting in the production of a large amount of lactate, which cannot be removed until the exercise is complete. Elevated levels of blood lactate tend to lower blood pH with consequent disturbance of metabolism/protein structure and beyond a tolerance level result in muscle fatigue or 'cramp'. Initially, lactate concentrations rise slowly but then increase sharply at a clearly defined point, termed the lactate threshold, which corresponds to the shift in metabolism to anaerobic within the muscle cells after exercise has begun. At this point, lactate is being produced faster than it can be metabolized and it accumulates, passing into the blood. Resting levels of blood lactate are around 1 mM, and in top athletes the lactate threshold can be as much as 4 mM, although there is considerable variation between individuals. Studies show that athletes can perform more muscle work before lactate levels raise significantly and that training at or around the lactate threshold can shift the threshold to reduce the adverse affects of lactate.

Even more importantly lactate has been shown to be involved in diseases such as myocardial infarction, severe congestive heart failure and pulmonary edma. These diseases are associated with the lack or excess of lactate in blood or muscle (Mascini 1985). In the present date, models have been formulated that suggest lactate rather than glucose is the major fuel for neurons thus linking energy metabolism to neurotransmitter release (Tan et al. 1992; Tsacopoulos and Magistretti 1996). According to the classical model of brain metabolism, increased energy requirements are met by an increase in blood flow that delivers oxygen and glucose to the extracellular compartments. In this model, blood flow is closely coupled with the delivery and utilization of glucose and oxygen.

A recent modification to this model includes the compartamentalization of energy metabolism. Increased energy requirements of activated neurons are met not by glucose, but by neuronal utilization of lactate provided by astrocytic glycolysis which itself is stimulated by glutamate uptake. Evidence in support of this model has principally come from *in vitro* experiments using primary cell cultures, brain slices and more recently NMR studies (Rusakov and Kullmann 1998; Schurr et al. 1988; Sibson et al. 1998). Also in support of this model figure 1-4 shows the physiological coupling of brain metabolism to neural activity which consists principally of glutamate-induced glycolysis in astrocytes (Schurr et al. 1988).

1.1.3 Importance of Glutamate

Glutamate is an important building block for polypeptides and accounts for over 10% of amino acid residues present in most proteins. It is also a constituent of many biologically active oligopeptides such as glutathione, a tripeptide present at high concentrations intracellularly and thought to be involved in cellular mechanisms dealing with oxidative stress (Tretter et al. 2003). Glutamate exists in two forms, D and L, in its isomeric nature it has an asymmetric alpha-carbon that can exist in two different configurations. *In vivo,* the L-form predominates and has maximal biological activity. In normal neural function, glutamate is responsible for most of the excitatory communications in the central nervous system (CNS). Nerve communication junctions (known as synapses) secrete and absorb glutamate more than any other neurotransmitter. Glutamate is involved, among other things, in memory and learning activities. However, when it is secreted in excessively large amounts, an exaggerated stimulus is created

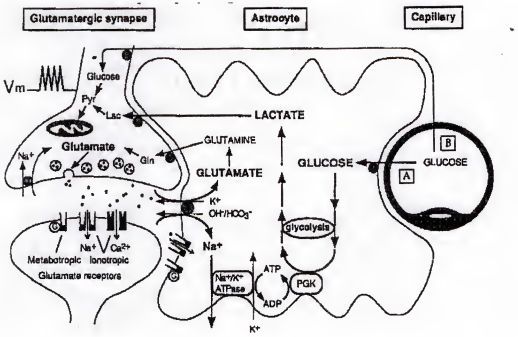

Figure 1-4. A schematic diagram showing the physiological coupling of brain lactate metabolism to neurotransmitter activity. (Copied from Tsacopoulos, M. and Magistretti, P.J. *J. Neurosci.* **1996**, 16, 877-885).

and expressed as an epileptic fit. The large amount of excess glutamate present in the brain over stimulates brain cells causing cell death, thus leading to the development of a stroke.

Stroke is the sudden development of focal neurological deficits usually related to impaired cerebral blood supply and oxygen delivery. Deprivation of the blood supply to a region of the brain results in reduced oxygen delivery. Decreased oxygen will lead to reduced synthesis of adenosine 5' triphosphate (ATP) in the axon terminal mitochondria. Thus, when the supply of oxygen is interrupted, an action potential arrives at the axon terminal and intracellular calcium rises, leading to the fusion of vesicles containing glutamate in the pre-synaptic membrane and the release of glutamate from the vesicles into the synaptic space.

The present accepted estimation of the quantum of glutamate contained in a vesicle is 5,000 molecules (Juurlink and Sweeney 1997). Once released into the synaptic cleft, glutamate binds to post-synaptic receptors, leading to direct or indirect depolarization of the post-synaptic neuron. If released in high concentrations, glutamate can have neurotoxic effects, leading to permanent brain damage.

Four to eight minutes of anoxia in the human brain is sufficient to produce irreversible damage (Smith 1995). This shortage of the oxygen supply to the brain can result in stroke, coronary arrest, or carbon monoxide poisoning. It has been known for at least the past decade that there is a window of opportunity for reduction of damage caused by cerebral ischemia. The window is not clearly defined but is not more than 24 hours after the ischemic episode. Cell death cannot be repaired in the infarct area, the

area of initial insult, but it can be reduced in the surrounding cell tissue by a number of pharmacological agents.

Drugs created for the reduction of ischemic damage are largely based on the accepted hypothetical model of ischemia. Experimental evidence suggests that prolonged neural depolarization and the resulting increase of intracellular sodium ions quickly deplete stored ATP when cells cannot undergo oxidative metabolism (Smith 1995). This depletion results in the release of glutamate in a Ca^{2+} dependent manner. Glutamate can also be released by a reversal of sodium-dependent uptake channels if the depolarization is large enough. The glutamate then stimulates (alpha)-amino-3-hydroxy-5-methyl-4-isoxazole propionic acid (AMPA), kianate, and N-methyl-D-aspartate (NMDA) glutamate receptors. Prolonged opening of the NMDA channels causes a large influx of Ca^{2+} into the cell, which activates a multitude of Ca^{2+}-dpendent processes, including catabolic enzymes that break down DNA. The end result is cell death through the actions of polyamines OH^- free radicals, proteases, endonucleases, and mitochondrial damage. After cell death, intracellular contents are released, including high concentrations of glutamate. This glutamate release results in a perpetuation of the ischemic event in surrounding neurons. Treatment is based on this hypothesized mechanism in attempt to block one or more of the pathways thought to lead to cell death.

Drugs discovered in the past few years, called use-dependent ischemic reducing drugs (blockers), give the best hope for reducing ischemic damage. These drugs block directly and indirectly, the voltage-gated sodium and/or calcium channels in a frequency-dependent (use-dependent) manner the more the cells fires, the more efficient the drugs' actions. This blockage prevents the release of neurotransmitters like glutamate. Since

excessive glutamate release is thought to be a main cause of ischemia, these drugs would reduce ischemic damage by indirectly blocking glutamate release. Two use-dependent ischemic reducing drugs, lamotrigine (3,5-diamino-6-[2,3-dichloropheny]-1,2,4-triazice) (Goldin 1995) and CNS 1237 (N-acenaphthyl-N'-methoxynaphthyl guanidine) (Turner 1993; www.worthington-biochem.com) have been shown to be effective in reducing ischemic damage. These drugs have also been shown to produce few, if any side-effects. These drugs may be very effective in preventing ischemic damage in human patients, especially if used during the first few hours after stroke, in preventing ischemic damage.

1.2 Enzymes

The existence of enzymes has been known for well over a century. Some of the earliest studies were performed in 1835 by the Swedish chemist Jon Jakob Berzelius who termed their chemical action catalytic. It was not until 1926, however, that the first enzyme was obtained in pure form, a feat accomplished by James B. Sumner of Cornell University. Sumner was able to isolate and crystallize the enzyme urease from the jack bean. His work earned him the 1947 Nobel Prize in chemistry. John H. Northrop and Wendell M. Stanley of the Rockefeller Institute for Medical Research shared the 1947 Nobel Prize with Sumner. They discovered a complex procedure for isolating pepsin. This precipitation technique devised by Northrop and Stanley has been used to crystallize several enzymes (Fersht 1999).

The Build-up of new tissue, replacement of old tissue, conversion of food to energy, disposal of waste materials, and reproduction are all the activities that we characterize as "life," this building up and tearing down takes place in the face of an apparent paradox. The great majority of these biochemical reactions do not take place

spontaneously. The phenomenon of catalysis makes possible biochemical reactions necessary for all life processes. Catalysis is defined as the acceleration of a chemical reaction by some substance which itself undergoes no permanent chemical change. The catalysts of biochemical reactions are known as enzymes and are responsible for bringing about almost all of the chemical reactions in living organisms. Without enzymes, these reactions take place at a rate far too slow for the pace of metabolism.

The oxidation of fatty acid to carbon dioxide and water is not a gentle process. When carried out in a test tube extreme condition of pH, high temperatures and corrosive chemicals are required. Yet in the body, such a reaction takes place smoothly and rapidly within a narrow range of pH and temperature. In the laboratory, the average protein must be boiled for about 24 hours in a 20% HCl solution to achieve a complete breakdown. In the body, the breakdown takes place in four hours or less under conditions of mild physiological temperature and pH. It is through attempts to understand more about enzyme catalysts, what they are, what they do and how they do it, that many advances in medicine and the life sciences have evolved.

1.2.1 Specificity of Enzymes

One of the properties of enzymes that makes them important as diagnostic and research tools is the specificity they exhibit relative to the reactions they catalyze. A few enzymes exhibit absolute specificity; that is they will catalyze only one particular reaction. Other enzymes will be specific for a particular type chemical bond or functional group. In general, there are four distinct types of specificity:

- Absolute specificity - the enzyme will catalyze only one reaction
- Group specificity – the enzyme will act only on molecules that have specific

functional groups, such as amino, phosphate and methyl groups.

• Linkage specificity – the enzyme will act on a particular type of chemical bond regardless of the rest of the molecular structure.

• Stereochemical specificity – the enzyme will act on a particular steric or optical isomer.

1.2.2 Naming and Classification

Except for some of the originally studied enzymes such as pepsin, rennin, and trypsin, most enzyme names end "ase". The International Union of Biochemistry (I.U.B) initiated standards of enzyme nomenclature that recommend enzyme names indicate both the substrate acted upon and the type of reaction catalyzed.

Enzymes can be classified by the kind of chemical reaction catalyzed:

1. Addition or removal of water
    a. Hydrolases – such as esterases, carbohydrases, nucleases, deaminases, amidases and proteases
    b. Hydrases such as fumarase, enolase, aconitase and carbonic anhydrase
2. Transfer of electrons
    a. Oxidase
    b. Dehydrogenase
3. Transfer of a radical
    a. Transglycosidases – of monosaccharides
    b. Transphosphorylases and phosphomutases – of a phosphate group

c. Transaimanses – of amino group

d. Transmethylases – of a methyl group

e. Transacetylases – of an acetyl group

4. Splitting of forming a C-C bond

a. Desmolases

5. Changing geometry or structure of a molecule

a. Isomerases

6. Joining two molecules through hydrolysis of pyrophosphate bond in ATP or other tri-phosphate

a. Ligases.

1.2.2.1 Dehydrogenases

Dehydrogenases are enzymes that utilize either NAD^+ or NADP as co-enzymes. The complex of the enzyme and co-enzyme is termed holoenzyme; the free enzyme is called apoenzyme. Some dehydrogenases are specific for just one of the co-enzymes and others use both. The reactions are readily reversible, so that carbonyl compounds may be reduced by NADH or NADPH via transfer of electrons from target molecules. The rates of reactions in either direction are conveniently measured by the appearance or disappearance of the reduced co-enzyme, since it has a characteristic ultraviolet absorbance at 340 nm, which provides an even more sensitive means of assay.

Lactate dehydrogenase has been isolated from many species, and is a tetramer with a molecular weight 140, 000 daltons. Lactate dehydrogenase is found in the cells of almost all body tissues. The enzyme is especially concentrated in the heart, liver, red blood cells, kidneys, muscles, brain, and lungs. The total LDH can be further separated

into five components or fractions labeled by number: LDH-1, LDH-2, LDH-3, LDH-4 and LDH-5. Each of these isoenzymes is used mainly by a different set of cells or tissues in the body. For this reason the relative amounts of a particular isoenzyme of LDH in the blood can provide valuable diagnostic information (Plaitakis 1999).

The entrapment, physical adsorption and immobilization of L-lactate dehydrogenase have all been successful methods for bio-analysis and detection of various diseases which are directly correlated with concentration variations of lactate found in the body. L-lactate dehydrogenase (LDH) catalyzes the reversible oxidation of L-lactate to pyruvate, using NAD^+ as a co-enzyme. The weakly fluorescent NAD^+ is thus converted to highly fluorescent NADH molecules (equation 1-1) the mechanism for the conversion is shown in figure 1-5.

$$\text{Lactate} + NAD^+ \xrightarrow{LDH} NADH + \text{Pyruvate} \qquad (1\text{-}1)$$

Similar to lactate dehydrogenase, glutamate has an enzyme specific for it which falls into the same class of enzymes known as glutamate dehydrogenase. Glutamate dehydrogenase carries out the oxidative deamination of glutamate to form ammonia and α-ketoglutarate. This is a liver enzyme, which can use either $NADP^+$ or NAD^+ (equation 1.2) as a major source of free ammonia in the liver for excretory purposes-urea synthesis (Xin and Wightman 1998). However, in the brain, and other organs without an active urea cycle, formation of glutamate and glutamine via amination of α-ketoglutarate (GDH reaction) and glutamate (glutamine synthetase reaction), respectively, is essential for ammonia detoxification. Similar to lacate dehydrogenase, glutamate dehydrogens has

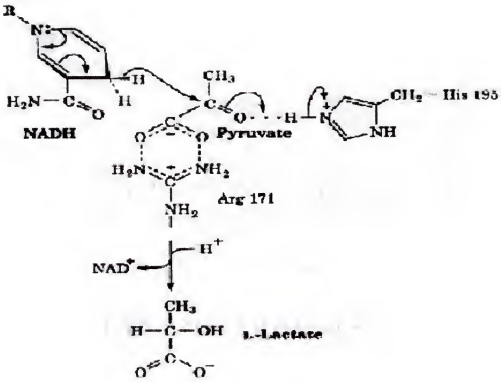

Figure 1-5. Model of LDH catalytic mechanism stereospecific transfer of hydride anion from NADH to pyruvate which is held in position by the Arg-171 side chain. (Copied from http://www.bio.mtu.edu/campbell/401lec16ball.pdf)

been used in electrochemical, amperometirc and fluorescent detection of glutamate in an attempt to understand pathophysiological effects of the neurotransmitter (Fersht 1999; Laidler 1987; Michealis and Menten 1913).

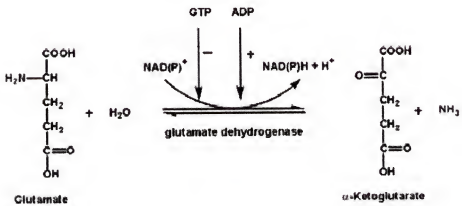

(1-2)

1.2.3 Enzyme Kinetics

Though enzymes are proteins, they may be associated with non-protein substances (Known as coenzymes or prosthetic groups) that are essential to the action of the enzyme. Some enzymes are catalytically inactive in the absence of certain substrates. For most enzymes, the catalytica activity is due to a relatively small region of the protein molecule termed the active site. The actions of enzymes show some resemblance to the catalytic action of acids and bases but are more complicated. The present treatment of enzyme kinetics is confined to the influence of concentrations, pH and temperature (Adams et al 1970).

It is also known that for these enzymatic reactions to proceed, some energy is needed. The quantity of energy needed is termed "the energy of activation." It is the magnitude of the activation energy which determines just how fast the reaction will proceed. It is believed that enzymes lower the activation energy for the reaction they are

catalyzing. Figure 1-6 illustrates this concept. The enzyme is thought to reduce the "path" of the reaction. This shortened path would require less energy for each molecule of substrate to be converted to be converted to product. Given the total amount of available energy, more molecules of substrate are converted when the enzyme is present (the shortened "path") than when it is absent. Hence, the reaction proceeds faster within a given period of time (Theorell and Chance 1951).

The simplest case is that of an enzyme-catalyzed reaction where there is a single substrate (aside from water). The dependence on substrate concentration in such cases is frequently as shown in Figure 1-7. The rate varies linearly with the substrate concentration at low concentration (first order kinetics) and becomes independent of substrate concentration (zero order kinetics) at high concentration. This type of behavior was first explained by Michaelis Menten and the reaction can be represented in equation (1-3) (Theorell and Chance 1951).

$$\underset{\text{Enzyme}}{E} + \underset{\text{Substrate}}{S} \longrightarrow \underset{\text{Enzyme Substrate Complex}}{ES} \longrightarrow \underset{\text{Product}}{P} + \underset{\text{Enzyme}}{E} \qquad (1\text{-}3)$$

In more difficult cases such as the class of enzymes known as dehydrogenases, which deal with dual substrates the kinetics can be much more difficult. In the dual substrate case, a number of mechanisms can be considered and are possible when an enzyme catalyses the reaction between the two substrates A and B. There may be the formation of binary enzyme-substrate complexes EA and EB, and the ternary complex

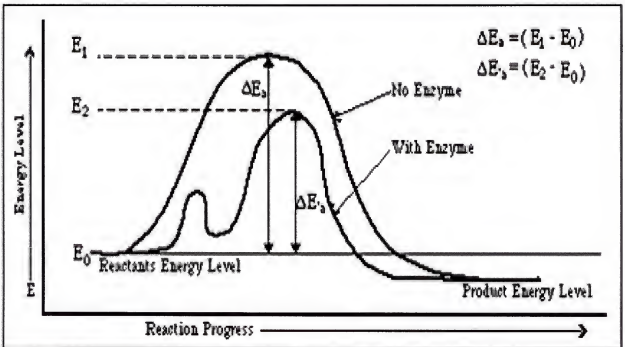

FIGURE 3
Energy of activation ΔE_a is less than $\Delta E'_a$ due to the effect of the enzyme on the substrate.

Figure 1-6. Plot of activation energy ΔE_a is less than $\Delta E'_a$ due to the effect of the substrate enzyme. (Copied from http://www.worthington-biochem.com/introbiochem/kinetics.html)

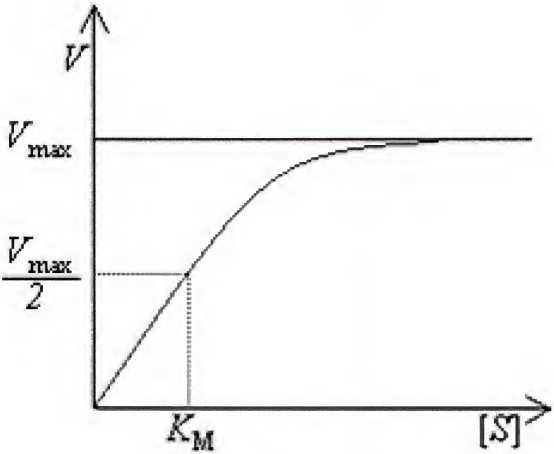

Figure 1-7. Diagram of reaction speed and Michaelis-Menten constant. The speed V describes the number of reactions per second that are catalyzed by an enzyme. With increasing substrate concentration [S], the enzyme is asymptotically approaching its maximum speed V_{max}, but never actually reaching it. Due to this phenomenon, no [S] at V_{max} can be given/determined. Instead, the characteristic value for the enzyme is defined by the substrate concentration at its half-maximum speed ($V_{max}/2$). This K_M value is also called Michaelis-Menten constant.

EAB. Sometimes the ternary complex is formed exclusively from one of the binary complexes and not from the other; for example equation 1-4 may occur but not equation 1-5. In this case the mechanism is said to be ordered; alternatively, the complex EAB may be readily formed from EA and EB, and the mechanism is said to be random.

$$EA + B \longrightarrow EAB \tag{1-4}$$

$$EB + A \longrightarrow EAB \tag{1-5}$$

Sometimes there is no evidence for the formation of a ternary complex; crystallographic studies have been done on dehydrogenases and they have hypothesized one mechanism for the enzyme lactate deydrogenase (Figure 1-8). Other enzymes in the class of dehydrogenases are currently being studied, but up to this point the mechanism for dehydrogenases is not well understood (Fardinia et al. 1993; Koshland 1953; Palleschi et al. 1951).

1.3 Current Detection Methods

The monitoring and detection of neurochemicals found in the brain is of great interest to a variety of different researchers with a wide spectrum of backgrounds ranging from clinical technologist, industrial researchers to academic scholars. Moreover, bio-

analytical techniques for the detection of neurochemicals are numerous and rapidly being developed, including methodologies for monitoring glutamate and L-lactate two substantially important chemicals (Chan and Nie 1998; Chang 1994; Cordek et al. 1999; Kobayashi and Martin; Lavine et al. 1998; Martin and Mitchell 1998 1999; Mitsubayashi et al. 1994; Pantano and Kuhr 1993; Tan et al. 1992; Xin 1998 Niwa 1998). Major techniques for the detection of glutamate and L-lactate use microelectrodes (Kar and Arnold 1992; Tan 1992; Wang and Arnold 1992), fiber-optic sensors (Dremel et al. 1991; Kar and Arnold 1992; Niwa 1998; Niwa 1996; Pantano and Kuhr 1993; Wang and Yeung 1997) and microdialysis coupled with chromatography techniques with optical or electrochemical detection (Chow et al. 1992; Jankowski et al. 1993; Xin 1998). These techniques have been useful for a variety of applications in lactate and glutamate analysis.

1.3.1 Microelectrodes

Electrochemical techniques that employ carbon fiber microelectrodes are becoming recognized as the tools of choice for answering questions about bio-chemical phenomena at the single cell level (Hu 1994; Zhou and Misler 1996; Zhou 1996). Many neuronal and neuroendocrine systems utilize chemical messengers that are easily oxidized. These include epinephrine, norepinephrine, dopamine, serotonin, and histamine, as well as smaller tryptophan and tyrosine containing polypeptide chains such as α-melanocyte stimulating hormone (α-MSH). Other compounds such as insulin, acetylcholine, choline, and glutamate may also be detected with the use of electron transfer mediators or enzyme modified electrodes.

Measurement of neurochemicals such as lactate and glutamate have been done using a variety of enzyme based electrochemical sensors.

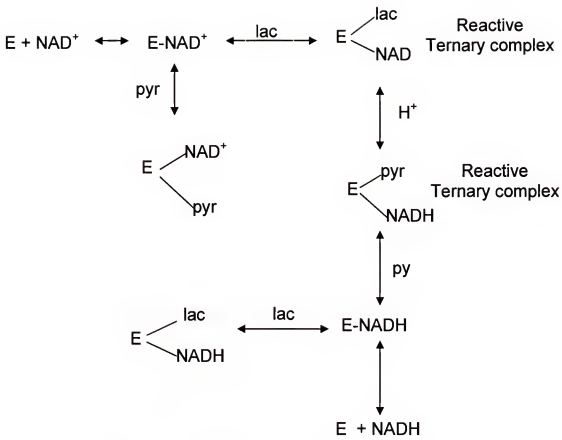

Figure 1-8. Suggested overall mechanism for L-lactate dehydrogenase.

The enzymes glutamate oxidase, glutamate dehydrogenase, lactate oxidase and lactate dehydrogenase have been immobilized inside polymer membranes giving response times in the 1 second range and detection limits from 10^{-6}-10^{-7} M concentration (Betzig et al. 1991; Cooper et al. 1997; Dempsey and Wang 1993; Hajizadeh et al. 199; Shengtian and Arnold 1996).

Similarly dual enzyme based electrodes for neurochemical detection has been fabricated with similar detection capabilities but increased signal to noise ratios for detection (Tan et al. 1992). The enzyme based electrodes are successfully able to detect and monitor neurochemicals. However these biosensors sometimes give false signals due to neurochemical interferences and also suffer from large over potentials.

1.3.2 Fiber Optic Probes

The use of fiber optic probes is a fairly new technology and is becoming more popular in bio-analytical applications. The fabrication of sub-micrometer optical fiber probe tips was first accomplished in 1991 (Betzig et al. 1991). Since then, the use of fiber optic probes as biosensors has become an increasingly popular technique. The capability of bringing the sample into close proximity for chemical sensing has made the fiber optic probe ideal as a biosensor. To date, fiber optic probes have been used for a vast array of applications. Initial applications of the fiber optic technology show the probes being used as pH sensors (Rosenzweig et al. 1995, 1996). From there the technology has been used for a wide range of bio-analytical studies (Gaddum 1961; Gaddum 1962; Mascini 1985; Tan et al. 1992; Wolfbeis and Trettnak 1989; Zhang 1997 1996; Zhou and Arnold). The use of fiber optic technology has made considerable progress in the area of bioanalysis. However most of these sensors are designed for

single point measurements, monitoring one specific location at any given time. With the 3 dimensionality of cells and their processes, and this may be a hindrance.

1.3.3 Microdialysis

Several years after the introduction of the push-pull cannula technique (Bito 1966; Ungerstedt 1982), it was proposed that the principles of dialysis could be applied to a method for sampling the extracellular fluid of the brain, thereby circumventing the problems associated with having a perfusion solution coming into direct contact with brain tissue. This method involves introducing a dialysis membrane between the perfusion solution and the extracellular fluid. Molecules that are sufficiently small to pass through the dialysis membrane will then diffuse across the membrane from an area of high concentration to an area of low concentration. First attempts in dialysis were done on dogs in which researchers attempted to determine amino acid levels (Wightman et al. 1987). These early attempts to dialyze the extracellular fluid of brain laid the foundation for subsequent work in this area.

Due to the parallel development of analytical methods, researchers began to use methods of high pressure liquid chromatography with electrochemical detection to achieve sufficient detection of neurochemicals such as dopamine, glutamate and lactate (Benvineste 1989; Andres et al. 1996). Using microdialysis with capillary electrophoresis, neurochemicals detection have been reported to be in 10^{-8}, 10^{-9} M level. Microdialysis provides information about qualitative changes in the extracellular concentration of a neurochemicals; however, because the mass transport of substances in brain tissue is different from aqueous solution, this difference in transport can lead to errors in detection (Murray et. al., 1995).

1.4 Nanotechnology

Nanoparticle technology has become an emerging field of research. It finds many applications in materials science, chemistry and biology. The attachment of bio-recognizable components to the surface of the discrete nanomaterials is one of the techniques for the preparation of assembled nanomaterials (Davis 1997; Kreuter 1991; Li et al. 1999; Mirkin et al. 1996; Shenton et al. 1998; Taleb et al. 1997, 1998). The array of nanomaterials into 2D and 3D superstructures has become an interesting field of research as they find a range of practical applications (Mirkin et al. 1996; Shenton et al. 1998; Taleb et al. 1997, 1998). In contrast there is still a demand for suitable nanomaterials based on solid supports for the development of efficient biosensors, biomarkers, drug delivery systems and for other biological applications (Marzouk et al. 1997; Sethi 1994). The knowledge of chemistry couples these two important aspects of nanoparticle research by providing nanoparticle synthesis methodologies and surface modification techniques. A variety of biomolecules (enzymes, antibodies, antigen, proteins), have the potential to control diseases and other problems within the human body. To study their activities *in vitro* biomolecules are being immobilized onto the various types of solid supports. Once they are found active on the surface they will be used for monitoring biological components. These developments will have potential applications in fields ranging from environmental monitoring to the production of monitoring devices for diagnosing infectious diseases (Liu and Tan 1999; Fang et al. 1999; Wagner and Schmid 1990). Solid supported biomolecules are thus becoming important tools for many biological studies (Bruchez 1998; Chan and Nie 1998; Fang and Tan 1998; Tan et al. 1997) and will be increasingly utilized as analytical tools of the future.

CHAPTER 2
FABRICATION AND CHARACTERIZATION OF 1ST GENERATION TWO-DIMENSIONAL BIOSENSOR FOR BIO-ANALYTICAL APPLICATIONS

2.1 Experimental

2.1.1 Instrumentation

The experimental set-up for the two-dimensional enzyme modified biosensor was based on an inverted Olympus fluorescence microscope (IX70-S8F). The set-up shown schematically in Figure 2-1 is similar to the microscope imaging system used for real-time neurotransmitter monitoring (Liu et al. 1997). An intensified charged coupled device (ICCD) (Princeton, EEV 512x1024) was used for capturing images and ultrasensitive analysis. The ICCD has the capability of imaging single molecules in solution and on a surface (Fangw et. al. 1999). The radiation source for the excitation of NADH molecules was a 350 nm laser beam from an Innova Ar^+ laser (Coherent Laser, Santa Clara, CA). We chose to use a laser instead of a lamp to ensure that NADH molecules were efficiently excited. The collection of NADH fluorescence was done through quartz microscope objectives with a 10 to 60X magnification. The optical signal was selected using a combination of long pass filters and a 465-interference filter (Oriel Corporation, Stratford, CT). The selected fluorescence signal was subsequently directed onto the ICCD. A PC computer with Winview software (Princeton Instruments, Princeton NJ) was used to control the ICCD system. The apparatus was put on a vibration free laser table to avoid variations during the imaging.

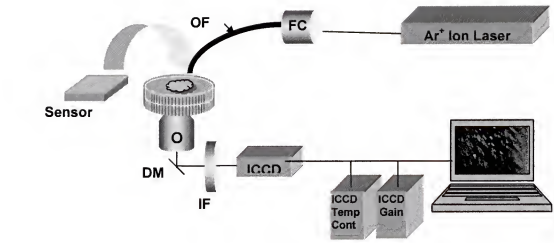

FC = Fiber Coupler
OF = Optical Fiber
O = Objective Lens
IF = Interference Filter
DM = Dichroic Mirror

10X Objective
460 Interference Filter
ICCD Parameters
75 Gain
-25^0 C

Figure 2-1. Schematic diagram of the optical set-up for two dimensional biosensor measurements.

This set-up has been used in the imaging of single living cells and single molecules (Trettnak and Wolfbeis 1989; Liu et. al., 1997).

2.1.2 Reagents and Materials

Lactate dehydrogenase (LDH) from Bovine Heart (550 units/mg) and glutamate dehydrogenase (GDH) from Bovine Heart (550 units/mg) was purchased from Roche Molecular Biochemicals (Germany). Lactate and glutamate was purchased from Sigma Chemical Co. (St. Louis, MO). Nicotinamide adenine dinucleotide (NAD^+) and gluteraldehyde (25% aqueous solution) were purchased from Acros Organics (Fairlawn, NJ). Trimethoxysilylpropyldiethylenetriamine (DETA), a silanization reagent was purchased from United Chemical Technologies (Bristol, PA). All other chemicals were of analytical reagent grade. Distilled deionized water was used for the preparation of all aqueous solutions.

2.1.3 2D Sensor Surface Modification

A batch of 6-10 flat silica plates was used in a single immobilization cycle. The flat silica plates (FSPs) were first cleaned by immersion in a solution of concentrated HCl/MeOH (1:1) for 30 minutes. They were then rinsed in deionized water and submerged in concentrated H_2SO_4 for 30 minutes. Following an adequate rinse in deionized water silanization of the FSPs was performed by immersion of the FSPs in a freshly prepared 1% (v/v) solution of DETA in 1mM acetic acid for 30 minutes at room temperature (23°C). The DETA-modified FSPs were thoroughly rinsed with deionized water to remove excess DETA. The silanized FSPs were dried under N_2 (gas) and fixed with heat in a 120°C oven for 5 minutes. Conjugation of the FSP was carried out using a bi-functional cross-linker, gluteraldehyde. The silanized sensors were kept in a 12.5%

(v/v) gluteraldehyde solution with 0.1 M potassium phosphate buffer solution (PBS) at pH 6.8 for 14 hours at room temperature.

Fluorescamine is intrinsically a non-fluorescent compound but reacts in milliseconds with primary aliphatic amines to yield a fluorescent complex as shown in Figure 2-2. It was employed to detect the amino groups on the flat silica plate surface. The flat silica plate was immersed in 1 mM fluorescamine-DMF solution in the range of for 4 to 60 minutes. Fluorescamine was subsequently used to confirm the binding of the glutaraldehyde to the aminosilane layer. A lack of fluorescence was a positive response. In the next step, it was particularly critical to remove all excess glutaraldehyde before placing the flat silica plate into the enzyme solution for immobilization (Zhang and Tan 2001). Therefore, meticulous rinsing with deionized water and complete drying under N_2 (g) followed conjugation. The un-reacted carboxyl termini of the bi-functional crosslinker were linkied to the primary amines on the target enzyme, as illustrated in Figure 2-3.

2.1.4 Enzyme Immobilization; LDH and GDH

LDH or GDH molecules were directly immobilized onto a flat silica plate surface by covalent binding. The mechanism for immobilization is a combination of several surface modification techniques (Sogowa and Takahashi 1978; Strver 1988Zhang, and Tan 2001). Conjugation of the LDH or GDH molecule is done through the use of gluteraldehyde, where one aldehyde group reacts with an amine from the amino-silane layer on the silica glass and the other aldehyde group reacts with the amine-containing bio-molecules. The gluteraldehyde is used not only for joining separate molecules, but also as a spacer arm that allows for greater accessibility and/or freedom to the attached

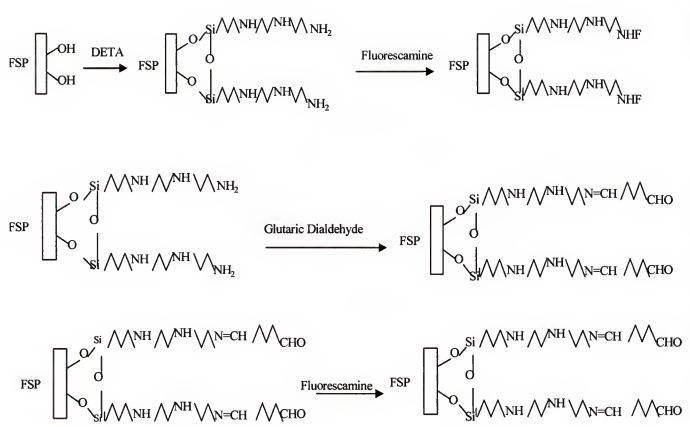

Figure 2-2. Detection of primary amines on a flat silica plate surface before conjugation.

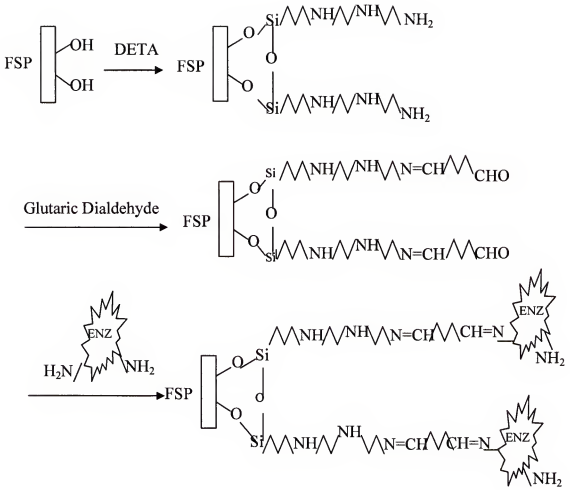

Figure 2-3. Enzyme immobilization onto a flat silica plate surface.

macromolecules such as LDH or GDH. Similarly glutaraldehyde is known to be essential to the activity of the enzyme reacting with its substrate.

2.1.5 Sensor Response Analysis

Measurements of the glutamate dehydrogenase and lactate dehydrogenase activity were carried out in the confines of channel created by arranging two glass slides adjacent to each other both on top of a third glass slide. An optical fiber was placed in the channel for excitation of the NADH molecules, generated by the enzymatic reaction of the immobilized enzyme and the injected substrate solution: the set-up is shown in Figure 2-4. The 2D enzyme sensor formed a sandwich with a clean glass slide. Substrate solution, containing different concentrations of lactate or glutamate and 1 mM NAD^+ in a 0.1 M PBS buffer at pH=7.8, was filled between the two plates.

Optical excitation from the laser was uniform in the imaging area using the 40X microscope objective; Figure 2-5 shows a pixel by pixel account of the fluorescence intensity across the imaging area. The microscopy system was used to monitor the enzymatic reaction over time. Usually, 100 fluorescence images were taken to monitor the fluorescence intensity increase due to NADH production from the reaction catalyzed by the immobilized LDH or GDH molecules on the FSP. Quantitative analysis of the data was performed with the software WinView. Individual spatial location can be chosen for time resolved analysis.

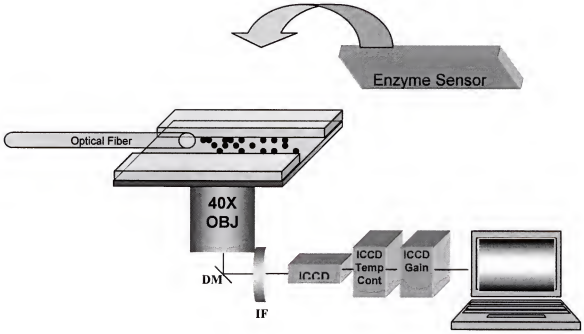

Figure 2-4. Schematic diagram of 2D enzyme biosensor characterization set-up.

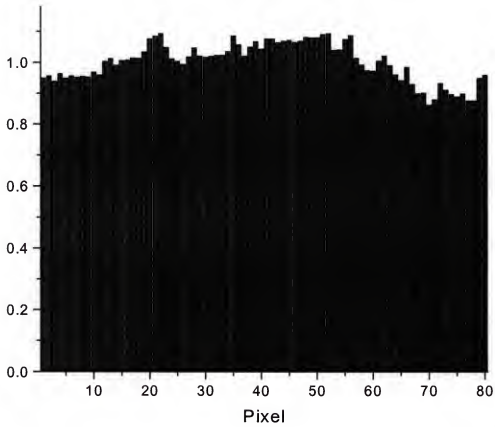

Figure 2-5. Bar graph representation of the uniformity of the laser excitation light across a viewing area.

2.2 Sensor Characterization

Solid support structures that are modified with biological components, whether it is enzymes, antibodies or DNA, need to be characterized to ensure that modification does not alter the activity of the biological component. In this instance we are dealing with enzymes, specifically glutamate and lactate dehydrogenase. Enzymes are catalyst, and when immobilized to a substrate they usually lose some of its catalytic activity. In addition, most enzymes are highly sensitive to their pH environment, and to guarantee optimal enzymatic conditions we have examined the effect of pH on the enzyme-immobilized sensor. Also, the concentration of an enzyme's substrate plays an important role in the enzyme's catalytic turnover rate: a range of substrate concentrations, [NAD^+], have been studied to ensure that the enzyme is used in a suitable working condition. We have also done selectivity, stability and response time experiments to further ensure excellent enzymatic activity. Optimized parameters assure that the immobilized enzyme will give maximal sensitivity for the detection of glutamate.

2.2.1 Effect of Immobilization Time on the 2D Enzyme Biosensor

To ensure maximal enzyme surface coverage on the flat silica plate, we have investigated the duration of the enzyme molecule reaction with a treated/activated flat silica plate. In order to develop an enzyme biosensor that has very good temporal resolution, having a high catalytic turnover rate in the presence of its substrates (NAD^+, lactate or glutamate), the immobilized enzymes must be orientated correctly so that the active sites on the enzymes are available for the substrates. Secondly, a sufficient amount of enzyme must be covalently attached to the silica plate surface, so that the detection of

the substrate can be determined at a high rate. Figure 2-6 illustrates how the 2D enzyme biosensor responds with maximum enzymatic activity when the immobilization of the enzyme is within a 20-30 hour time period, although after 5-7 hours immobilized enzyme is present on the flat silica plate, and the generation of NADH can be detected.

Currently, surface spectroscopies have been utilized in attempt to confirm enzyme surface coverage on substrates (Zhang, and Tan 2001), but we chose to use the immobilized enzyme itself as an indicator of maximum immobilized of enzyme concentration. There are two methods that can be employed to confirm the point at which no additional enzyme can be immobilized. The first of which uses the absolute increase in NADH signal produced in a given time, while the second makes use of the enzymatic reaction rate. Both methods confirmed the trend shown in Figure 2-6. The immobilization plot shows that after approximately 25 hours the enzyme immobilization time of the enzyme does not affect the activity, but an increase in immobilization time may disrupt the immobilized enzyme conformation and active site accesibility.

2.2.2 NAD^+ Effect on the 2D Enzyme Sensor Performance

As mentioned earlier, NAD^+ is a vital component of GDH and LDH enzymatic reactions and the effect of its concentration during lactate and glutamate measurements has been studied. The sensor response for different NAD^+ concentrations, while having a constant substrate (0.5mM) of either lactate or glutamate is shown in Figures 2-7 and 2-8. When the concentration of NAD^+ was increased, the sensor responded in an asymptotic approach to a maximum enzyme activity. Thus the immobilized enzyme's activity on the FSP is in essence independent of the co-substrate when the concentration of NAD^+ is above 1 mM.

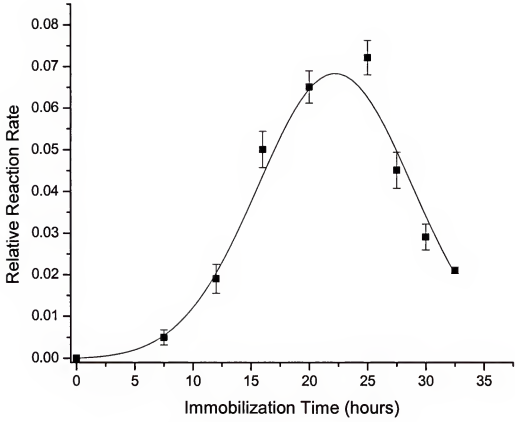

Figure 2-6. Effect of immobilization time on the 2D enzyme sensors response. Testing solution conditions are 1 mM NAD+ and 4 mM glutamate

2.2.3 Influence of pH on the Enzyme Sensor

The environment in which a biosensor is used may have a significant effect on its response; therefore the influence of pH was investigated. The results are shown in Figures 2-9 and 2-10. The sensor had its highest activity in a pH range 6.8-8.9. The reaction of the substrates lactate or glutamate with NAD^+ under the catalysis of LDH or GDH is a process that releases H^+/NH_4^+ thus a high pH is advantageous to the positive reaction. However, too high a pH may result in both the decomposition of NAD^+ and instability of the enzyme. Optimum response in the physiological pH range is an advantage for both of these sensors. All GDH/LDH enzyme sensor measurements were performed at pH 8.5 by using a Tris-HCl buffer.

2.2.4 Enzyme Probe for Sensitive Neurochemical Detection.

The enzyme immobilized two-dimensional sensor is a highly sensitive probe down to the micromolar range. The response curve for both LDH/GDH enzyme biosensors were obtained under the optimal conditions presented in Figure 11 and 12. We used initial reaction rates to characterize the sensor's sensitivity for monitoring lactate/glutamate changes. According to the Michaelis equation, at constant enzyme concentration the initial rate is directly proportional to the substrate concentration when the concentration is much less than K_m (Strver 1988) (K_m, the Michaelis constant, is equal to the substrate concentration at which the reaction rate is half of its maximal value). Reaction rates were calculated for the first 100 data points, (25 ms for each point) of continuous monitoring of the production of NADH at different lactate/glutamate concentrations. Figure 11 and 12 shows that the lactate and glutamate sensors have a linear response ranged of 0-1 μM.

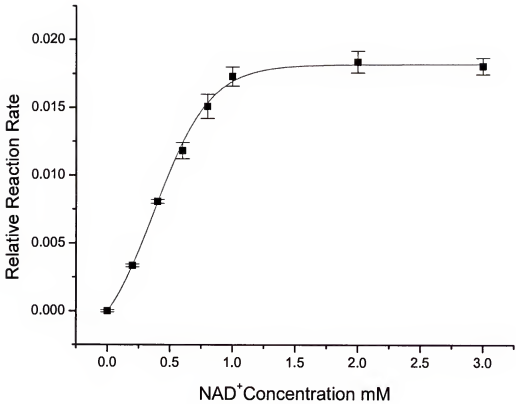

Figure 2-7: Effect of NAD^+ concentration on the activity of lactate sensor at pH 80 (Tris-HCl buffer) in the presence of 0.5 mM lactate

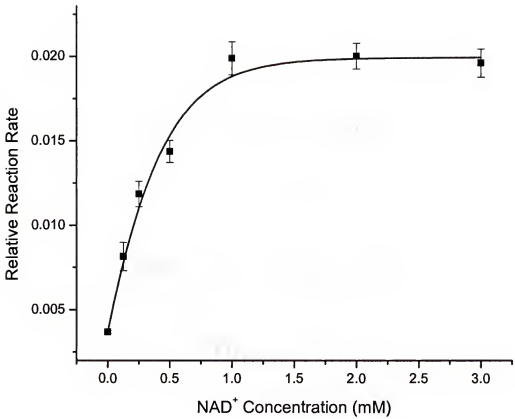

Figure 2-8: Effect of NAD^+ concentration on the activity of glutamate sensor at pH 80 (Tris-HCl buffer) in the presence of 0.5 mM glutamate

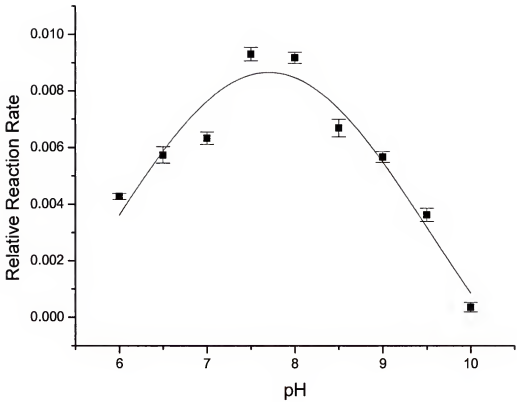

Figure 2-9: Effect of pH on immobilized LDH. Experimental conditions 0.1 mM $NaHPO_4$-NaH_2PO_4 (pH = 5.7-6.8), 0.1mM Tris-HCl buffer (pH = 7.0-8.9), 0.1mM Na_2CO_3-$NaHCO_3$ buffer (pH = 9.1-10.2), 0.5 mM lactate and 1mM NAD^+.

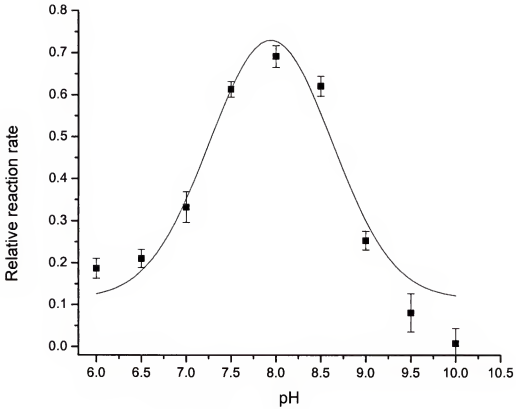

Figure 2-10. pH effect on the immobilized GDH enzyme: Experimental conditions .0.1 mM Na_2HPO_4-NaH_2PO_4 (pH = 5.7-6.8), 0.1 mM Tris-HCl buffer (pH = 7.0-8.9), 0.1 mM Na_2CO_3-$NaHCO_3$ buffer (pH = 9.1-10.2), 0.5 mM glutamate and 1mM NAD^+.

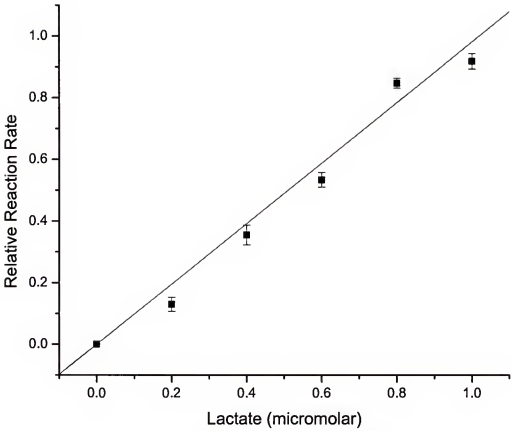

Figure 2-11. Calibration curve for L-lactate under optimal conditions.

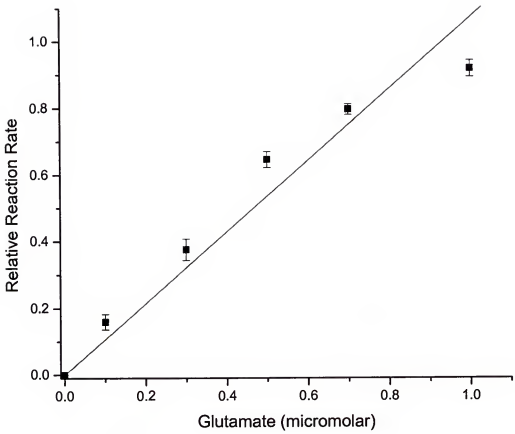

Figure 2-12. Calibration curve for glutamate under optimal conditions.

The LDH immobilized sensor has a detection limit of 0.2 μM and the GDH biosensor a detection limit of 0.1 μM.

Compared with previously reported neurochemical sensors, the 2D enzyme immobilized biosensor prepared in this work is geometrically larger. However this biosensor is comparable in sensitivity with other lactate/glutamate probes that have been reported. There are five possible reasons/factors that contribute to the high sensitivity of the present sensor. The first factor is the direct covalent immobilization of the enzyme molecules on the FSP surface without membrane, gel, or any other carriers. Second, our 2D structure allows for more enzymes to be immobilized, increasing the overall sensitivity of the sensor. Third our sensor designs attaches a large spacer between the FSP surface and the enzyme molecules through long chains. Fourth, due to the excellent enzyme surface coverage, the sensor can detect multiple analytes simultaneously. The fifth reason is the highly sensitive optical detection (containing an ICCD and laser-induced fluorescence system) built for the sensor application.

2.2.5 2D Enzyme Biosensor Stability

The lifetime of sensors, especially those employing biologically active materials such as enzyme or antibodies, is a major concern. The 2D enzyme sensor was stored in pH 6.8 PBS buffer at 4°C when not in use. The stability of the system was initially evaluated based on hourly response measurements on a 4 mM substrate sample under optimal conditions as shown in Figures 13 and 14. The 2D enzyme sensor showed good stability in the first couple of days. A significant degradation in the sensor's response was observed after the second day. Optimal storage conditions were found to be at 4 °C.

2.2.6 2D Enzyme Biosensor Selectivity

Both lactate and glutamate dehydrogenases are highly selective in their reaction with lactate and glutamate over other substrates, because of this the 2D enzyme sensor offers high selectivity for both lactate and glutamate. The selectivity of the 2D enzyme biosensor probe for its target substrate was demonstrated by attempting to report any response to other α-hydroxy acids and those compounds that are the most common interferences in physiological samples. As shown in Table 2-1 no responses were observed for the majority of the compounds tested. For lactate, only acetamidophenol showed a low response at a concentration of 10 mM which is about 2.3 % of the response for lactate at the concentration of 0.2 mM. Similarly, potential interferences for glutamate were examined; ascorbate and cysteine initiated a small response. Potential interferences from NMDA was also evaluated due to its structural similarities to glutamate, Table 2-2 shows selectivity results.

2.2.7 2D Sensor Response Time

For most biological sensors, the time the sensors need to achieve a steady-state response after the introduction of a sample is reported as the response time. We define the response time for the enzyme sensor as the time required for the 2D sensor to generate sufficient NADH for detection. The shortest response time of the sensor corresponds to the lowest required optical signal generated by NADH. We used the standard deviation of the base line to estimate the response time of the sensor. The 2D sensor has demonstrated response times less than 100ms for 0.5 mM concentration of the respective substrate. The 2D biosensors prepared in this work were ready for experimental measurements directly after rinsing with buffer. A great benefit of the 2D biosensor was

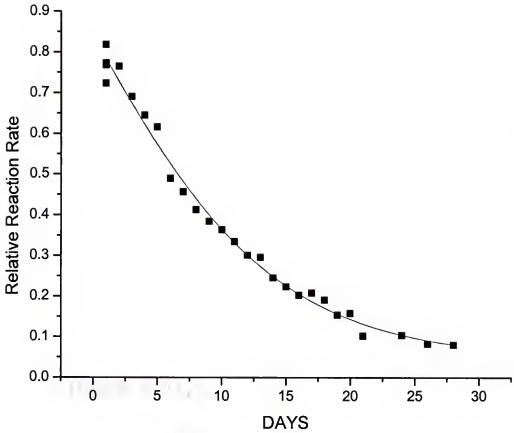

Figure 2-13. Response to 4 mM glutamate and 1mM NAD^+ as a function of biosensor age.

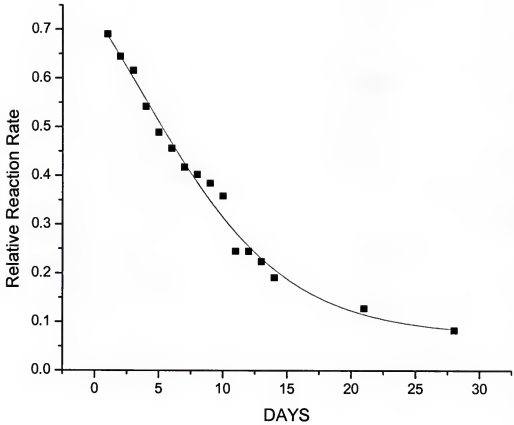

Figure 2-14. Response to 4mM lactate and 1mM NAD^+ as function of the 2D biosensors age.

Table 2-1. Relative response of LDH sensor to potential physiological interferences

Compound	% Response	Compound	% response
Lactate	100	Ascorbic acid	0
Malonic acid	0	Uric acid	0
Glycolic acid	0	L-cysteine	0
Isocitric acid	0	Glutathione	0
Quinic acid	0	Acetamidophenol	2.3

Compound	% Response	Compound	% response
L-Glutamate	100	L-glycine	0
ADP	0	H2O2	0
L-ascorbate	5.2	L-lactate	0
L-cyseine	3	NMDA	0
L-glutamine	0	Urate	0

Figure 2-2. Relative responses of GDH 2D enzyme sensor to potential physiological interferences

its short recovery time and the fast response time is due to the direct immobilization of the enzyme molecules onto the flat silica plate.

2.3 2D Spatially Resolved Imaging

The two-dimensional sensor for the monitoring of neurochemicals has excellent spatial and temporal resolution. Also the two-dimensional sensor has the advantage of capturing simultaneous measurements at multiple points. To further show the 2D enzyme biosensors capability, we used 5 μm diameter polycarbonate membrane holes with a depth of about 10 μm as the reactors for ultra-sensitive neurochemical detection (Tan and Yeung 1997, Bang and Tan 1999). The membrane holes are comparable in size to single biological neuron cells. The 2D dimensional enzyme biosensor was placed on top of the polycarbonate membrane wells as shown in Figure 2-17. The fluorescence intensity increase generated by the enzyme biosensor was monitored using a fluorescence microscope with an ICCD. As seen in the Figure 2-17 the 2D biosensor is able to spatially resolve the fluorescence increases generated by the enzymatic reaction. This capability will allow a better understanding of biological processes through spatially resolved images that show a complete picture of important cellular events.

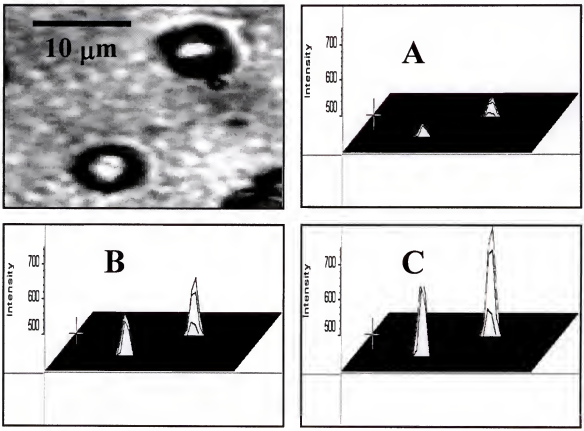

Figure 2-17. Spatially Resolved Imaging: Top left is an image of a section of 5 μm membrane holes. A-C: The graphical representation of fluorescence intensity increase due to NADH formation. A is the image of frame 1, B is frame 50, and C is frame 100. The dwell time for the experiment was 1 sec/frame.

2.4 Conclusions

In conclusion, a highly sensitive optical biosensor with two-dimensional imaging capabilities has been developed for spatially resolved imaging and monitoring of neurochemicals. The two-dimensional sensor is based upon the direct immobilization of dehydrogenase class enzymes onto a flat silica plate. The silanization, cross-linking and chemical modification have been used to coordinate the enzyme molecules to the flat silica plate. The enzyme molecules attached to the flat silica plate have exhibited high enzymatic activity, and have been characterized. Both LDH and GDH 2D biosensors have shown sensitive detection limits of 0.1 and 0.2 μM respectively. The sensitivity of these biosensors though geometrically larger have comparable sensitivity levesl to other neurochemicals detection methods. These highly selective and stable sensors will be useful to give a more encompassing view of cellular activities when the release of a neurotransmitter can be mapped and spatially resolved. The two-dimensional imaging biosensors can also enable us to monitor many cells simultaneously, providing better biochemical imaging of cellular functions and interactions.

CHAPTER 3
SYNTHESIS OF PURE SILICA NANOPARTICLES FOR BIOANALYSIS AND FABRICATION OF 2ND GENERATION TWO-DIMENSIONAL BIOSENSOR

3.1 Introduction

There are many interesting areas in nanotechnology (Hari 1999 Kobayashi and Martin 1999; Martin and Mitchell 1998). One of the most important aspects of this field is the preparation and development of nanomaterials, such as nanoparticles. There have been a variety of techniques for preparing different types of nanoparticles (Bruchez et al. 1998; Chan and Nie 1998; Chang et al. 1994; Couvreur et al. 1995; Tadros 1993). The nanoparticles can be made with different materials and be as small as 1 nm (Andres et al. 1996; Clark et al. 1999; 1996; Li et al. 1999; Mirkin et al. 1996; Murray et. al., 1995; Taleb et al. 1997, 1998; Santra et al. 2001; Qhobosheane et al. 2001; Shenton et al. 1998) There are a few important nanoparticle research areas of current interest related to biochemical analysis: preparation of nanoparticles with small and uniform sizes and the biochemical modification of nanoparticles for unique biochemical functionality.

Biomolecular surface modification adds specific functionality to a large variety of substrates (Cordek et al 1999.; Fang et al 2000. Ingersoll and Bright 1997, 1999; 1999; Pantano and Walt 1999). There have been recent advances in nanoparticle surface modification (Andres et al. 1996; Bruchez et. al 1996; Chan and Nie 1998; Clark et al. 1999; Li et al. 1999; Murray et al. 1995; Mirkin et al. 1996; Shenton et al. 1998; Taleb et al. 1997, 1998). These biochemically modified nanoparticles have different surface properties that provide new opportunities for their effective applications of nanoparticles

in a wide variety of fields (Chang et al. 1994; Chan and Nie 1998; Hari 1999; Kobayashi and Martin 1999Martin and Mitchell 1998). Recently, semiconductor nanocrystals (quantum dots) have been functionalized to couple biomolecules for bio-labeling (Bruchez et al. 1998; Chan and Nie 1998). Nanoparticles with biocompatible surfaces are useful for a variety of applications in biochemical analysis, such as biosensors and biomarkers.

Of the many techniques to prepare nanoparticles, the water-in-oil microemulsion (W/O microemulsion) is one the most widely used methods to prepare nanomaterials of small size. (Chang et al. 1994; Li et al. 1999; Shiojiri et al. 1998; Stathatos et al. 1997). In this method, reversed micelles are formed; water nanodroplets are formed in an organic medium, and used as nanoreactors for the formation of nanoparticles. The water/oil ratio can be carefully adjusted to control the particle size. Particles prepared by the reverse microemulsion method show good promise in size control and further miniaturization.

Silica based solid supports have been used effectively for the immobilization of various biomolecules such as enzymes, proteins, DNA etc (Davis 1997; Kreuter 199; Kar and Arnold 1992; Wang and Arnold 1992). It has been proven to be an excellent substrate suitable for many surface immobilization mechanisms, and a rich database has been developed. Using the various methods biomolecules have been immobilized on silica surfaces for applications ranging from biosensors to interfacial interaction studies. There is a rich database developed for silica surface modification. By combining the size advantage of nanoparticles and the ease of surface modification of silica, one expects that nanometer scale biosensors could be prepared. Nevertheless, there has been limited research work on the development of nanoparticle-based biosensors or biomarkers. Even

though there are various types of polymeric nanoparticles commercially available for biochemical applications (Bangs Laboratories Inc.), there exist limitations that restrict their applications as biosensor arrays or individual biosensors. The polymeric nanoparticles have a severe self-aggregation in biological media. Also they have a wide size distribution. As a result of these shortcomings, they have not been used effectively for sensitive bio-analytical measurements.

In this chapeter we describe novel silica nanoparticle based biomolecule immobilization demonstrating their biological activities for the development of potential biosensors and also their applications as biomarkers. The material, silica is well studied and proven to be a unique material for the present applications. Of the many methods, we have employed two simple approaches for the preparations of silica nanoparticles, an aqueous solutions reaction (Stober and Fink 1968) and water-in-oil microemulsions, for the preparation of uniform silica nanoparticles, including pure silica nanoparticles and dye-doped silica nanoparticles.

Also this chapter will show that silica based nanoparticles are better biocompatible solid supports for enzymes than polystyrene microspheres. We have demonstrated the biochemical funtionalization ability of the silica nanoparticle with two different enzymes, glutamate dehydrogenase (GDH) lactate dehydrogenase (LDH). These enzymes are involved in similar enzymatic reaction with their co-substrates glutamate and lactate, respectively (Hu and Wilson 1997; Mascini et al 1985). Using the pure silica nanoparticle synthesis method, we were able to add a fresh layer of silica on a flat silica plate as well as an assembly of nanoparticles. This technique has provided more surface area with a larger amount of pure silica content. Commercially available ordinary

microscopic slides with 64% silica content can now be modified to obtain more surface area with large amount of pure silica content. This approach is much less expensive than buying pure silica plates. The more biomolecules on the surface of the flat silica plate, the higher the sensitivity. It is thus quite reasonable that the high silica content surface is a much better support for the covalent immobilization of a large amount of biomolecules.

Here we also report a novel silica nanoparticle based membrane dye prepared by the W/O microemulsion technique. The dye molecule is a complex of ruthenium ion and bipyridyl, (Tris(2,2'-bipyridyl)dichlororuthenium(II)hexahydrate, Rubpy). The highly luminescent water-soluble dye becomes water insoluble when doped inside the silica network. Using these dye-doped nanoparticles we have modified the outside silica surface of the nanoparticles in such a way that they can bind with a cell membrane. To demonstrate the functionality of the dye-doped nanoparticles we have used PTK2 cells and leukemia cells for staining. Our result show that dye doped nanoparticles can efficiently stain cell membranes.

3.2 Experimental Section

3.2.1 Materials

Lactate dehydrogenase (LDH) from hog muscle (550 units/mg) and glutamate dehydrogenase (GDH) from beef liver (120 units/mg) were purchased from Roche Molecular Biochemicals (Germany). Lactate and glutamate were purchased from Sigma Chemical Co. (St. Louis, MO). Nicotinamide adenine dinucleotide (NAD^+) was purchased from Acros Organics (Fairlawn, NJ). Water soluble 1-[3-(Dimethylamino)propyl]-3-ethylcarbodiimide hydrochloride (WSC), Tris(2,2'-bipyridyl) dichlororuthenium(II) hexahydrate (RuBpy), tetraethylorthosilicate (TEOS), lauroyl

chloride and succinic anhydride were purchased from Aldrich Chemical Co. (Milwaukee, WI). Trimethoxysilylpropyldiethylenetriamine (DETA), a silanization reagent was purchased from United Chemical Technologies (Bristol, PA). All other chemicals were of analytical reagent grade. Distilled deionized water (Easy pure LF) was used for the preparation of all solutions. Commercial microspheres were purchased for comparison experiments with the nanoparticles produced in tour lab. Carboxylate modified approximately 1-1.5 μm in size were obtained from Bangs Laboratory. We used the company's recommended protocol to immobilize the enzyme.

3.2.2 Apparatus

Emission spectra was recorded on the Perkin Elmer Spectrofluorometer, model LS50B. The size of the silica nanoparticles was measured by the Hitachi Transmission Electron Microscope (TEM). The growth of the silica nanoparticles onto the coverslips were confirmed by the Scanning Electron Microscopy (SEM). Optical and fluorescence images of the dye-doped silica nanoparticles were taken using an inverted fluorescence Microscope (Olympus, Japan).

3.2.3 Nanoparticle Synthesis

Synthesis of the pure silica nanoparticles was carried out following the Stober synthesis (Stober and Fink 1968). 5.0 ml of ethanol (95% v/v) was added to a conical flask and mixed with 100 μl of TEOS. The flask was then cooled to $0^{o}C$ and placed floating in an ice cooled ultrasonicator bath. 5.0 ml of ammonium hydroxide (NH_4OH, 28-30 wt %) was added to the solution while ultrasonicating. After 1 hour of sonication, the nanoparticles were centrifuged out of solution, and were washed thoroughly (5-6 times) with both water and acetone, and finally air-dried.

Pure silica nanoparticles were grown onto a flat silica plate through the Stober synthesis. Flat silica plates were cleaned by immersion into a solution of HCl/MeOH for 30 minutes. Subsequently the cleaned plates were placed inside the conical flask containing 5.0 ml of ethanol (95% v/v) with 100 μl of TEOS. The flask was then cooled to 0°C and placed floating in an ice cooled ultrasonicator bath. 5.0 ml of ammonium hydroxide (NH_4OH, 28-30 wt %) was added to the solution while ultrasonicating. After 1 hour of sonication, the flat silica plates were removed from solution and placed in a beaker of deionized water and acetone and ultrasonicated to remove any physically absorbed nanoparticles. This procedure was repeated 2 to 3 times.

The dye-doped particles were synthesized using the water-in-oil microemulsion [Triton X-100/cyclohexane/n-hexanol (4.2:1:1 v/v)/water] technique. RuBpy was chosen as the dye in this specific application. The water to surfactant molar ratio was 10 and the final dye concentration in the mixture was 0.1 M. TEOS and NH_4OH were used for the silica particle synthesis with volume ratio of TEOS to NH_4OH of 1.7. The dye-doped nanoparticles were isolated from the microemulsion with acetone.

3.2.4 Nanoparticle Characterization

Silica nanoparticles were characterized by the TEM and SEM measurements. TEM images of the dye-doped silica particles show that the particles are 60 nm in size and uniform. Nanoparticle deposited coverslips were characterized by SEM. The size of the pure silica particles is in the range of 100-120 nm. Fluorescence emission spectra show that the dye-doped particles have characteristic bright red emission at 595 nm when excited at 450 nm.

3.2.5 Silica Nanoparticle Surface Modification

Pure silica nanoparticles they were added to a solution of silanization agent. Silanization of the particles were performed by immersion in freshly prepared 1% (v/v) solution of distilled DETA and 1mM acetic acid for 30 minutes at room temperature (23°C). The DETA modified particles were thoroughly rinsed with deionized water and ultracentrifuged to remove excess DETA. The silanized particles were then treated with 10% succinic anhydride in dimethylformamide solution under an argon atmosphere and stirred for 6 hrs. The resulting carboxylate modified particles were washed with deionized water and centrifuged two to three times. Carboxylate modified particles were then added to an activation buffer solution (pH 4.6, acetic acid-sodium acetate) with 1% WSC and stirred for 15 mins. Activated nanoparticles were then washed in PBS buffer (coupling buffer, pH 6.8) thoroughly. Figure 3-1a shows the surface modification procedures for the pure silica nanoparticles.

3.2.6 Enzyme Immobilization

LDH and GDH solution with concentration of 1×10^{-5} M were prepared in 0.1 M PBS at pH 6.8. The nanoparticles were immersed in the LDH/PBS or GDH/PBS solution for 23 hours at room temperature to allow the enzymes to be immobilized on the surface (Figure 3-1a). The particles were subsequently washed and ultrasonicated to remove any physically adsorbed enzyme molecules on the silica surface. The particles were either used immediately for testing or stored in a PBS buffer at 4°C for later use.

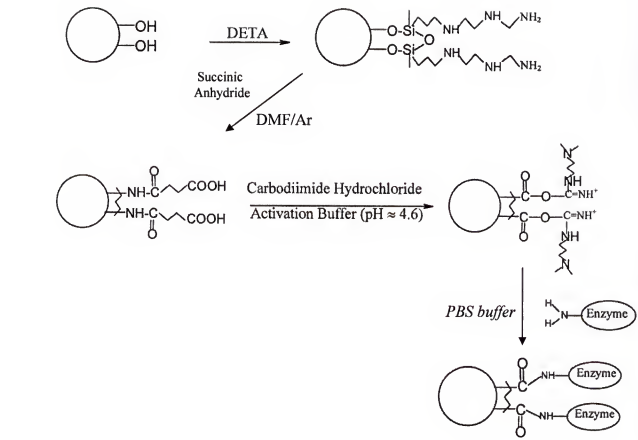

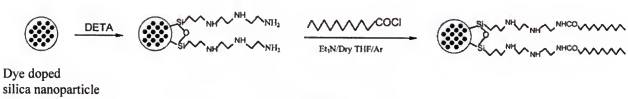

Figure 3-1. Surface modification of pure silica nanoparticles for enzyme immobilization (a), and surface modification of the dye doped silica nanoparticles for membrane probing (b).

3.2.7 Biochemical Modification of Dye-Doped Silica Nanoparticles

The biological membrane consists mainly of phospholipid bilayers. The interior of the membrane is hydrophobic in nature. Therefore, membrane probes should be designed in such a way that it can bind to the hydrophobic part of the membrane. With this knowledge, we have modified the silica surface of the dye-doped nanoparticles. The silica surface was silanized by DETA as described earlier. The amine-functionalized particles were then treated with lauroyl chloride in dry tetrahydrofuran in an argon atmosphere for 6 hours (Vogel 1978 (Figure 3-1b). The presence of the amide group (-NHCO-) was confirmed by the IR spectroscopy (Figure 3-2). These functionalized nanoparticles, used as a membrane probe, were then tested with PTK2 cells and leukemia cells. The cells were obtained in a dish with approximately 2.0 ml culture medium. 20 μl of functionalized dye-doped particles in (1% (v/v) DMSO was added to the cell dish and incubated for 6 hours. After thoroughly rinsing the cells with PBS buffer (pH 6.8), fluorescence images were taken.

3.2.8 Spectroscopic Measurement

Preliminary spectroscopic measurements were done on the pure silica nanoparticles to determine whether the nanoparticles were functionalized with enzyme. Emission spectra were recorded on an LS50B Perkin Elmer Spectrofluorometer. Measurements of the GDH activity were carried out in a 3 ml cuvette. The substrate solutions of glutamate with 2 mM NAD^+ in a PBS buffer (pH 6.8) were used for the enzymatic activity study. A known amount of the enzyme-immobilized nanoparticles was added to the cuvette. The reaction was allowed to take place and, upon 350 nm excitation, NADH fluorescence was

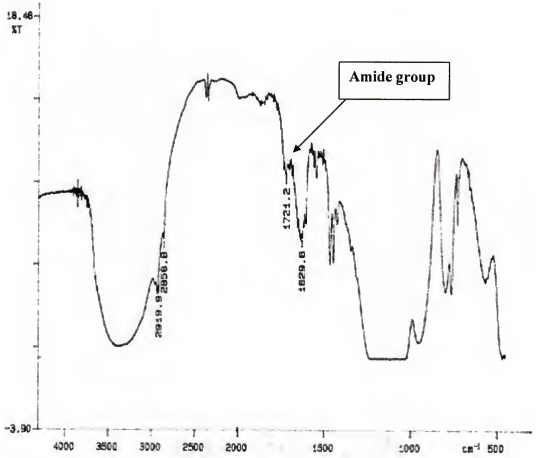

Figure 3.2. IR spectra of the lauroyl derivatized membrane dye

monitored at 465 nm with time. All measurements were carried out at room temperature (23°C).

3.3 Results and Discussion

3.3.1 Uniform Silica Based Nanoparticles

Three different types of silica nanoparticles of uniform sizes have been prepared. The first type of nanoparticles prepared in this work is the dye-doped silica particles. The silica nanoparticle with membrane dye were prepared by the W/O microemulsion technique. The highly luminescent water-soluble dye, Rubpy, becomes water insoluble when doped inside the silica network of the nanoparticles. TEM image of the nanoparticles show that the particles are 62 nm in size, and their size distribution is extremely uniform with a standard deviation of less than 2% (Based on a calculation done on 30 nanoparticles shown in Figure 3-3). Fluorescence emission spectra show that the dye-doped particles have characteristic bright red emission at 595 nm when excited at 450 nm. The second type of nanoparticles is the pure silica nanoparticles. They have also been prepared with similar sizes and uniformity in size distribution. The third and final type of nanoparticles prepared are 100-120 nm in diameter and have been grown directly on a glass slide (Figure 3-4). This third type of nanoparticle is the basis of the 2nd generation two-dimensional sensor due to the silica surface area enhancement on the flat silica plate.

3.3.2 Particle Surface Modification

Microspheres purchased from Bangs laboratories were already modified with carboxylate groups. Lactate dehydrogenase and glutamate dehydrogenase was covalently

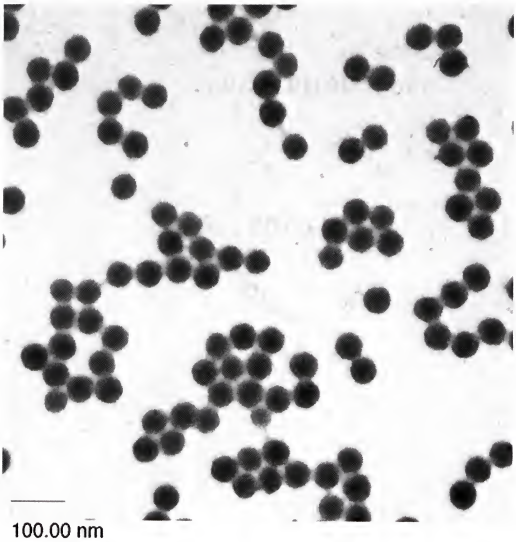

Figure 3-3: TEM image of the dye doped silica nanoparticles. The Particle sizes was determined to be about 60 nm. The relative standard deviation in size distribution is 1.6%

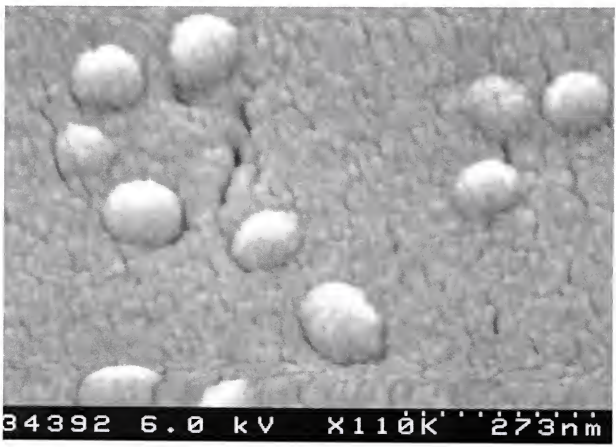

Figure 3-4: SEM Image of pure silica nanoparticles grown onto a flat silica plate (FSP).

immobilized onto these polystyrene based microspheres following the company's protocol.

The freshly prepared silica nanoparticles were functionalized with enzymes or membrane binding reagents. The nanoparticles prepared in this work all have a surface that can be functionalized. These surfaces can be modified with different reagents for a variety of applications. Two major modification mechanisms were used in this work as shown in Figure 3-1. Both of these schemes rely on the creation of primary amine functional groups onto the particle silica surface. Fluorescamine, which becomes highly fluorescent upon reacting with primary amines, was used to test the efficiency of the silanization. The fluorescamine assay was used for the monitoring of the first two steps in both immobilization processes. We observed a positive fluorescamine response in the first step confirming that DETA was successfully used for the silanization of the nanoparticles, leaving free primary aliphatic amine groups on the surface. After the succinic anhydride treatment in Figure 1a, nanoparticles were carboxylated and a negative fluorescamine response confirmed no free amine groups were left on the nanoparticle surfaces. Once the nanoparticles were carboxyl modified, the particles were used for the immobilization of enzyme molecules (LDH and GDH). Similarly, in figure 3-1b, we show that the amine-functionalized particles can also be linked with a membrane functional group. We treated the nanoparticles with lauroyl chloride in dry tetrahydrofuran in the presence of an argon atmosphere for 6 hours. Lauroyl-derivatized nanoparticles became poorly soluble in water because of the presence of hydrophobic lauroyl groups on their surface. They tended to aggregate in aqueous solution. These particles showed negative fluorescamine response indicating that amine groups on the

particle surfaces had been consumed. It is expected that the lauroyl group can bind to the lipid bilayer of the cell membrane. It is clear that the nanoparticles can be functionalized with desired biomolecules by attaching the required functional groups on their surfaces.

3.3.3 Enzyme Immobilized Nanoparticles for Glutamate and Lactate Analysis

Lactate dehydrogenase and glutamate dehydrogenase were both covalently immobilized onto individual pure silica nanoparticles prepared in this work. The immobilized enzyme molecules display excellent enzymatic activity. The enzymatic activity of the immobilized LDH/GDH was monitored by following the reaction between lactate/glutamate with NAD^+ when the LDH/GDH immobilized nanoparticles were added to the substrate solution as shown in Figure 3-5. The fluorescent signal from the product NADH was measured as a function of reaction time.

The detection limit for glutamate by the GDH immobilized nanoparticles was determined when 10 μl of a GDH immobilized nanoparticle suspension was added to a 3 ml of substrate solution. A series of glutamate solutions were tested as shown in Figure 3-6. The detection limit was determined to be 0.5×10^{-6} M. Similar results were obtained with LDH for the detection of lactate. The detection limit for the enzyme immobilized nanoparticles can not be directly compared with results obtained by other means (Cordek et al. 1999; Wang and Arnold 1992) as the exact amount of enzyme molecules immobilized on the nanoparticle surfaces is not known. However, it can be used as a way to compare relative capacity of different nanoparticle probes prepared with similar procedures.

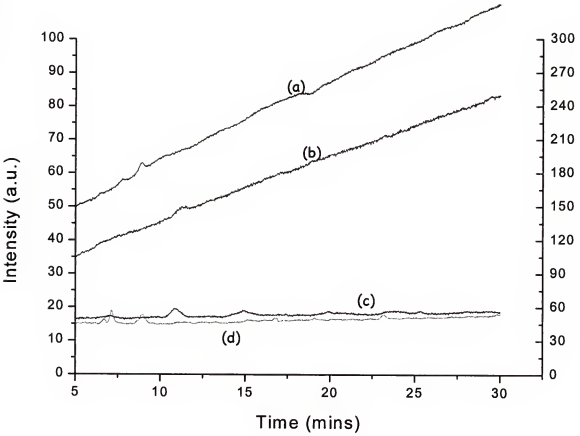

Figure 3-5. Comparison of LDH and GDH immobilized nanoparticles vs. microspheres. NADH was monitored over time as a product of the enzymatic reaction catalyzed by the enzyme molecules immobilized on the surface of the particles. (a) GDH nanoparticles, (b) LDH nanoparticles, (c) LDH microspheres, (d) GDH microspheres.

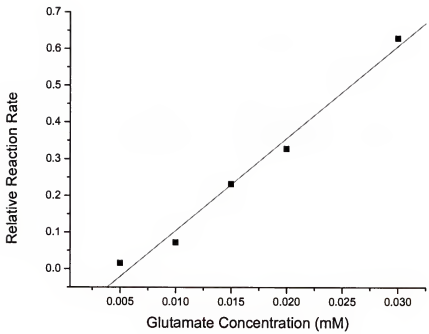

Figure 3-6. Effect of glutamate concentration on the relative enzymatic reaction rate of GDH immobilized nanoparticles. Based on this curve, the detection limit of glutamate has been determined. 10 μl GDH nanoparticle (.1mg particle/ml particle concentration) is used and the NAD^+ concentration is 2mM. The reaction was carried out at pH-6.8 PBS buffer.

3.3.4 Enzyme Immobilized Silica Nanoparticles for 2nd Generation 2D Sensor

Pure silica nanoparticles have been grown onto a flat silica plate using the Stober synthesis (Stober and Fink, 1968). During the Stober synthesis pure silica nanoparticles are formed. By cleaning the flat silica plates with an HCl/MeOH combination, all silica atoms were made available for polymerization to form a fresh silica layer of silica and also nanoparticles. As discussed in earlier chapters the silica content of glass plates are approximately 64%, so the available silanol groups for enzyme modification are limited. The addition of a fresh layer of silica and silica nanoparticles thus increases the amount of silica available for surface modification allowing more enzymes to be immobilized and and increasing the detection sensitivity for lactate and glutamate.

Previous detection limits for the two-dimensional sensor which is based on the commercial flat silica plate is in the low micromolar range for lactate and glutamate analysis. Figures 3-7 and Figure 3-8 confirms that the placement of the commercial flat silica plates into the Stober synthesis and the addition of a fresh layer of silica allow for a lower detection limit due to a higher amount of immobilized enzyme. The detection limit of this 2nd generation two-dimensional sensor has been lowered by an order of magnitude. The new detection limit of 40 nanomolar for neurochemicals analysis thus enhances our ability to detect extracellular neurochemical release from samples and was used as the primary sensor for the detection of lactate and glutamate from tissue slices.

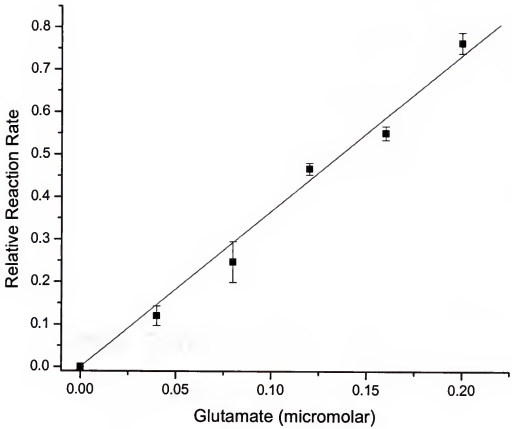

Figure 3-7. Calibration curve for glutamate analysis under optimal conditions

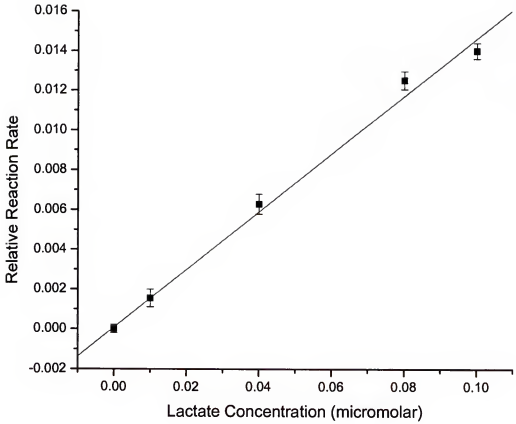

Figure 3-8. Calibration curve for lactate under optimal conditions

3.3.5 Lifetime and Sensor Response for Glutamate and Lactate

Biosensor lifetime is an important factor to consider especially when one has to consider that these biosensor are based on the use of biological active components. The lactate and the glutamate sensors were stored in PBS buffer, pH 6.8 when not in use. The stability of the enzyme-immobilized particles was based on a daily response measurement. Both the lactate and the glutamate sensors showed similar results for their stability over a two-week period (Figure 3-9). 93% of their enzymatic activities remained after a two week period, with daily fluctuations of 4%. The sensor began to degrade after a two-week period, which is most likely due to the natural degradation process of enzymes. For most enzyme sensors the time that the sensor needs to achieve a steady state response after the introduction of a sample is known as the response time. We define the response time for the enzyme sensors as the time required for the enzyme-immobilized nanoparticles to generate sufficient NADH for the detection. We used the standard deviation of the baseline to estimate the response time of the sensor. The nanoparticles have response times in the millisecond range. The fast response time of the sensors is due to the direct immobilization of the enzyme molecule onto the nanoparticle surface which allows for easy access to the active center of the enzyme.

3.3.6 Comparison Between Enzyme Immobilized Microspheres and Nanoparticle

Nanoparticles prepared in this work were directly compared with commercially available microspheres 0.5 μm in diameter. We used the same amount of enzymes for the immobilization on the same amount of particles (nano and micro). We then took an equal amount of particles for the same enzyme assay and compared their enzymatic activities. In order to compare them fairly, we used optimized procedures for the

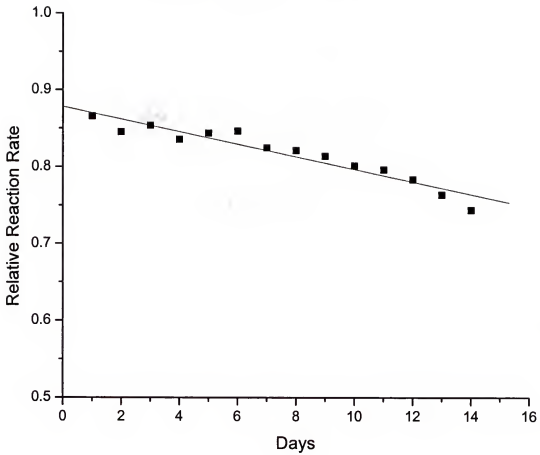

Figure 3-9: Response to 4mM glutamate and 1mM NAD^+ as function of the 2D biosensors age.

immobilization of LDH (or GDH) on both particles. We took 1 mg of each type of enzyme-immobilized particles to run the enzyme assay. Microspheres purchased from Bangs laboratories were already modified with carboxylate groups. Lactate dehydrogenase was covalently immobilized to these polystyrene-based microspheres following the company's protocol. Enzyme immobilized microspheres were always dispersed by ultrasonication before use. The enzymatic activity was monitored, as shown in Figure 3-5c and d. It was clear that the microsphere-based probes have higher sensitivity, about one order of magnitude lower than that of the nanoparticle-based probes. This applied to both LDH and GDH nanoparticles. This is most likely due to the fact that the nanoparticles have a larger surface area than the microspheres; therefore more enzyme molecules are attached to the nanoparticle surface which gives higher sensitivity. Moreover, the commercially available microspheres are difficult to handle. Due to the polymeric composition of the nanoparticles, they have a tendency to agglumerate, resulting in a higher fluctuation in their optical signal as shown in Figure 3-5c and d. In addition, the microspheres tended to stick to the centrifuge tubes, both glass and plastic, during centrifugation and ultrasonication. These problems were not observed with the silica nanoparticles prepared in this work.

3.3.7 Dye-Doped Nanoparticle for Modification and Application as a Membrane Probe

We have prepared particle suspension (5mg/ml) in dimethylsulfoxide (DMSO) solution by ultrasonication. To test the functionality of the lauroyl-derivatized dye particles as membrane-probes two types of cells were employed: PTK2 cells and leukemia cells. PTK2 cells were obtained in a dish with approximately 2.0 ml culture medium. 20 μl of dye doped particles in (1% (v/v)) DMSO was added to the cell dish and

incubated for 6 hours. After washing with the PBS buffer (pH 6.8) images were taken by the fluorescence microscope. Figure 3-10a and Figure 3-10b show both optical and fluorescence images of two different PTK2 cell dishes. The optical image (left panel) corresponds well to the fluorescene (right panel). Thus results are very reproducible. Leukemia cells (mononuclear lymphoid cells, about 2 millions/ml) were obtained as a suspension in cell medium. In a similar way 50 μl of cell suspension was diluted with 1ml PBS buffer and treated with the dye-doped particles. The particles were ultrasonicated before adding to the cell medium. Figure 3-11a shows the optical and fluorescence images of the leukemia cells. This result shows that lauroyl derivatized dye-doped nanoparticles can bind very well to the cell membrane. We also observed particle aggregation when they were added to the cell medium. Proper washing is needed to remove unbound particles. Our control experiment with non-functionalized dye-doped nanoparticles did not show any staining (Figure 3-11b). Presently we are optimizing various parameters including cell viability for the efficient cell staining. We are also studying the photostability, dye-distribution and the effect of the quencher on the dye doped silica nanoparticles, and their use to recognize inter- and intra- cellular antigen (by the cellular uptake mechanism) via antibody-antigen recognition principle. All these results will be communicated shortly.

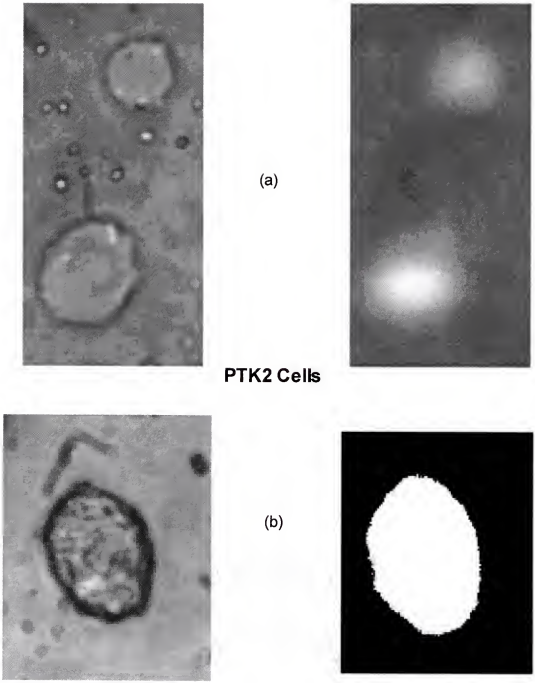

Figure 3-10. Cell staining by optical and fluorescence microscopy: left panel, optical images of PTK2 cell; right panel, fluorescence image of PTK2 cell. After staining with the dye-doped nanoparticles containing membrane functional groups, the cells show strong fluorescence

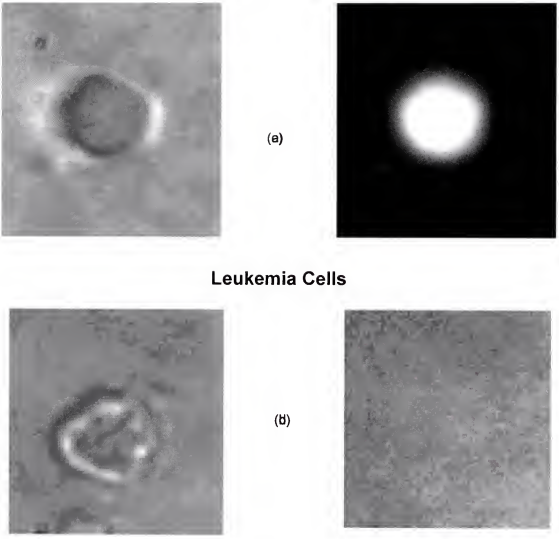

Figure 3-11. Cell staining by optical and fluorescence microscopy: left panel of image A optical images of leukemia cells; right panel of image A shows fluorescence image of leurkemia cell; after staining with the dye doped nanoparticles containing membrane functional group, the cells have strong fluorescence. Right panel of image B is the control after washing with non-functionalized particles.

3.4 Conclusion

Two different types of silica nanoparticles of uniform sizes have been synthesized and biochemically modified for specific function. They can be functionalized with enzyme molecules and biomembrane probes. The surface modification of the nanoparticles has added unique biofunctionality for these nanoparticles. We have used lactate dehydrogenase and glutamate dehydrogenase for enzyme immobilization onto the nanoparticles. The immobilized nanoparticles have shown excellent enzymatic activities and excellent detection capability. Direct comparisons with commercially available microspheres have shown that the nanoparticles have at least one order of magnitude better enzymatic activities due to larger surface areas for enzyme immobilization.

Also pure silica nanoparticles have been polymerized onto the flat silica plate for the fabrication of the 2nd generation 2D enzyme biosensor. The biosensor has shown enhanced detection capabilities down to 40 nanomolar. The increase in analytical detection capabilities has shown to be an order of magnitude better than the original 2D enzyme biosensor.

To further demonstrate the nanoparticle's bio-applicability, we have also used dye-doped silica nanoparticles as biomarkers for cell staining. The dye molecules inside the nanoparticles are stable, and there is no direct contact between the dye molecules and their surrounding environments that could affect their optical properties. This work demonstrates and easy approach of combining nanotechnology with biomolecules for biochemical analysis and biotechnology applications.

CHAPTER 4
ASSEMBLY OF NANOPARTICLES FOR BIOENHANCED NANOMATERIAL

4.1 Introduction

Continuous exploration of new applications of nanoparticles and related nanomaterials is indispensable for the continual development of the science and technology of nanomaterials (Ha et al. 2001). The assembly of nanomaterial in the form of thin films and the organization of nanoparticles into highly ordered arrays on various supports has been the focus of intense research during the last three decades as the ability to do so have many implications in material science and biotechnology (Lee et al. 1996; Ulman 1996). As modern science is evolving away from the manipulation of sets of individual molecules toward the description and manipulation of systems of molecules, the sizes of building blocks subjected to be assembled on substrates are currently experiencing an increase from subnanometer to nanometer scale (Kulak et al. 2000; Whitesides and Ismagilov et al. 1999). It is therefore necessary to develop novel methods to organize these materials in the form of highly ordered single layer to multilayer arrays on substrates. Such methods will also be of great use in the development, application and diversification of nanotechnology.

Currently a large amount of efforts has been placed into generating thin film layers of metallic and silica particles for characterization of surface properties that may be exhibited once arranged into an array (Caruso et al. 2001; Jeng et al. 2003; Kachan and Ponyavina 2002; Ping et al. 2001Sbrana et. al., 2002; Rutnakornpituk et al. 2002; Yu et

al. 2003). However, despite the availability of a large number of methods to prepare monolayers of nanoparticles on various substrates, the methods that are available for the covalent attachment of these materials are not as accessible. Yoon and co-workers first reported methods in which to covalently attach zeolite crystals to a variety of substrates (Choi et al.. 2000; Ha et al. 2001; Lee et al. 1996; Lee et al. 2001; Kulak et al. 2000; Park et al. 2002; Um et. al 2002). This covalent chemistry can be easily applied to nanomaterials including pure silica nanoparticles.

Within the specialized areas of nanotechnology, the fabrication and surface modification of nanoparticles whether metallic (gold) or pure silica particles for biomedical application has been an important and relevant research area for us. There have been recent advances in silica nanoparticle surface modification (Andres et al. 1996; Chan and Nie 1998; Li et al. 1999; Mirkin et al. 1996; Murray et al. 1995; Shenton et al. 1998; Taleb et al. 1997). The pure silica nanoparticle's biocompatible surface allows them to be useful for a variety of applications for biochemical analysis (Santra et al. 2001; Qhobosheane et al. 2001; Tapec et al. 2002). The utilization of individual nanoparticles for biosensing and biomarking has been a promising area of nanotechnology and offers many advantages and displays unique properties. Similarly, assembled nanomaterials have its own properties, but yet and still the ease of removal of the particles from the substrate inhibits the utilization of the properties that may be exhibited upon assembly. There is a need for covalent assembly of nanoparticles for bioenhanced nanomaterials.

Due to the similar functional groups that are shared between the zeolite crystals and pure silica nanoparticles, we were able to adapt the zeolite chemistry and attach pure silica nanoparticles to a glass substrate. In this chapter we discuss the capabilities of

synthesizing nanoparticles and covalently assembling them on a 2D glass substrate. Also we show that the pure silica nanoparticles can be controllably assembled thru the use of photolithography. Finally, the covalently assembled nanoparticles can be modified and used as a biosensor for possible bio-applications.

4.2 Experimental Section

4.2.1 Materials

Glutamate dehydrogenase (GDH) from beef liver (120 units/mg) was purchased from Roche Molecular Biochemicals (Germany).Tetramethyl rhodamine labeled streptavidin was purchased from Molecular probes (Eugene, Oregon). Glutamate was purchased from Sigma Chemical Co. (St. Louis, MO). Nicotinamide adenine dinucleotide (NAD^+) was purchased from Acros Organics (Fairlawn, NJ), (3-chloropropyl)trimethoxysilane (CPTMS), n-propyl trimethoxysilane (NP-TMS), tetraethylorthosilicate (TEOS), lauroyl chloride, anhydrous toluene and succinic anhydride were purchased from Aldrich Chemical Co. (Milwaukee, WI). Trimethoxysilylpropyldiethylenetriamine (DETA), a silanization reagent was purchased from United Chemical Technologies (Bristol, PA). Photoresist plates were purchased from Nanofilm (West lake, CA).All other chemicals were of analytical reagent grade. Distilled deionized water (Easy pure LF) was used for the preparation of all aqueous solutions.

4.2.2 Preparation of Pure Silica Nanoparticles.

Synthesis of the pure silica nanoparticles was carried out following the Stober synthesis (Stober and Fink 1968). 5.0 ml of ethanol (95% v/v) was taken in a conical flask and mixed with 100µl of TEOS. The flask was then cooled to 0^oC and placed

floating in an ice cooled ultrasonicator bath. 5.0 ml of ammonium hydroxide (NH_4OH, 28-30 wt %) was added to the solution while ultrasonicating. After 1 hour of sonication, microparticles were centrifuged out of solution and washed thoroughly (5-6 times) with both water and acetone, and finally air-dried.

4.2.3 Silica Nanoparticle Characterization

Silica nanoparticles have been characterized by a Hitachi Transmission Electron Microscope, model H7000. Optical and fluorescence images of the assembled silica nanoparticles were taken by an inverted Olympus fluorescence microscope (model IX708F).

4.2.4 2D Assemblies of Silica Nanoparticles

Pure silica nanoparticles with an average size of a few 100 nanometers were washed and cleaned using a solution of acetone and water to activate available silanol (-OH) groups for covalent attachment and then dried. A batch of 1-3 flat silica plates was used in a single 2D assembly synthesis. The flat silica plates (FSPs) were first cleaned by immersion in a solution of concentrated HCl/MeOH (1:1) for 30 minutes. They were then rinsed in deionized water and submerged in concentrated H_2SO_4 for 30 min. Activated flat silica plates where immersed into a solution containing toluene (20 ml) and CPTMS (0.1M) and refluxed under argon for 3 hours. Pure silica nanoparticles (2.0 mg) were then added to the solution containing the modified flat silica plates. Both pure silica nanoparticles and surface modified flat silica plates were refluxed for an additional 3 hours. To ensure that only covalently attached nanoparticles remained, flat silica plates were washed and sonicated in toluene. A schematic of synthesis procedure is shown in Scheme 4-1.

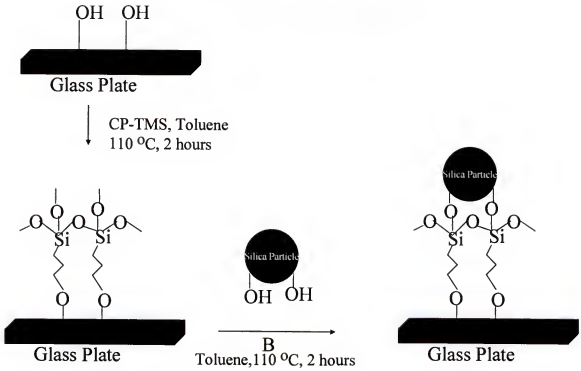

Scheme 4-1: Schematic illustration for the covalent attachment of microparticles onto a 2D glass substrate.

4.2.5 Controlled Assembly of Nanoparticles.

The formation of patterned nanoparticle assemblies was done with the use of photoresist borosilicate plates. Activated photoresist glass plates were exposed to UV light with a photomask on top of the plate. After exposure to UV light, photoresist plates were placed in chrome etch solution to remove the chrome layer and make glass available for surface modification. Patterned photoresist plates were immersed into a solution of concentrated HCl/MeOH (1:1) for 30 minutes followed by immersion in a solution of H_2SO_4 (30 minutes) to activate the silanol groups. The activated glass plate was then placed into a toluene and CPTMS solution and refluxed for 3 hours. Surface modified photoresist plates were then washed in toluene, and placed into a solution of toluene (20 ml) and nanoparticles(2.0 mg) and again refluxed for another 3 hours. Nanoparticle assembled plates were then placed in a solution of acetone/water to remove photoresist followed by a chrome etch solution to remove the chrome layer. Glass plates were washed and sonicated in toluene to ensure that only covalently attached particles were present.

4.2.6 Surface Modification of Nanoparticle Assembly.

To demonstrate the biosensing capabilities of the assembled nanoparticles, we have attached the enzyme glutamate deyhdrogenase (GDH) to the pure silica nanoparticles. Silanization of the nanoparticle assembly was performed by immersion in a freshly prepared 1% (v/v) solution of distilled DETA and 1mM acetic acid for 30 minutes at room temperature (23°C). The DETA modified silica nanoparticles were thoroughly rinsed with deionized water to remove excess DETA. The silanized particles were then treated with 10% succinic anhydride in dimethylformamide solution under an argon

atmosphere and stirred for 6 hours. The resulting carboxylate modified particles were washed with deionized water and centrifuged two to three times. Using the Bangs Labs (Bangs laboratories Inc.) protocol the carboxylate modified particles were functionalized with enzyme. A GDH solution with concentration of $1x10^{-5}$ M was prepared in 0.1 M PBS at pH 6.8. The nanoparticle assembly was immersed in the GDH/PBS solution for 23 hours at room temperature to allow the enzymes to be immobilized on the surface. The nanoparticle assembly was subsequently washed and ultrasonicated to remove any physically adsorbed enzyme molecules on the silica surface.

4.3 Results and Discussion

4.3.1 Nanoparticle Assembly Characterization.

The Stober synthesis can yield particles in the range of submicrometer to nanometer. These nanoparticles have been characterized with microscopy and spectroscopic methods. The assembly of pure silica nanoparticles has been characterized by SEM. Figure 4-1 shows the typical results of nanoparticle assembly onto a 2D glass substrate, a low concentration of particles was used to clearly show the covalent attachment of particles. To demonstrate the close packed assembly that can be attained from the synthesis procedure a high concentration of nanoparticles (0.1mg/ml) was used in the reaction (Figure 4-2).

4.3.2 Nanoparticle Array Density Studies.

The 2D assembly of nanoparticles with controlled density can offer many advantages that can not be obtained when generating thin films. The covalent attachment of the nanoparticles was based upon the addition of various amounts of pure silica

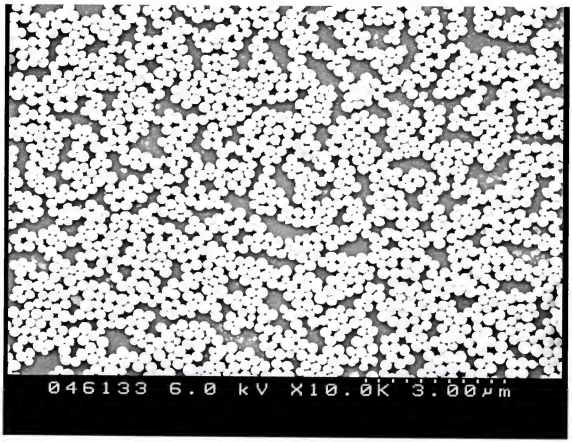

Figure 4-1. SEM images of microparticles covalently attached to glass slide A low concentration of microparticles was used in the synthesis to clearly show covalent attachment

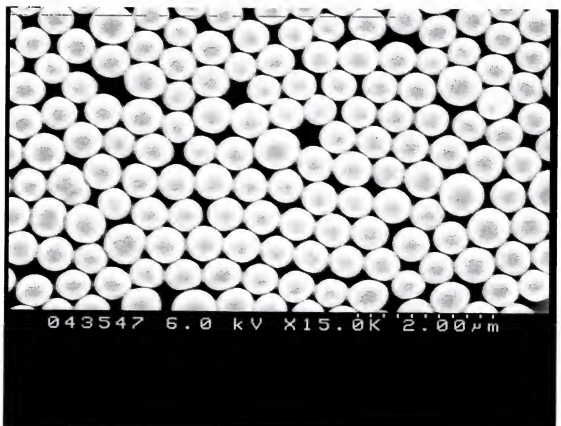

Figure 4-2. SEM images of a closed pack structure that can be obtained after the microparticle synthesis procedure.

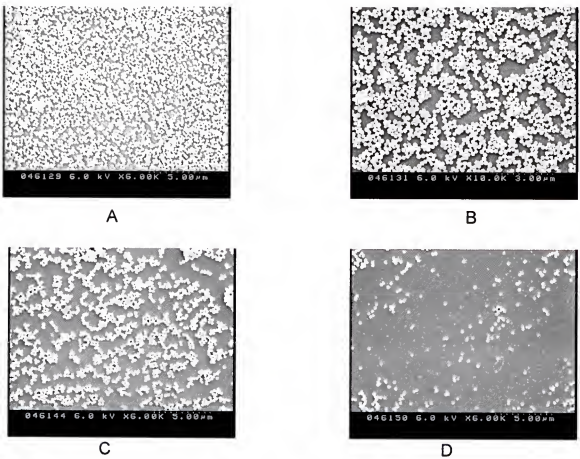

Figure 4-3. Density control experiments; A) 0.2g; B)0.08g; C) 0.04g; D)0.01g of microparticles used for synthesis.

nanoparticles ranging from 0-0.2 grams. Based on SEM results, we found that as the particle concentration in the reaction media increases the packing density increases linearly. The maximum packing density of the nanoparticles was found to occur when 0.2 grams of nanoparticles was added into the synthesis reaction. Higher concentrations of nanoparticles were used and the packing density remained the same. Figure 4-3 shows how varying the amount of pure silica nanoparticles to the reaction medium yields different surface coverage on the glass slide.

4.3.3 Localized Assembly of Nanoparticles.

The technology of photolithography has allowed the capability of controlling the fabrication of various patterns. The assembly of particles into ordered patterns can offer advantages over films of particles. The assembly of ordered patterns of nanoparticles can have future implications in biosensor development. These ordered assemblies may be functionalized with different sensing elements and allows for the capability of simultaneous detection of multiple analytes. To demonstrate localized covalent attachment of silica nanoparticles, photolithography was used to fabricate glass surfaces of circles and square patterns. The patterned borosilicate plates were allowed to proceed thru the same reaction procedure for the flat silica plates. The pure silica nanoparticles were able to attach to the areas which were activated. At the conclusion of the reaction, we found that the nanoparticles only attached in the circle and square areas of glass. Optical images of the patterned nanoparticle array were obtained by modifying the nanoparticle surface with tetramethyl-rhodamine labeled avidin. The dye labeled avidin was physically absorbed onto silica particles as shown in Figure 4-4. Avidin is a well known biomolecule that gives strong physical absorption to silica and has been utilized to

attach DNA and other biomolecules to the solid support structures for bioanalysis. The assembly of these nanoparticles in an ordered fashion offers the possibilities of multiple analyte modification and detection.

4.3.4 Enzyme Immobilized Nanoparticle Array for Glutamate Analysis.

Silica substrates have shown to be very good supports for biomolecule immobilization (Cordek et al. 1999; Fang et al. 1999; Ingersoll and Bright 1997; Pantano and Walt 1995). These immobilized biomolecules on silica substrates have been used for a wide range of applications including biosensing and biomarking. The 2D array of covalently attached nanoparticles has been modified with the enzyme GDH for the detection of glutamate. Glutamate is the primary neurotransmitter responsible for learning and memory. Glutamate dehydrogenase when in the presence of its substrate nicotinamide adenine dinucleotide (NAD^+) and glutamate undergoes a catalytic reaction to produce the fluorescent product NADH. Measurement of GDH activity was taken; Figure 4-5 shows a typical plot of the response that is given when the GDH immobilized nanoparticle array is in the presence of its co-substrates. These results show that the assembled microparticles can be used for bioanaylsis.

4.4 Conclusion

In conclusion, we have adopted covalent chemistry techniques for the two-dimensional assembly of pure silica nanoparticles. We have shown that by varying particle concentration it is possible to control the surface density of nanoparticles. With the use of photolithography we were able to localize and control the covalent attachment of the nanoparticles. Fluorophore labeled avidin and glutamate dehydrogenase were utilized to further show that after covalent attachment of the particles, the remaining

surface was available for biomodification and can possibly be used in the future for biosensing. In addition, the covalent attachment of particles in the nanometer range can further offer advantages that may not be possible with individual nanoparticles.

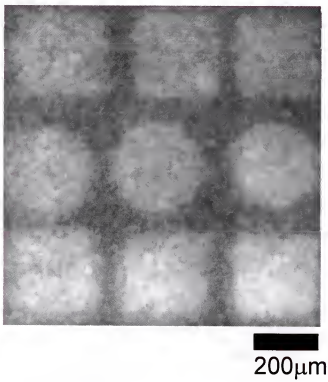

Figure 4-4. SEM image of the glass patterned with covalently bound silica microparticles modified with TMR-Avidin.

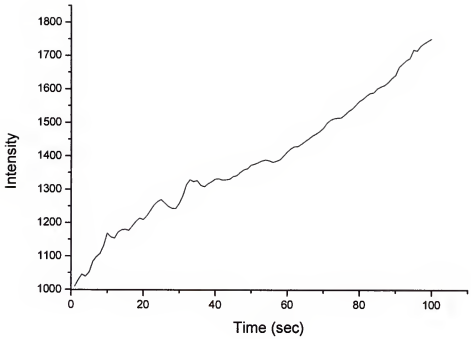

Figure 4-5. Response of GDH immobilized microparticle array. A standard testing solution of 4mM Glutamate and 1mM NAD^+ was used.

CHAPTER 5
A TWO-DIMENSIONAL IMAGING BIOSENSOR FOR THE MONITORING OF LACTATE RELEASE FROM BRAIN SLICES

5.1 Introduction

The determination of L-lactate is essential in clinical analysis for the diagnosis of lactate acidosis, which may be caused by anaerobic metabolism (Trettnak and Wolfbeis, 1989). Other diseases such as myocardial infarction, severe congestive heart failure and pulmonary edma are also associated with the lack or excess of lactate in blood or muscle (Mascini et al. 1984; Toffaletti 1989). In the brain, it has been reported that it is lactate, not glucose, which protects the neurons from apoptosis during ischemia and fuels the recovery of synaptic function from hypoxia (Hu and Wilson, 1997; Mascini et. al., 1985). Considerable efforts have been made regarding the development of L-lactate sensors for metabolite determination in body fluids, such as blood (Hu et al.; 1993 Schurr et al. 1997), saliva (Palleschi et al. 1991), and sweat (Fardnia et al. 1993; Mitsubayashi et al. 1994).

Current detection techniques for L-lactate have been spectrophotometric, fluorometric and electrochemical. Recently, a variety of L-lactate biosensors have been developed for *in vitro* and *in vivo* analysis (Cordek et al. 1999; Castanohn-Lobo et al. 1997; Liu and Tan 1999; Shimojo et al. 1993; Villamil-Fernandez et al. 1997). These sensors consist of microelectrodes (Castanohn-Lobo et al. 1997; Shimojo et al. 1993; Villamil-Fernandez et al. 1997) or fiber optical devices (Liu and Tan 1999). These sensors are able to monitor cellular events and study lactate release. However most

of these sensors are designed for single point measurements, i.e. monitoring one specific location at any given time. It is necessary to monitor a group of cells or a brain tissue in order to gain a complete understanding of many interesting cellular events. A precise, rapid, and spatially resolved determination of lactate among a group of cells and/or tissues is critically important for better elucidation of neurological mechanisms and the overall impact of a drug. Therefore, there is a great need for the development of imaging techniques for real-time monitoring of lactate release. A more encompassing view of cellular activity may thus be obtained where the release of lactate can be studied more effectively.

A two-dimensional (2D) biosensor has the capability for spatially resolved imaging (Bang and Tan, 1999; Lavine et al. 1998; Michael et al. 1998). This capability can either be used for multiple analytes or for spatially resolved imaging. There have been some efforts in 2D biosensor development for imaging (Bang and Tan 1999), while most of the 2D sensing has been centered on or intended for multiple analyte detection. For example, an array of optical fibers has been used in monitoring multiple genes (Michael et al. 1998), and a microwell array system (Lavine et al. 1998) has been used to create an electronic tongue. These biosensors have show advantages in analytical sensitivity and multiplexibility. However, they have not been used for monitoring spatially resolved events.

In this chapter, we will combine the imaging capability of a conventional optical/fluorescence microscope and the biochemical sensing capability of enzyme based biosensors to create a 2D imaging biosensor for the monitoring of lactate released from brain slices. The imaging biosensor is able to capture multiple points across a surface.

This optical biosensor is based on the immobilization of an enzyme, lactate dehydrogenase, on the surface of a flat silica plate. The immobilized enzyme molecules can catalyze a reaction between lactate and a weakly fluorescent NAD^+ to give a highly fluorescent product NADH:

$$\text{Lactate} + NAD^+ \xrightarrow{LDH} \text{Pyruvate} + NADH + H^+ \tag{4.1}$$

The production of NADH is monitored by an imaging system and is used for the analysis of lactate. In this chapter, we will describe the development and the application of this 2D biosensor for studies of lactate release from a mouse brain slice.

5.2 Experimental and Methods

5.2.1 Apparatus

The experimental set-up for the characterization of the 2D LDH sensor was based on an inverted Olympus fluorescence microscope (IX70-S8F). The set-up is shown schematically in Chapter 2, Figure 2-1. An intensified charged coupled device (ICCD) (Princeton, EEV 512x1024) was used for capturing images and for ultrasensitive analysis. The ICCD has the capability of imaging single molecules in solution and on a surface (Fang et. al. 1999). The radiation source for the excitation of NADH molecules was a 350 nm laser beam from an Innova Ar^+ laser (Coherent Laser, Santa Clara, CA). The layout of the set-up is similar to the microscope imaging system we used before for real-time neurotransmitter monitoring (Zhang and Tan 2000). We chose to use a laser instead of a lamp to ensure that NADH molecules were efficiently excited. The collection of NADH fluorescence was done through quartz microscope objectives ranging from 10 to 60X in magnification. The optical signal was selected using a combination of long pass filters and a 465-interference filter. The selected fluorescence signal was subsequently directed

onto the ICCD. A PC computer with Winview software (Princeton Instruments, Princeton NJ) was used to control the ICCD system. The apparatus was put on a vibration free laser table to avoid localization variations during the imaging process. This set-up has been used to image single living cells and single molecules (Bui et. al. 1999; Zhang and Tan 2000).

5.2.2 Reagents

Lactate dehydrogenase (LDH) from Bovine Heart (550 units/mg) was purchased from Roche Molecular Biochemicals (Germany). Lactate was purchased from Sigma Chemical Co. (St. Louis, MO). Nicotinamide adenine dinucleotide (NAD^+) and gluteraldehyde (25% aqueous solution) were purchased from Acros Organics (Fairlawn, NJ). Trimethoxysilylpropyldiethylenetriamine (DETA), a silanization reagent was purchased from United Chemical Technologies (Bristol, PA). All other chemicals were of analytical reagent grade. Distilled deionized water was used for the preparation of all these aqueous solutions.

5.2.3 2nd Generation 2D Sensor Fabrication

A batch of 6-10 flat silica plates was used in a single immobilization cycle. The flat silica plates (FSPs) were first cleaned by immersion in a solution of concentrated HCl/MeOH (1:1) for 30 minutes. They were then rinsed in deionized water and submerged in concentrated H_2SO_4 for 30 minutes. Growth of a pure silica layer and nanoparticles were done by placing the clean glass slides into the Stober synthesis (Stober and Fink 1968). Silanization of the nanoparticle synthesized on the grown FSP surface was performed by immersion of the FSPs in a freshly prepared 1% (v/v) solution of DETA in 1mM acetic acid for 30 minutes at room temperature

(23°C). The DETA-modified FSPs were thoroughly rinsed with deionized water to remove excess DETA. The silanized FSPs were dried under N_2 (g) and fixed with heat in a 120°C oven for 5 min. Conjugation of the FSP was carried out using a bifunctional cross-linker, gluteraldehyde. The silanized sensors were kept in a 12.5% (v/v) gluteraldehyde solution with 0.1 M potassium phosphate buffer solution (PBS) at pH 6.8 for 14 hours at room temperature. In the last step the unreacted carboxyl termini of the bifunctional cross-linker were linking to the primary amines on the target enzyme LDH. An LDH enzyme solution with a concentration of $1x10^{-5}$ M was prepared in 0.1M PBS at pH 6.8. The 2D sensors were immersed in the solution for 17-20 hours at room temperature to allow LDH to be immobilized on the surface. The 2D sensors were stored in PBS at 4°C when not in use.

5.2.4 Sensor Response Analysis

Measurements of the LDH activity were carried out in the set-up shown in previously in Chapter 2, Figure 2-1. The 2D lactate sensor formed a sandwich with a clean glass slide. Substrate solution, containing different concentrations of lactate and 1 mM NAD^+ in a 0.1 M PBS buffer at pH=7.8, was filled between the two plates. Optical excitation from the laser was uniform in the imaging area with a 40X microscope objective. The microscopy system was used to monitor the enzymatic reaction over time. Usually, 100 fluorescence images were taken to monitor the fluorescent intensity increase due to NADH production from the reaction catalyzed by the immobilized LDH molecules on the FSP. Quantitative analysis of the data was performed with Winview software and individual spatial location can be chosen for time resolved analysis. Lactate release from the brain slice can thus be monitored.

5.2.5 Monitoring Lactate Release from Brain Slice

The detailed procedures for obtaining the brain slice can be found in the literature[21]. Briefly, 20-21 day old male mice were euthanized in the presence of CO_2 and decapitated. The local IACUC committee approved these procedures. Brains were removed rapidly and cooled down to 4°C. Coronal slices (100 μm thick) (bregma -1.0 mm to bregma -1.6 mm) were prepared (VT1000S, Leica) with the speed setting on 2 and the frequency setting on 5 at room temperature in artificial cerebral spinal fluid (ACSF) containing: 124 mM NaCl, 26 mM $NaHCO_3$, 3 mM KCl, 2mM $CaCl_2$, 2mM $MgSO_4$, 1.25 mM NaH_2PO_4, and 10 mM glucose. The brain slices were freshly prepared in an ACSF solution before they were transferred to 35 mm culture dishes on ice filled with buffers compatible with the 2D sensor (PBS pH = 8.0) containing 1 mM NAD^+.

5.3 Results and Discussion

5.3.1 Covalent Immobilization of LDH on Nanoparticle Modified FSP

LDH molecules were directly immobilized onto a flat silica plate surface by covalent binding. The mechanism for immobilization is a combination of several surface modification techniques (Liu et. al. 1997; Trettnak and Wolbeis 1989; Zhang and Tan 2001). Conjugation of the LDH molecule was done using of gluteraldehyde, where one aldehyde group reacts with an amine from the amino-silane layer on the silica glass and the other aldehyde group reacts with the amine-containing biomolecules. The gluteraldehyde is used not only for joining separate molecules but also as a spacer arm that allows for greater accessibility and/or freedom to the attached macromolecules, such as LDH. This spacer is known to be essential to the activity of the LDH reacting with its substrate.

5.3.2 Influence of pH and NAD^+ Effects on Lactate Sensor Performance

The response of the biosensor is dependent upon pH and substrate concentrations. We have investigated the influence of pH and NAD^+ concentration on the lactate sensor performance. The sensor had its highest activity in the pH range of 7.8-8.2 it peaked around pH 8 as shown in Chapter 2, Figure 2-9. The reaction of lactate and NAD^+ catalyzed by LDH is a process of releasing H^+, so a high pH is advantageous to the forward reaction. However, if the pH is too high, the enzyme becomes unstable and the decomposition of NAD^+ may occur. For this reason all subsequent measurement were done at pH 8.0 in 1 mM PBS buffer.

NAD^+ is a vital component of this enzymatic reaction. Its effect on the lactate sensor's performance was previously studied (Cordek et. al. 1999; Liu and Tan 1999), also shown in Chapter 2, Figure 2-7. The lactate sensors were tested with different NAD^+ concentrations, while the lactate concentration (0.5 mM) remained constant. As the concentration of NAD^+ was increased, the sensor responded in an asymptotic approach to a maximum enzymatic activity. The sensor was in essence independent of the co-substrate when the NAD^+ concentration was above 1 mM. The concentration of NAD^+ in all further experiments was then set to 1 mM.

5.3.3 2nd Generation 2D Biosensor for Lactate Detection

The LDH two-dimensional imaging biosensor is highly sensitive with an analytical sensitivity down to the submicromolar range. In our experiments, 100 images (either full frame or subframe, depending on the sample) were taken to monitor the time course of NADH production when different concentrations of lactate were used. As shown in Chapter 2, Figure 2-11, the 2D biosensor responded linearly to lactate

concentration changes. The relative reaction velocity was plotted against lactate concentration. The velocity was based on initial reaction rate and has been found to be an accurate way to characterize the 2D biosensor's sensitivity for monitoring its substrates (Cordek et al. 1999; Liu and Tan 1999). The relative reaction rate obtained was based on initial reaction rates. The velocity obtained was based on all 100 images. According to the Michaelis equation at constant enzyme concentration, the initial rate is directly proportional to the substrate concentration when the concentration is much less than K_m (Stervr 1988) (K_m, the Michaelis constant, is equal to the substrate concentration at which the reaction rate is half of its maximal value). Reaction rates were calculated based on the slope of the plot of intensity vs. time. The absolute intensity of each pixel in each image was averaged, and the velocity was then determined using the duration of the imaging process (for example, 25 ms for each point for the images taken in Figure 2-10). The lactate response curve shown in Figure 2-11 is reproducible and was obtained under optimal conditions. The biosensor has a linear response range of 0-10 μM.

5.3.4 Selectivity and Stability of the 2nd Generation 2D Biosensor

The longevity and durability of biosensors pose major concerns for storage, especially when the sensor is intended for biological use. When not in use, the LDH sensor was stored in PBS pH 6.8 at 4°C. The basis for the determination of the biosensor's stability was a series of experiments done over an 8-hour period. During the 8-hour period, the biosensor was tested using a 0.5 mM lactate sample under optimal conditions. The LDH sensor showed good stability, and was stable over a 7-10 day period. The LDH sensor was also very selective in its detection of lactate. The selectivity of the sensor was tested by measuring responses from 9 α-hydroxy-acids (Malonic acid,

Glycolic acid, Isocitric acid, Quinic acid, Ascorbic acid, Uric acid, L-cysteine, Glutathione, Acetamidaphenol), which most commonly interfere with determination of lactate in physiological samples. No responses were observed for the majority of compounds tested. Only acetamidophenol showed a response that was 2.3% of the response of that for lactate.

5.3.5 Response Time of the 2D Biosensor

For most biological sensors, the time the sensors need to achieve a steady-state response after the introduction of a sample is reported as the response time. We define the response time for the lactate sensor as the time required for the LDH sensor to generate sufficient NADH for detection. The shortest response time of the sensor corresponds to the lowest detectable optical signal generated by NADH. We used the standard deviation of the base line to estimate the response time of the sensor to be less than 100 ms for 0.5 mM lactate solution. The fast response time is due to the direct immobilization of the enzyme molecules onto the flat silica plate. Another great benefit of the LDH biosensor was its short recovery time. The LDH biosensors prepared in this work were ready for experimental measurements directly after rinsing with buffer.

5.3.6 2D Imaging of Lactate from Tissue Slice

To demonstrate the spatially resolved sensing and imaging capability of the 2D biosensor, we applied the sensor to monitor lactate release from mouse brain slices. Lactate release is the preferred form of fuel under hypoxia conditions. The brain slices were prepared freshly in an ACSF solution as described in the experimental section. Before the KCl experiments, we performed strict control experiments to make sure that there was no appreciable fluorescence signal increase under the following conditions: (1)

the buffer together with the 2D biosensor with KCl bathing and without KCl bathing; (2) the brain slice with the biosensor but without KCl stimulation; (3) the brain slice and KCl bathing but without the 2D sensor; (4) the 2D biosensor with brain slice and KCl but without NAD^+; and (5) the 2D biosensor with NAD^+ without KCl. These experiments assured us that there were no false signal in lactate monitoring when the brain slice was used. Similarly, control experiments were done to determine how much lactate would be present after tissue slicing in comparison to the lactate released from a stimulated slice followed by a determination of the amount of lactate present after washing. We found that lactate present after slicing and also after washing following stimulation is less than 10% of the total amount of that after stimulation using KCl (Figure 5-1). We also found that the tissue slice in oxygenated buffer gave approximately 75-80 % of the signal of that in non-oxygenated buffer (Figure 5-2). Reproducibility among the same batch of biosensors was within ± 4.2% before brain slice release experiments. The mouse brain was cut into slices and tested inside a dish, which contained 1 mM NAD^+. The brain slice sat on a glass slide and was bathed with the buffer solution. The 2D lactate biosensor was placed on the top surface of the brain slice during lactate release experiments.

Figure 5-3 illustrates a typical result from such an experiment in which the enzymatic reactions between the immobilized enzyme, NAD^+, and the released extracellular lactate, to produce the fluorescent product NADH. The mouse brain is enriched in a glutamatergic neuronal network. Before a stimulation reagent was added, an optical image was taken, as shown in Figure 5-3a, to show the localization of the

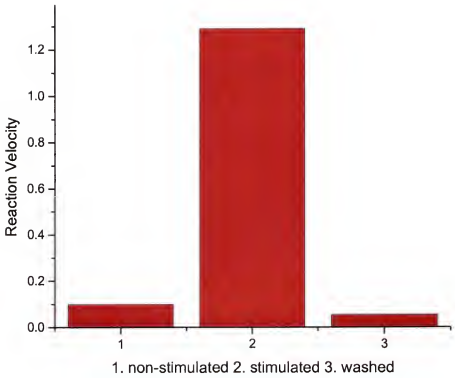

Figure 5-1: Bar graphs representing reaction rates dependrnt on lactate concentration; (1) total amount of lactate before stimulation; (2) total amount of lactate present after stimulation with KCl; (3) Lactate level after washing of tissue slice.

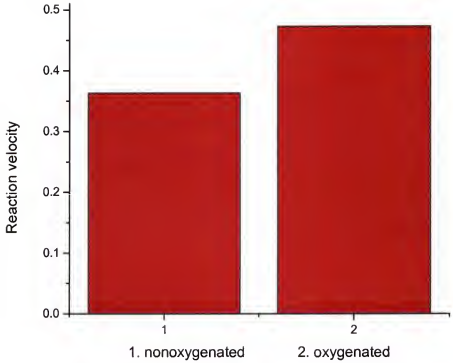

Figure 5-2: Bar graph schematic of total lactate concentration of lactate present after stimulation of tissue slice. (1) Mouse brain was sliced and placed in non-oxygenated buffer and stimulated with KCl (2) Mouse brain was slice and placed in oxygenated buffer and stimulated with KCl.

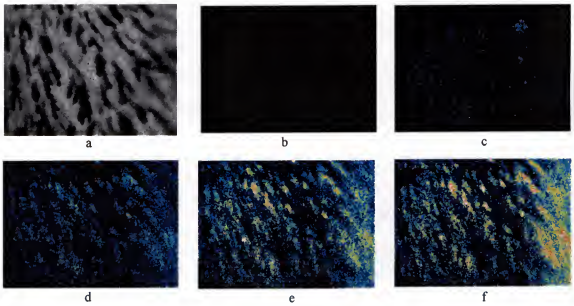

Figure 5-3: Images of brain slice. The scale bar shows the size of the brain slice imaging area. a) Optical image of the rat brain slice, b) First fluorescence image (1/100th second), c) 25th second image, d) 50th second. image, e) 75th second. Image, f) 100th second image.

different morphological structures of the brain slices. A background fluorescent image was taken prior to the injection of KCl, which serves as the background signal for all subsequent fluorescent images. A stock KCl solution was injected into the culture dish at a final concentration of 50 mM to enhance neuronal activity of the brain slice and to stimulate lactate release. From Figure 5-3, it is clear that lactate has been released from the brain slices. The full image, which encompasses a large area of the brain slice, provides the capability to study local heterogeneity in lactate release. The relationship between the stimuli concentration and the amount of lactate released was investigated. The KCl concentration was changed and the amount of lactate released was monitored. As shown in Figure 5-4, the higher the KCl concentration used for stimulation, the faster rate the lactate was released from the brain slice. However, there was little variation in the lactate release when the KCl concentration was higher than 50 mM.

5.3.7 Real-Time Imaging of the Brain Slice

The 2D biosensor is able to image lactate release on a regional and pixel-by-pixel basis in real-time. To show that the LDH enzyme is uniformly immobilized on the FSP, we monitored the enzymatic reaction on a pixel-by-pixel basis across the focused region of the substrate solution. In a test sample with given lactate concentration, we calculated the intensity change over time on a pixel-by-pixel basis. The results showed that the deviation of all pixels in the imaging was minimal, with a 2.5% RSD. The 2D sensor showed it could detect lactate uniformly, providing evidence that the LDH enzyme was homogenously immobilized on the FSP. This result indicates that any deviation in lactate is not due to the sensor itself but the variations in the tissue sample used in the study.

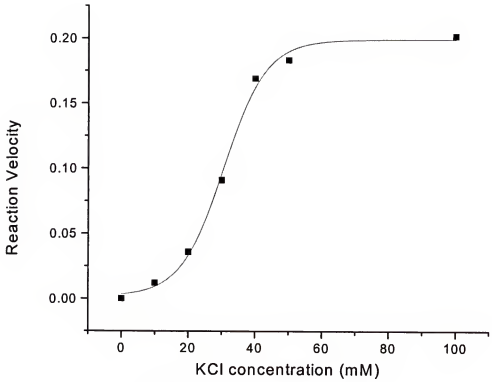

Figure 5-4: Effect of KCl concentration on the release rate of lactate from brain tissue slices.

The lactate release was monitored on a regional basis. 100 fluorescent images of the brain slices were taken after KCl stimulation, each being 1 second apart. As shown in Figure 5b, the first fluorescence image is dark, but as the image number increases from Figure 5c to 5f, different areas of the brain slice becomes brighter, indicating lactate release and NADH generation from the specific area. It is clear that different areas of the brain slice have different amounts of lactate released. To illustrate spatially resolved imaging on a regional scale, we have chosen three typical areas in Figure 5-3 to plot the time course of lactate release, shown in Figure 5-5a.

The 2D sensor could be used for spatially resolved imaging. Three separate areas of an 80 x 80 μm region of the brain slice were selected from Figure 5-5a. In each of these regions, 3 areas (4μm x 4μm) were highlighted and lactate release was followed. These three regions had different amounts of lactate released, as shown in Plot 1 in Figure 5-5. However, lactate release kinetics in the same region was similar. To further demonstrate molecular diffusion plays a minimal role in the spatially resolved 2D imaging biosensor, we chose 3 neighboring 2x2 pixels (D-F) and monitored lactate release. As seen in Figure 5-5 plot 2, the release kinetics between close by regions can be spatially resolved. The released lactate concentration and release kinetics for D, E and F areas were not the same. We further show the spatial resolution in plot 3 by analyzing the fluorescence intensity across the tissue slice. In summary, Figure 5-5 shows that lactate release is not uniform across the hippocampal slice, but rather regional specific.

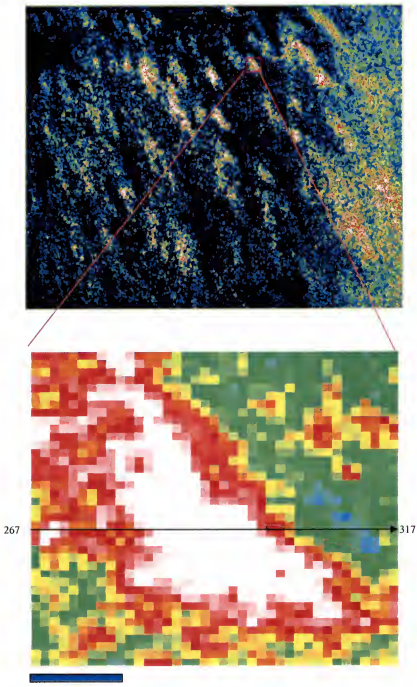

Figure 5-5a: Image of 80 x 80 μm region of the brain slice.

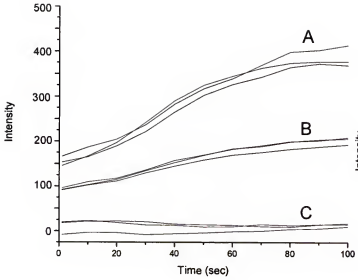

Plot 1

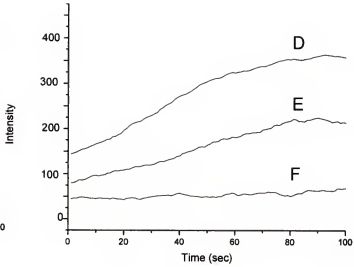

Plot 2

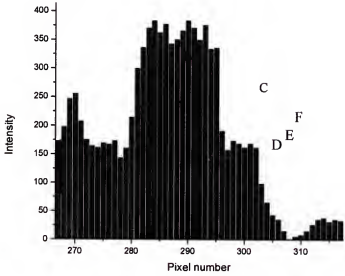

Plot 3

Figure 5-5b: Plot 1: Three areas, 4 μm x 4 μm, were chosen in areas A-C. Their responses to lactate release are shown in Plot 2: Three adjacent 2x2 pixels (D-F) were monitored to show spatial concentration variations during lactate release. Plot 3: Fluorescence intensity analysis across one horizontal line of the tissue sample to show the sharp changes from pixel tom pixel in the 2D imaging

The variations in the amount of lactate released may be a reflection of the fact that neuronal activity, in particular, the excitatory activity of glutamate as neurotransmitter (Schurr et al. 1997). This present study, to the best of our knowledge, is the first to report such a focal increase of lactate across a surface of neuronal network. In any event, the real-time determination of the newly released lactate from the mouse brain slices clearly demonstrates the feasibility of an effective and practical application of our two-dimensional lactate biosensor for monitoring of dynamic lactate release from living specimen.

5.4 Conclusion

In conclusion, a highly sensitive optical biosensor with two-dimensional imaging capabilities has been developed for real-time monitoring of brain slice lactate release upon stimulation. The two-dimensional biosensor was prepared by direct immobilization of lactate dehydrogenase molecules onto a flat silica plate surface through a covalent immobilization mechanism. The biosensor was able to spatially differentiate lactate concentration variations with conventional optical microscopic resolution. This relatively simple biosensor has the capability to effectively detect lactate down to a concentration of 10 nM. The two-dimensional biosensor responds uniformly and has a fast response time. We studied the impact of KCl on lactate release from the brain slices. Different areas of the brain slices have different amounts of lactate release. The imaging of lactate release showed that the two-dimensional imaging biosensor is a feasible approach to study cellular communications and possibly other biological processes that require simultaneous temporal and spatial resolutions. The two-dimensional biosensor has the capability of monitoring simultaneously many cells in one image.

CHAPTER 6
NICOTINE STIMULATION OF BRAIN SLICES FOR THE MONITORING OF GLUTAMATE

6.1 Introduction

Cigarette smoking is a major cause of many diseases in the United States. Smoking is directly linked to over 400,000 deaths due to cancer, stroke and cardiovascular disease every year in the U.S. In the United States, less than 10 percent of the nearly 20 million people who quit smoking for a day remain abstinent one year later. With only 2 to 3 percent of smokers succeeding in their attempts to quit smoking cigarettes is considered among the most addicting drugs (Emmons et al. 1997; Hasukami et al. 1995; Johnson and Gold 1996). Alongside 50,000 non-smokers are killed each year due to side stream smoke or better known as second hand smoke. This form of smoke is released into the air from a lighted cigarette or exhaled by a smoker. The passive smoker in the room with active smokers does not have the advantage of the filter. The smoke contains higher levels of substances such as carbon monoxide, nicotine, and other additives.

Nicotine, which is a substance found in cigarettes and other tobacco products, has been shown to interact with nicotinic receptors in the central nervous system, which facilitates the release of neurotransmitters such as dopamine, norepinephrine, acetylcholine, serotonin and most importantly glutamate (Matta et al. 1995Rose et al. 1999; Summers and Giacobini, 1987; Toth et al. 1992; Wonnacott et al. 1990). In

addition to the facilitation of neurotransmitter release more recent electrophysiological studies have focused on the ability of nicotine to enhance excitatory synaptic activity (Barrantes et al. 1995; McGhee et al. 1995; Vidal and Changeux 1993). These electrophysiological studies have shown a model, which suggests that presynaptic activation occurs in which ionotropic nicotine receptors activate calcium influx, which enhances the release of glutamate and the subsequent firing of excitatory postsynaptic potentials (McGhee and Role 1996). This proposed mechanism is also supported by neurochemical data. Thus both locally perfused and peripherally injected nicotine have been shown to stimulate the extra-cellular levels of glutamate in the striatum (Toth et al. 1992) and nucleus accumbens (Reid and Berger 1997) respectively. Recent evidence suggests that nicotine effects on dopamine neurons are mediated by glutamate (Garcia-Munoz et al. 1996). The neurotransmitter dopamine plays an important role in the reward pathways of the brain. This neural circuitry reinforces behaviors that are essential to the survival of an individual. Stimulating neurons in these areas of the brain brings on pleasant, happy feelings so the person will continue the actions. Thus nicotine activates these reward pathways and causes the smoker to continue the use of cigarettes even though they are causing harm to themselves in the form of cardiovascular diseases and stroke.

In this chapter, we report how different levels of nicotine intake can vary the amounts of glutamate released in brain slices. Through the use of an intensified charged coupled device (ICCD) and a well characterized enzyme biosensor we monitor and imaged glutamate release (Bang and Tan 1999; Lavine et al.. 1998; Michael et al. 1998). The imaging biosensor is based on the immobilization of the enzyme glutamate

dehydrogenase (GDH) on a flat silica plate (FSP) thus providing two-dimensional (2D) imaging capabilities. The immobilized enzyme molecules can catalyze a reaction between glutamate and the weakly fluorescent NAD^+ to give a highly fluorescent product NADH. The production of NADH can be monitored by the ICCD system and used for the analysis of nicotine-induced glutamate from mouse brain slices.

6.2 Experimental and Methods

6.2.1 Apparatus

The experimental set-up for the detection of glutamate from brain tissue slices was based on an inverted Olympus fluorescence microscope (IX70-S8F). The set-up is shown schematically in Chapter 2, Figure 2-1. An Intensified Charged Coupled Device ICCD (Princeton, EEV 512x1024) was used for capturing images and for ultrasensitive analysis. The ICCD has the capability of imaging single molecules in solution and on a surface (Fang et al. 1999). The radiation source for the excitation of NADH molecules was a 350 nm laser beam from an Innova Ar^+ laser (Coherent Laser, Santa Clara, CA). The layout of the set-up is similar to the microscope imaging system we used for real-time neurotransmitter monitoring (Zhang and Tan, 2000). The collection of NADH fluorescence was done through quartz microscope objectives with 10 to 60X magnification. The optical signal was selected using a combination of long pass filters and a 465-interference filter. The selected fluorescence signal was subsequently directed onto the ICCD. A PC computer with Winview software (Princeton Instruments, Princeton NJ) was used to control the ICCD system. The apparatus was put on a vibration free laser table to avoid localization variations during the imaging process. This set-up has been

used in the imaging of single living cells and single molecules (Bui et al. 1999; Zhang and Tan 2000).

6.2.2 BioSensor Fabrication

Flat silica plates (FSP) (a batch of 6-10), were first cleaned by immersion into a solution of concentrated HCl/MeOH (1:1) for 30 minutes. FSPs were then washed with deionized (DI) water and re-submerged into a solution of concentrated H_2SO_4 for an additional 30 minutes. Silanization of the FSPs was performed by immersion of the FSPs in a freshly prepared 1% (v/v) solution of DETA in 1mM acetic acid for 30 minutes at room temp (23°C). The DETA-modified FSPs were thoroughly rinsed with deionized water to remove excess DETA. The silanized FSPs were dried under N_2(g) and fixed with heat in a 120°C oven for 5 minutes. Conjugation of the FSP was carried out using the bi-functional cross-linker, gluteraldehyde. The silanized sensors were kept in a 12.5% (v/v) gluteraldehyde solution with 0.1M potassium phosphate buffer solution (PBS) at pH 6.8 for 14 hours at room temperature. In the last step the un-reacted carboxyl termini of the bi-functional cross-linker interact with the primary amines on the target enzyme GDH. A GDH enzyme solution with a concentration of $1x10^{-5}$ M was prepared in 0.1M PBS at pH 6.8. The biosensors were immersed in the solution for 17-20 hours at room temperature to allow GDH to be immobilized on the surface. The biosensors were stored in PBS at 4°C when not in use.

6.2.3 Sensor Characterization

Substrates that are modified with biological components, whether it is enzymes, antibodies or DNA need to be characterized to ensure that modification does not alter the activity of the biological component. In this instance we are dealing with enzymes,

specifically glutamate dehydrogenase. Enzymes are catalyst, and when immobilized to a substrate they might lose some of its catalytic activity. Similarly, enzymes are highly sensitive to their pH environment; to guarantee optimal enzymatic conditions we have examined the effect of pH on the enzyme-immobilized sensor. Also a range of substrate concentrations [NAD^+] were used to ensure that the enzyme was used in optimal conditions. Most importantly, selectivity and stability experiments were performed to ensure excellent enzymatic activity. Optimized parameters assure that the immobilized enzyme will give maxium sensitivity for the detection of glutamate.

6.2.4 Preparation of Biological Samples

The detailed procedures for obtaining brain slices, approved by the local IACUC committee, can be found in the literature (McGhee and Role 1999). Briefly, 20-21 day old male mice were euthanized in the presence of CO_2 and decapitated. Brains were removed rapidly and cooled down to 4°C. Coronal slices (100 μm thick) (bregma -1.0 mm to bregma -1.6 mm) were prepared (VT1000S, Leica) with the speed setting on 2 and the frequency setting on 5 at room temperature in artificial CSF containing: 124 mM NaCl, 26 mM $NaHCO_3$, 3 mM KCl, 2mM $CaCl_2$, 2mM $MgSO_4$, 1.25 mM NaH_2PO_4, and 10 mM glucose. The brain slices were freshly prepared in an artificial cerebral spinal fluid (ACSF) solution before they were transferred to 35 mm culture dishes on ice filled with buffers compatible with the biosensor (PBS buffer, pH = 8.0) containing 1 mM NAD^+ before the experiments were conducted.

6.2.5 NAD^+ Effect on Glutamate Sensor Performance

Since NAD^+ is required for the reaction, the effect of NAD^+ concentration on the GDH sensor activity was established. Sensor response was monitored for 0.5 mM glutamate solutions with various concentrations of NAD^+. As shown in Figure 6-1, when the concentration of NAD^+ was increased, the sensor responded in an asymptotic approach to maximum enzymatic activity. The GDH activity on the probe is in essence independent of the co-substrate when the concentration of NAD^+ is above 1 mM. Therefore a NAD^+ concentration of 1 mM was used in all subsequent experiments.

6.2.6 Influence of pH on the Glutamate Sensor

The environment in which a biosensor is used may have an effect on its response; therefore the influence of pH was investigated. The results are shown in Figure 6-2. The sensor has its highest enzymatic activity in the pH range of 6.8-8.9. The reaction of glutamate and NAD^+ under the catalysis of GDH is a process that released H^+, thus a high pH is advantageous to the positive reaction. However, too high a pH may result in both the decomposition of NAD^+ and instability of the enzyme. The optimum response over a physiological pH range is an advantageous virtue for this sensor. All subsequent measurements were performed at pH 8.5 in PBS buffer.

6.2.7 GDH Probe for Sensitive Glutamate Detection

The enzyme-immobilized biosensor can detect glutamate as low as the sub-micromolar range. We used initial reaction rate, based on 100 images, to characterize the sensor's sensitivity for monitoring glutamate changes According to the Michaelis equation, at constant enzyme concentration, the initial rate is directly proportional to the substrate concentration when the concentration is much less than K_m (Michael et al. 1998)

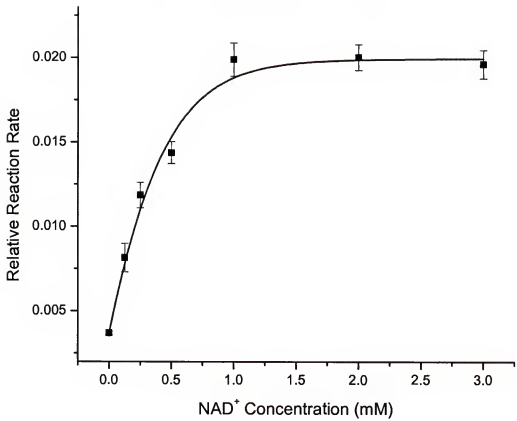

Figure 6-1: Effect of NAD^+ concentration on the activity of glutamate sensor at pH 80 (Tris-HCl buffer) in the presence of 0.5 mM glutamate

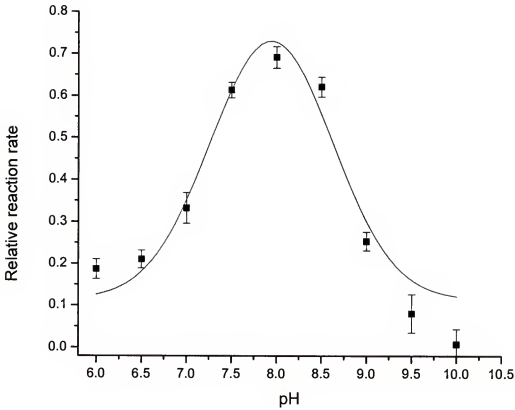

Figure 6-2. pH effect on the immobilized GDH enzyme Experimental conditions . 0.1 mM Na_2HPO_4-NaH_2PO_4 (pH = 5.7-6.8), 0.1 mM Tris-HCl buffer (pH = 7.0-8.9), 0.1 mM Na_2CO_3-$NaHCO_3$ buffer (pH = 9.1-10.2), 0.5 mM glutamate and 1mM NAD^+.

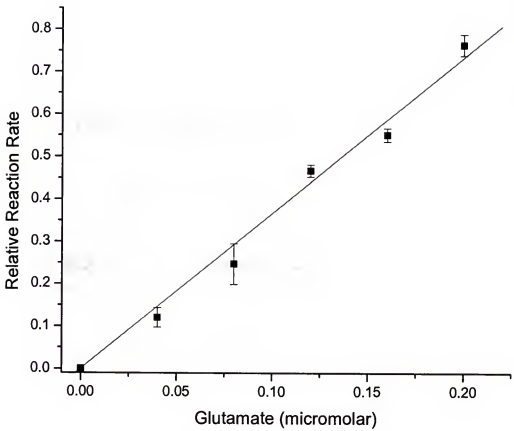

Figure 6-3: Calibration curve for glutamate analysis under optimal conditions

(K_m, the Michaelis constant, is equal to the substrate concentration at which the reaction rate is half of its maximal value). Reaction rates were calculated based on the slope of the plot of intensity vs. time. The absolute intensity of each pixel in each image was averaged, and the velocity was then determined using the duration of the imaging process (for example, 25 ms for each point for the images taken in Figure 6-3). The glutamate response curve shown in Figure 6-3 is reproducible and was obtained under optimal conditions. The biosensor has a linear response range from 0-0.2 μM with a LOD of 0.04 μM.

6.2.8 Glutamate Sensor Stability and Selectivity

The lifetime of sensors, especially those employing biologically active materials such as enzyme or antibodies, is a major concern. The glutamate sensor was stored in pH 6.8 PBS buffer at 4 °C when not in use. The glutamate sensor showed good stability in the first 24-48 hours of use (Figure 6-4). An obvious degradation in the sensor's response was observed after 10 days. GDH itself is highly selective in its reaction for glutamate over other substrates, so the GDH sensor offers high selectivity for glutamate. The selectivity of the GDH sensor probe for its substrate was demonstrated by monitoring any response to other α-hydroxy acids (Malonic acid, Glycolic acid, Isocitric acid, Quinic acid, Ascorbic acid), compounds which are the most common interference, no responses were observed for the compounds tested (Figure 6-5).

6.3 Biological Application of the Imaging Biosensor

This enzyme biosensor has two-dimensional imaging capabilities and to demonstrate this novel capability we tested this biosensor on brain tissue slices for the real-time monitoring of glutamate release. Initially we examined KCl and $CaCl_2$ as stimulants for the monitoring of glutamate release. It is well known that Ca^{2+} and K^+ can

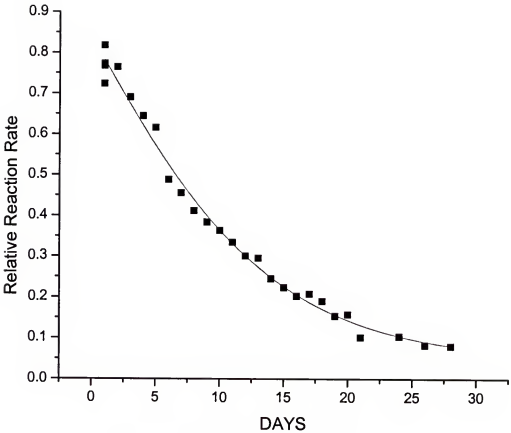

Figure 6-4: Response to 4 mM glutamate and 1mM NAD^+ as a function of sensor age.

Compound	% Response	Compound	% response
L-Glutamate	100	L-glycine	0
ADP	0	H_2O_2	0
L-ascorbate	5.2	L-lactate	0
L-cyseine	3	NMDA	0
L-glutamine	0	Urate	0

Figure 6-5: Relative response of the GDH 2D enzyme sensor to potential physiological interferences

bind to intracellular ligand-gated channels in the cell membranes, thereby influencing the opening/closing of ion channels. Upon the opening of the channels, there is an influx of ions causing the vesicles to migrate and fuse to the cell membrane and thus release neurotransmitters, more specifically glutamate in the case of glutaminergic neurons. To ensure real time monitoring of glutamate release, the following control experiments were done: (1) the buffer together with the 2-D biosensor with $CaCl_2$ bathing and without $CaCl_2$ bathing, (2) the brain slice with the biosensor but without $CaCl_2$ stimulation, (4) the brain slice and $CaCl_2$ bathing but without the 2-D sensor, (3) the 2D biosensor with brain slice and $CaCl_2$ but without NAD^+ and finally (5) the 2D biosensor with NAD^+ but without $CaCl_2$. Similar control experiments were done with KCl. These experiments confirmed that no false positive would be observed during glutamate detection from brain slices. Similarly, control experiments were done to determine how much glutamate would be present after tissue slicing in comparison to the glutamate released from a stimulated slice. We found that glutamate present after slicing is less than 10% of the total amount of that after stimulation using KCl or $CaCl_2$. Figure 6-6 shows the effects of both calcium chloride ($CaCl_2$) and potassium chloride (KCl) on glutamate release from the brain slice.

6.3.1 Nicotine Stimulation of Brain Tissue Slices for Glutamate Release

As with the most addictive substances, humans have devised a number of ways of delivering nicotine to their bodies. Nicotine readily diffuses through small blood vessels and into the bloodstream. Once in your bloodstream, nicotine flows almost immediately to your brain. While nicotine is in your brain, it binds specifically to the nicotinic receptors located on the various neurons including glutaminergic neurons in different

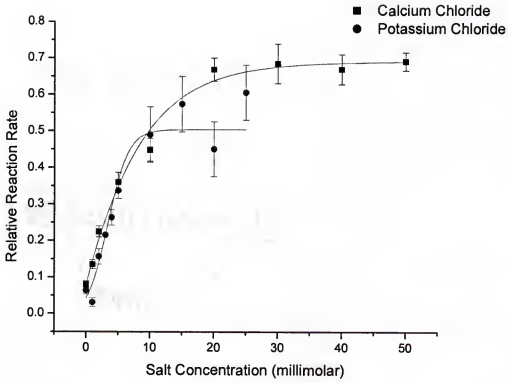

Figure 6-6: Effect of physiological salts on the release rate of glutamate from brain tissue: Calcium chloride,- ■ Potassium chloride-. ●

regions of the brain, thus opening ion channels and allowing the influx of ions and causing the release of glutamate. Typically the nicotine levels in the brain range from 0.1-0.5 μM (Alkondon et al. 2000). On average these levels are easily attainable after a person has smoked one cigarette. We monitored nicotine's effect on glutamate release. As previously discussed, control experiments were done to ensure that there were no false positive signals. A range of (-) Nicotine di (+)tartrate (Sigma, St. Louis, MO) solutions were made and applied to the tissue slice. Figure 6-7 graphically shows the response of the tissue slices as the concentration of nicotine was increased the levels of glutamate release responded linearly. Glutamate release responded in an asymptotic approach as the amount of nicotine added to the tissue slice was increased. Concentrations below 0.5 μM nicotine was applied to the tissue slice and no noticeable glutamate release was detected.

When comparing the potency of nicotine and the physiological salts one must consider the fact that the mechanistic pathways that are taken to stimulate glutamate release are very different. In nicotine's case, the mechanism involves the binding to cholindric receptors thus opening channels for the influx of ions to facilitate glutamate release. On the contrary potassium chloride and calcium chloride both act as intracellular ligands causing the opening of the channels and again influencing the release of glutamate. Figures 6-6 & 6-7 show calibration plots for KCl, $CaCl_2$ and nicotine. Reaction rates are directly related to the amount glutamate that is being released. We found that micromolar concentrations of nicotine induce glutamate levels that are comparable to release levels seen when millimolar concentrations of the salt are used. These findings confirm that the potency of nicotine in comparison to the physiological

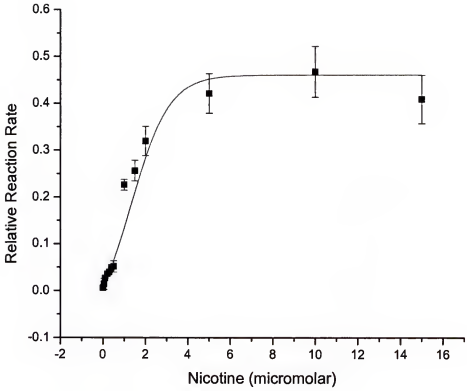

Figure 6-7: Nicotine's stimulatory effect on the mouse tissue slice for glutamate release

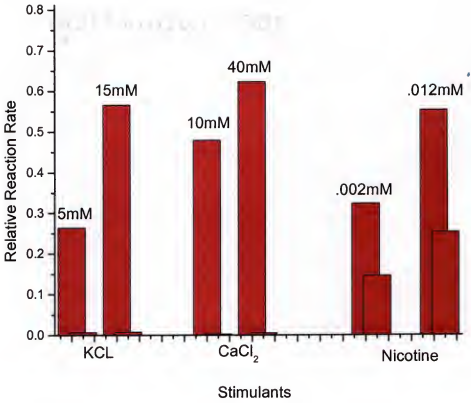

Figure 6-8: Comparison of KCl, $CaCl_2$ and nicotine ability to re-stimulate the mouse brain slice. Concentrations were chosen based on the calibration plots of the stimulant.

salts is greater and much more relevant when trying to understand the role nicotine plays in addiction. In addition we found that upon re-stimulation of the brain tissue slices the salts did not induce any substantial glutamate release, but on the contrary, nicotine's ability to induce further glutamate release was easily detected (Figure 6-8). These results thus confirm that the mechanism of stimulation of glutamate release between the salts and nicotine are quite different. Similarly, this result proves the well known depolarizing action of salts on biological samples, which cause the opening of channels and the release of cell contents.

6.3.2 Imaging of Glutamate Release from Brain Slice

From previous results, it is clear that the homogenously immobilized GDH biosensor allows for the detection and measurement of glutamate from the tissue slices. Figure 6-9 illustrates a typical result from such an experiment in which the enzymatic reactions between the immobilized enzyme, NAD^+, and the released glutamate produces the fluorescent product NADH. The slices were prepared in ACSF solution before they were placed into the dish containeing 1 mM NAD^+. Before a stimulation reagent was added, an optical image was taken, as shown in Figure 6-9a, to show the localization of the different morphological structures of the brain slices. A background fluorescent image was taken prior to the injection of nicotine, which served as the background signal for all subsequent fluorescent images. The brain slices released glutamate due to nicotine stimulation. From Figure 6-9, it is clear that glutamate was released from the brain slices. The full image, which encompasses a large area of the brain slice, allows the study of local heterogeneity in glutamate release. In the monitoring of glutamate release on a regional basis, 100 fluorescent images of the brain slices were taken after nicotine

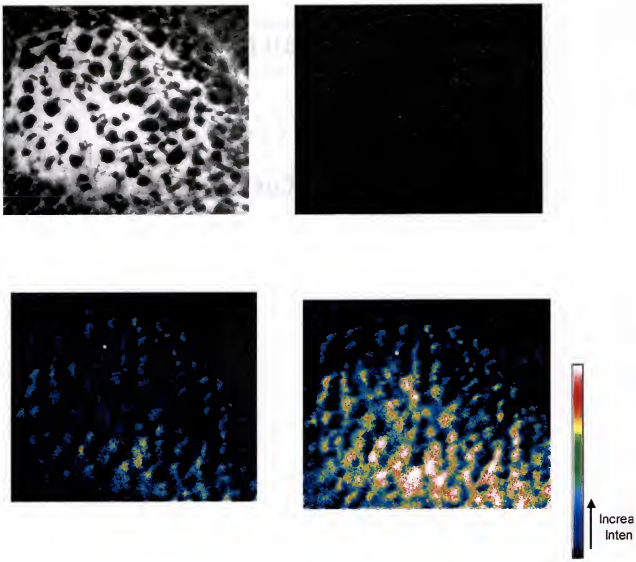

Figure 6-9: Images of brain slice. The scale bar shows the size of the brain slice imaging area. a) Optical image of the rat brain slice, b) First fluorescence image (1 sec), c) 50 sec. image, d) 100 sec. image.

stimulation, each being 1 second apart. As shown in Figure 6-9a, the first fluorescence image is dark, but as the image number increases from Figure 6-9b to 6-9d, different areas of the brain slice become brighter, indicating glutamate release from the specific areas.

6.4 Conclusion

A highly sensitive optical biosensor with two-dimensional imaging capabilities has been developed for real-time monitoring of glutamate release. It was used initially to measure glutamate release by physiological salts such as calcium chloride and potassium chloride because of their well known roles in the facilitation of neurotransmitter release. More importantly, this is the first time such a 2D sensor was used to define the vital role of nicotine in glutamate release. This relatively simple biosensor has the capability to effectively detect glutamate down to a concentration of 40 nM. The combination of the highly sensitive ICCD and the imaging sensor allowed the monitoring of glutamate release throughout different areas of the brain slices. Glutamate is known to be involved in learning and memory by enhancing the connections between various sets of neurons essential for cognition. To the best of our knowledge, this present study is the first to report such a focal increase of glutamate across a surface of neuronal network. The real time monitoring of newly released glutamate from mouse brain slices clearly demonstrates the feasibility of an effective and practical application of our imaging glutamate biosensor for real-time imaging of dynamic glutamate release from living specimens.

CHAPTER 7
SUMMARY AND FUTURE DIRECTIONS

7.1 Summary

The development of biosensors has made and will continue to make a dramatic impact in the research and industrial world of sensor technology. Research efforts in this dissertation have been focused on the development, enhancement and application of a two-dimensional enzyme based biosensor for the detection and imaging of the neurochemicals lactate and glutamate. In the detection of these neurochemicals enhanced levels of detection sensitivity are needed for the elucidation of cellular and subcellular process involved with these neurochemicals. Nanotechnolgy has played a major role in the enhancement of biosensor development in attempt to monitor and detect these processes. These neurochemicals play a vital role in the diagnosis of diseases, food chemistry and body biochemistry. The 2D enzyme biosensor technology has the potential to be used for diagnostic measures which will hopefully lead to the development of drugs for therapeutic measures.

Chapter 2 presents work directed towards the fabrication and characterization of the enzyme based two-dimensional sensors. To study the activity of the immobilized enzyme, we investigated the effects of $[NAD^+]$ and pH. We also examined the selectivity, stability and the response time of the biosensors. Although the creation of the two-dimensional sensor was successful, significant improvement in sensitivity, spatial

resolution as well as applicability would be required for practical utilization of this novel enzyme biosensor. New advances in nanotechnology such as nanoparticle synthesis and surface modification would improve sensitivity for the detection of the neurochemicals lactate and glutamate, which would in turn enhance the possibilities of neurochemical detection from single cells.

Chapter 3 depicts work in the area of nanotechnology primarily utilization of pure and dye-doped silica nanoparticles for bioanalysis, biomarking and enhanced detection of neurochemicals thru the development of our 2nd generation two-dimensional enzyme sensors. Through the fabrication and characterization of nanoparticles have been well studied, the surface modification and application of these nanoparticles as biosensors and biomarkers are yet and still an area of great interest with a wide range of possible research application. In particular chapter 3 discusses the application of dye-doped nanoparticles for the biomarking of leukemic cells. Also individual pure silica nanoparticles were utilized for the detection of neurochemicals. We found that the enhanced surface properties demonstrated by pure silica nanoparticles allows for more enzymes (i.e. higher concentration) to be immobilized thus increasing detection capabilities.

The surface area properties displayed by the nanoparticles lead to the development of the 2nd generation 2D enzyme biosensor for neurochemical detection. By placing flat silica plates into the Stober synthesis, a fresh layer of silica nanoparticles was polymerized on the FSP. We were able to utilize the high silica content and immobilize a higher concentration of enzyme onto the plate. Characterization experiments of the 2nd generation enzyme biosensor showed that the immobilized enzyme responds was similar

to that observed for the 1st generation sensor, but major differences were found in the limits of detection. The enzyme biosensor detection limits were decreased by two orders of magnitude, which greatly enhanced our capabilities for neurochemical detection.

Chapter 4 discusses work that also utilized nanotechnology in combination with surface immobilization chemistry for the fabrication of nanomaterials for enhanced bio-detection. In this chapter pure silica nanoparticles were synthesized via the Stober synthesis and reverse microemulsion process for covalent 2D assembly of nanoparticles. In the previous chapter we were able to utilize the enhanced surface properties of the silica particles, but not the maximum level of enhancement because the particles were being polymerized to the glass plate and we had to limit control over particle size. In this chapter, we synthesized the silica particles first, and then adopted a covalent attachment procedure, commonly used in zeolite chemistry for the nanoparticle attachment. Thru the use of halogenated silanes such as chloropropyl trimethoxy silane (CPTMS), we were able to control surface coverage density and also utilize lithography techniques for patterned assembly of the silica nanoparticle. In future application the patterned assembly of nanoparticles was then modified with biomolecules to demonstrate biosensing capabilities. Furthermore, the patterned assemblies of nanoparticles can be used for multianalyte detection.

Chapters 5 and 6 describes the application of the 2D enzyme biosensor. In Chapter 5, the enzyme biosensor was used for the detection of lactate from brain tissue slices. Multiple control experiments were done to ensure that the lactate being detected was due to the stimulation of the tissue slice. Potassium chloride a well known binding

ligand was used as a stimulant for neurotransmitter release. Glutamate release from brain tissue slices was the focus Chapter 6. The 2D GDH immobilized enzyme sensor was used for sensitive detection of glutamate. In this study, we examined the effects of physiological salts KCl and $CaCl_2$ on the tissue slice. For a more in depth study we monitored nicotine's effect on the brain tissue slices, both studies confirmed that the enzyme biosensors were capable of detecting neurochemicals from the brain tissue slices. Also in both chapters, we were able to simultaneously image the release events from the tissue slices. These two chapters demonstrate the capabilities of the 2D enzyme biosensors and show that they could be utilized for neurochemical detection from individual cells.

7.2 Future Work

7.2.1 Future Work for Nanoparticles

In Chapter 3, we synthesized pure silica and dye-doped nanoparticles for bioanalysis. Both types of nanoparticles have been utilized, but for more in-depth studies of the biomodified particles, continued studies in the area of neurotransmitter detection from a biological sample can be evaluated. The enhanced detection capabilities of individual enzyme immobilized particles can be utilized by strategically placing them in between two separate neuron cells for synaptical detection of glutamate release. From the biomarking point of view, dye-doped nanoparticles have show excellent stability and are useful for membrane staining or labeling. Continued efforts in the direction of cancerous cell detection would be advantageous.

7.2.2 Future Work for 2D Assembly of Nanoparticles

The assembly of pure silica nanoparticles for enhance biomaterial immobilization will be further explored. Results show that the adoption of zeolite covalent chemistry can be easily applied to nanotechnology. Furthermore, advances in photolithography enable the formation of ordered assemblies of nanoparticles which are also easily modified after attachment. This capability can be used to develop an ordered array of nanoparticles which can then be applied for mutli-analyte detection.

7.2.3 Future Work for 2D Enzyme Biosensor for Neurochemical Detection.

In Chapter 2, we fabricated a two-dimensional sensor which was based on the covalent immobilization of enzymes to a flat silica plate. The two-dimensional enzyme sensors have been characterized and in chapters 5 and 6 we applied the sensors for neurochemical detection from mouse brain tissue slices. The two-dimensional biosensor shows that it is feasible to detect neurochemicals from brain tissue samples. More in-depth study of neurochemicals and their roles in the cell will have to be done. Therefore it will be necessary to study neurochemical release from individual neuron cells. Glutamate, a major neurotransmitter in the brain is amain neurochemical involved in many processes and diseases. Concentrations variations in the release of glutamate from neuron cells in attempt to communicate with nearby cells are a mechanism that not well understood. The two-dimensional enzyme biosensor coupled with our imaging technologyis able to spatially monitoring neurochemical release. Monitoring these events on a cellular level will help understand mechanisms behind communication, learning, memory and more importantly disorders linked to glutamate release.

LIST OF REFERENCES

Adams, M.J.; Ford, G.C; .Koekoek, R.; Lentz, P.J.; McPherson, A.; Rossman, M.G.; Smiley, I.E.; Schevitz, R.W.; Wonnacot, A.J. *Nature* **1970,** 227, 1098.

Andres, R.P.; Bielefeld, J. D.; Henderson, J. I.; Janes, D. B.; Kolagunta, V. R.; Kubiak, C. P.; Mahoney, W. J.; Osifchin, R. G. *Science*, **1996**, *273*, 1690-1693.

Bang, L; Tan, WH. *Anal. Chim. Acta.,***1999**, 401, 91-94.

Bangs Laboratories Inc., 9025 Technology Drive Fishers, IN 46038-2866, USA, 1-800-387-0672.

Belay, A.; Collins, A.; Tautgirdas, R.; Kissinger, P. T.; Gorton, L.; Csoregi, E. *J Pharm. and Biomed. Analysis* **1999**, 19, 93-105.

Benvineste, H. *J. Neurochem.* **1989,** 52, 1667-1679.

Betzig, E.; Trautman, J. K.; Harris, T. D.; Weiner, J. S.; Kostelak, R. L. *Science* **1991**, 251, 1468-1470.

Bito, R.; Davson, H.; Levin E. M.; Murray, M.; Snider, N. *J. Neurochem.* **1966**, 13, 1057-1067.

Bruchez Jr. M.; Moronne, M.; Gin, P.; Weiss, S.; Alivisatos, A. P. *Science* **1998,** 281, 2013-2016.

Bui, J.D.; Zelles, T.; Lou, H. J.; Gallion, V. L.; Phillips, M. I.; Tan, W. *J. Neurosci. Meth.* **1999**, 89, 9-15.

Caruso, F.; Spasova, M.; Saigueirino-Maceira, V.; Liz-Marzan, L.M. Adv. Mat. 2001, 13, 14, 1090.

Castanohon-Lobo, M. J. Ordieres-Miranda, A. J.; Bianco-Tunon, P. Anal. Chim. Acta 1997, 346, 165-174.

Castillo, J.; Davalos, A; Noya, M. Lancet 1997, 349, 79-83. Chan, W. C. W.; Nie, S. Science 1998, 281, 2016-2018.

Chang, S. Y.; Liu, L.; Asher, S. A., J. Am. Chem. Soc. 1994, 116, 6745-6747.

Chen, G; Ewing, A. G. Crit. Rev. Neurobiol. 1997, 11, 4560-4565.

Choi, S.Y.; Lee, Y.J.; Park, Y.S.; Chun, Y.S.; Ha, K.; Yoon, K.B J. Chem. Soc. 2000, 122, 5201-5209.

Chow, R. H.; Von Ruden, L.; Neher, E. Nature 1992, 356, 60-63.

Chung, L. A. Anal. Biochem. 1997, 248, 195-201.

Clark, H. A.; Kopelman, R.; Tjalkens, R.; Philbert, M. A. Anal. Chem. 1999, 4837.

Collins, R. C.; Dobkin, B. H.; Choi, D. W. Annals of Internal Medicine 1989, 110 992-1000.

Cooper, J. M.; Foreman, P. L.; Glidle, A.; Ling, T. W.; Pritchard, D. J. J. Electroanal. Chem. 1995, 388, 143-149.

Cordek, J.; Wang, X.; Tan, W. Anal. Chem. 1999, 71, 1529-1533.

Couvreur, P.; Dubernet, C.; Puisieux, F. Eur. J. Pharm. Biophar. 1995, 41, 2.

Davis, S. S. *Trends Biotechnol.* **1997**, *15*, 217-224.
Dempsey, E. and Wang, J.; *Talanta* **1993**, 40, 445-451.
Diemer, N. H.; Valente, E.; Bruhn, T.; Berg, M.; Jorgensen, M. B.; Johansen, F. F. *Progress in Brain Research* **1993**, 96, 105-118.
Dremel, B. A.; Schmid, R. D.; Wolbeis, O. S. *Anal. Chim. Acta.* **1991,** 248, 351-359.
Fang, X. H and Tan, W. *Anal. Chem.* **1999** 71, 3101-3105.
Fang, X. H.; Liu, X.; Schuster, S.; Tan, W. *J. Am. Chem. Soc.*, **1999**, *121*, 2921-2922.
Fardinia, M.; Palleschi, G.; Lubrano, G. *Anal. Chim. Acta.* **1993**, 278, 35.
Fersht, A. *Structure and Mechanism in Protein Science* W. H. Freeman and Company New York, **1999**, Ch. 3.
Gaddum, J. H. *Pharmacological Analysis of Central Nervous Action.* London: Permagon Press, **1962**, 1-6.
Gaddum, J. H. *Physiol* (London) **1961**, 155.
Goldin, S. M *NY. Acad. Of Sci.* **1995**, 210-229.
Gonzales, R.A.; Jaworski, J.N., *Neurotransmitter Review* **1997,** No.2, 107.

Ha, K.; Lee, Y.J.; Chun, Y.S.; Park, Y.S.; Lee, G.S.; Yoon, K.B. *Advanced Materials* **2001**, 13, 8, 594-596.
Hajizadeh, K. Halsall, H. B.; Heineman, W. R. *Talanta* **1991**, 38, 37-47.
Hari Singh Nalwa *Handbook of Nanostructured Materials and Nanotechnology*, San Diego, Academic Press, Vol IV, **1999**, 621.
Haupt, M.T.; Gilbert, E.M.; Carlson, R.W. *Am. Rev. Resp. Dis.* **1985,** 131, 912.

Hu, Y.; Mitchell, K. M.; Albahadily, F. N.; Michaelis, E. K.; Wilson, G. S. *Brain Research* **1994**, 659, 117-125.
Hu, Y.; Wilson, G. S. *J. Neurochem.* **1997,** 69, 1484-1490.
I.C.B.R., the University of Florida.
Ingersoll, C. M.; Bright, F. V., *Anal. Chem.* **69**, 1997, 403A.
Jankowski, J. A.; Schroeder, T. J.; Ciolkowski, E. L.; Wightman, R. M. *J. Bio. Chem.* **1993**, 268, 14694-14700.
Jeng, R.J.; Chang, C.C.; Chen, C.P.; Chen, C.T.; Su, W.C. *Polymer* **2003**, 44, 143-155.
Juurlink, B.H.J.; Sweeney, M.I. *Neurosci and Biobehavioral Review* **1997**, 21(2), 121-128.
Kachan, S.M.; Ponyavina, A.N. *Surface Sci.* **2002**, 507-510, 603-608.
Kar, S.; Arnold, M. A. *Anal. Chem.* **1992**, 64, 2438-2443.
Kobayashi, Y.; Martin, C. R. *Anal. Chem.* **1999,** 71, 3665-3672.
Koshland, D. E. *Biol. Revs.* **1953**, 28, 416.
Kreuter, J. *J. Control Release*, **1991**, *16*, 169-176.
Kulak, A.; Lee, Y.J.; Park, Y.S.; Chun, Y.S.; Ha, K.; Yoon, K.B *J. Chem. Soc.* **2000**, 122, 9308-9309.

Kulak, A.; Lee, Y.J.; Park, Y.S.; Yoon, K.B. *Angew. Chem., Int. Ed.* **2000**, 39, 950.
Lada, M.; Vickroy, T. W.; Kennedy, R. T. *Anal. Chem.* **1997,** 69, 4560-4565.
Laidler, K.J. *Chemical Kinetics 3rd ed.*, HarperCollins Publishers, **1987,** Ch. 10.
Lavine, J. J.; Savoy, S.; Clevenger, M. B.; Ritchie, J. E.; McDoniel, B.; Yoo, S. J.; Anslyn, E. V.; McDevitt, J. T.; Shear, J. B.; Neikirk, D. J. *J. Am. Chem. Soc.* **1998,** 120, 6429-6430.
Lee, G.S. Lee, Y.J.; Yoon, K.B *J. Chem. Soc.* **2001**, 123, 9769-9779.
Lee, G.S.; Ha, K.; Yoon, K.B *Tetrahedron* **2000**, 56, 6965-6968.
Li, M.; Schnablegger, H.; Mann, S. *Nature*, **1999**, *402*, 393-395.
Li, T.; Moon, J.; Morrone, A. A.; Mecholsky, J. J.; Talham, D. R.; Adair, J. H. *Langmuir* **1999**, *15*, 4328-4334.
Liu, B.; Hu, R.; Deng, J. *Anal. Chem.* **1997**, 69, 2343-2348.
Liu, X.; Tan, W. *Mikrochim Acta* **1999**, 131, 129-135.
Liu, X.; Tan, W., *Anal. Chem.* **1999**, *71*, 5054-5059.
Martin, C. R.; Mitchell, D. T. *Anal. Chem.* **1998,** 70, 322A-327A.
Marzouk, S. A. M.; Cosofret, V. V.; Buck, R. P. *Analytical Chemistry*, **1997**, *69*, 2646-2652.
Mascini, M.; Fortunati, S.; Moscone, D.; Palleschi, G.; Benedetti, M.; Fabietti, P. *Clin. Chem.* **1985**, 31, 451.
Mascini, M.; Mosconed, D.; Palleschi, G. *Anal. Chim. Acta* **1984,** 157, 45.
Michael, K. L.; Taylor, L. C.; Schultz, S. L.; Walt, D. R. *Anal. Chem.* **1998,** 70, 1242-1248.
Michealis, L.; Menten M. L. *Biochem. Z.* **1913**, 49, 333.
Mirkin, C. A.; Letsinger, R. L.; Mucic, R. C.; Storhoff, J. J. *Nature*, **1996**, *382*, 607-609.
Mitsubayashi, K.; Suzuki, M.; Tamiya, W.; Karube, I. *Anal. Chim. Acta.* **1994**, 289, 27.
Murray, C. B.; Kagan, C. R.; Bawendi, M. G. *Science*, **1995**, *270*, 1335-1338.
Nicholls, D.G. *Proteins , Transmitters and Synapses* Blackwell Science, Oxford London, 1994.

Nichols, J.G.; Martin, R.A.; Wallace, B.G. <u>*From Neuron to Brain*</u> 3rd ed. Sinauer Associated, Inc. Sunderland, Mass. USA, 1992.

Niwa, O.; Kurita, R.; Tsutomu, H.; Torimitsu, K. *Anal. Chem.* **1998,** 70 89-93.

Niwa, O.; Torimitsu, K.; Morita, M.; Osborne, P.; Yamamoto, K. *Anal. Chem.* **1996,** 68, 1865-1870.
Palleschi, G.; Faridnia, M.; Lubrano, G.; Guilbault, G. *Anal. Chim. Acta.*, **1991**, 245, 151.
Pantano, P.; Kuhr, W.G. *Anal. Chem.* **1993**, 65, 623-630.
Pantano, P.; Walt, D. R. *Anal. Chem.* **1995**, 481A.
Park, J.S.; Lee, G.S. Lee, Y.J.; Park, Y.S.; Yoon, K.B *J. Chem. Soc. Comm.* **2002**.

Ping, D.H.; Ohnuma, M.; Hono, K.; Watanabe, M.; Iwasa, T.; Masumoto, T. *J. Appl. Phys.* **2001**, 90, 9.
Plaitakis, P.; Shashidharan, P. Amyotrophic Lateral Sclerosis, Glutamate, and Oxidative Stress, http://www.acnp.org/G4/GN401000148/CH.html 1999.
Qhobosheane, M.; Santra, S.; Zhang, P.; Tan WH *Analyst* **2001**, 126, 1274-1278.
Rosenzweig, Z.; Kopelman, R. *Anal. Chem.* **1995**, 67, 2650-2654.
Rosenzweig, Z.; Kopelman, R. *Anal. Chem.* **1996**, 68, 1408-1413.
Rusakov, D. A. and Kullmann, D.M. *J. Neurosci.* **1998**, 18, 9, 3158-70.
Rutnakornpituk, M.; Thompson, M.S.; Harris, L.A.; Farmer, K.E.; Esker, A.R.; Riffle, J.S.; Connolly, J.; St. Pierre, T.G. *Polymer*, **2002.**
Santra, S.; Wang, K.; Tapec, R.; Tan, W. *Biomed. Opt.* **2001**, 6 (2), 160-166.
Sbrana, F.; Parodi, M.T.; Ricci, D.; Di Zitti, E. *Catalysis Today* **2002.**
Schurr, S.; West, C.A.; Rigor, B. M. *Science* **1988**, 3240, 1326-1328.
Sethi, R. S. *Biosensors & Bioelectronics*, **1994**, *9*, 243-264.
Shengtian, P. and Arnold, M. A. *Talanta* **1996**, 43, 1157-1162.
Shenton, W.; Pum, D.; Sleytr, U. B.; Mann, S. *Nature*, **1998**, *389*, 585-587.
Shiojiri, S.; Hirai, T.; Komasawa, I. *Chem. Commun.* **1998**, *14*, 1439-1440.
Sibson, N.R.; Dhankhar, A.; Mason, G.F.; Rothman, D.L.; Behar, K.L.; Shulman, R.G. *Proc. Natl. Acad. Sci. USA* **1998**, 95, 316-321.
Smith, S.E.; Meldrum, B.S. *Stroke* **1995,** 26 117-121.
Sogowa, K.; Takahashi, K. *J. Biochem.* (Tokyo), **1978**, 83, 4242.
Stathatos, E.; Lianos, P.; DelMonte, F.; Levy, D.; Tsiourvas, D. *Langmuir* **1997**, *13*, 4295-4300.
Stober, W., Fink, A. J, *Colloid and Interf. Sci.*, **26,** 1968, 62.
Strver, L; Biochemistry, 3rd Ed. Freeman, New York, **1988**, p. 189.
Tadros, T. F. *Adv. Colloid Int. Sci.*, **1993,** 46, 1.
Takata, T.; Hirai, H.; Shigemoto, T.; Okada, Y. *Neuroscience Letters* **1995,** 189, 21-24.
Taleb, A.; Petit, C.; Pileni, M. P. *Chem. Mater.*, **1997**, *9*, 950-959.
Taleb, A.; Petit, C.; Pileni, M. P. *J. Phys Chem B*, **1998**, *102*, 2214-2220.
Tan, W. *Trends in Analytical Chemistry* **1998**, 17, 501-513.
Tan, W.; Haydon, P. G.; Yeung, E. S. *Applied Spectroscopy* **1997**, 51, 1139-1143.

Tan, W.; Shi, Z. Y.; Smith, S.; Birnbaum, D.; Kopelman, R. *Science* **1992**, 258, 78-781.
Tan, W.; Yeung, E. *Anal. Chem.* **1997**, 69, 4242.
Tapec, R.; Zhao, X.; Tan. WH *J. Nanosci. Nanotech.* **2002**, 2, 3, 405-409.
Theorell, H.; Chance, B. *Acta. Chem. Scand.* **1951**, 5, 1127.
Toffaletti, J.B. *Clin. Chem. News.* **1989**, 9, 14.
Tretter, L.; Repassy, R.; Adam-Vizi, V. *Neurochem. Intl.* **2003**, 42, 5, 393-400.
Trettnak, W. and Wolfbeis, O. S. *Fresen. Z. Anal. Chem.* **1989**. 334, 427-430.
Trettnak, W. and Wolfbeis, O.S. *Anal. Lett.* **1989**,22, 2191-2197.
Tsacopoulos, M. and Magistretti, P.J. *J. Neurosci.* **1996**, 16, 877-885.
Turner, T.J. *Proc. Natl. Acad. Sci. USA.* **1993**, 90, 9518-22.
Ulman, A. *Chem. Rev.* **1996,** 96, 1533.

Um, S.H.; Lee, S.G.; Lee, Y.J.; Koo, K.K.; Lee, C. Yoon, Y.B. *Langmuir* **2002,** 18, 4455-4459.
Ungerstedt, U.; Herrera-Marshcitz, M.; Jungnelius, U.; Ståhle, L.; Tossman, U, Zetterstöm, T. *Advances in Dopamine Research.* **1982,** 219-231.
Villamil-Fernandez, M. J.; Ordieres-Miranda, A. J.; Bianco-Tunon, P. *Anal. Chim. Acta* **1997,** 345, 37-43.
Vogel, A.I. in "*Vogel's Textbook of practical organic chemistry, including qualitative organic analysis*", 4th ed., Longman, New York, **1978.**
Wagner, G., Schmid, R. D. *Food Biotechnology,* **1990,** *4,* 215-240.
Wang, A. J.; Arnold, M. A. *Anal. Chem.* **1992,** 64, 1051-1055
Wang. Z.; Yeung, E. S. *J. Chromatogr. B. Biomed. Sci. Appl.* **1997,** 695, 59-65.
Whitesides, G.M; Ismagilov, R.F. *Science* **1999,** 284, 89.
Wightman, R.M.; Brown, D. S.; Huhr, W.G.; Wilson, R.L. *Voltammetry in the Neurosciences.* **1987,** 103-108.
Wolfbeis, O. S. and Trettnak W. *Proc. SPIE* **1989,** 1172, 287-292.
Xin, Q.; Wightman, M. R. *Anal. Chem.* **1998,** 70, 1677-1681.
Yu, Y.Y.; Chen, C.Y.; Chen, W.C. *Polymer* **2003,** 44, 593-601.
Zhang, and W. Tan, *Fresen. Z. Anal. Chem* **2001,** 369, 302-307.
Zhang, W.; Chang, H.; Rechnitz, G.A. *Anal. Chim. Acta.* **1997,** 350, 59-65
Zhou, X.; Arnold, M. A. *Anal. Chem.* **1996** *68,* 1748-1754.
Zhou, Z.; Misler, S. *J. Bio. Chem.* **1996,** 270, 270-277.
Zhou, Z.; Misler, S.; Chow, R. H.; *Biophysical Journal* **1996,** 70, 1543-1552.
Zivin, J. A.; Choi, D. W. *Scientific American,* 56-63, **1991.**

BIOGRAPHICAL SKETCH

Monde Qhobosheane was born on June 2, 1975. He was born and raised in Syracuse, NY. Monde attended a private Seventh-Day Adventist Christian academy for his secondary schooling. He then attended the University of Pittsburgh and studied chemistry and received a Bachelor of Science degree in this field in 1997. Thereafter he further pursued a Ph.D in bio-analytical chemistry under the supervision of Dr. Weihong Tan. He will receive his Doctorate of Philosophy in analytical chemistry from the University of Florida in May of 2003.

I certify that I have read this study and that in my opinion it conforms to acceptable standards of scholarly presentation and is fully adequate, in scope and quality, as a dissertation for the degree of Doctor of Philosophy.

Weihong Tan, Chairman
Associate Professor of Chemistry

I certify that I have read this study and that in my opinion it conforms to acceptable standards of scholarly presentation and is fully adequate, in scope and quality, as a dissertation for the degree of Doctor of Philosophy.

James D. Winefordner
Graduate Research Professor of Chemistry

I certify that I have read this study and that in my opinion it conforms to acceptable standards of scholarly presentation and is fully adequate, in scope and quality, as a dissertation for the degree of Doctor of Philosophy.

Charles R. Martin
Professor of Chemistry

I certify that I have read this study and that in my opinion it conforms to acceptable standards of scholarly presentation and is fully adequate, in scope and quality, as a dissertation for the degree of Doctor of Philosophy.

Benjamin A. Horenstein
Associate Professor of Chemistry

I certify that I have read this study and that in my opinion it conforms to acceptable standards of scholarly presentation and is fully adequate, in scope and quality, as a dissertation for the degree of Doctor of Philosophy.

Howard M. Johnson
Graduate Research Professor of Microbiology and Cell Science

This dissertation was submitted to the Graduate Faculty of the Department of Chemistry in the College of Liberal Arts and Sciences and the the Graduate School and was accepted as partial fulfillment of the requirements for the degree of Doctor of Philosophy.

May, 2003

_____

Dean, Graduate School